THE IDENTIFICATION OF A SOLAR SIGNAL IN CLIMATE RECORDS OF THE LAST 500 YEARS USING PROXY AND MODEL-BASED ANALYSIS AND THE IMPLICATIONS FOR NATURAL CLIMATE VARIABILITY

A Dissertation Presented

By

ANNE M. WAPLE

Submitted to the Graduate School of the University of Massachusetts Amherst in partial fulfillment of the requirements for the degree of

DOCTOR OF PHILOSOPHY

September 2006

Department of Geosciences

UMI Number: 3242309

UMI®

THE IDENTIFICATION OF A SOLAR SIGNAL IN CLIMATE RECORDS OF THE LAST 500 YEARS USING PROXY AND MODEL-BASED ANALYSIS AND THE IMPLICATIONS FOR NATURAL CLIMATE VARIABILITY

A Dissertation Presented

by

ANNE M. WAPLE

Approved as to style and content by:

_____
Raymond S. Bradley, Chair

_____
Robert M. Deconto, Member

_____
William D. McCoy, Member

_____
Jonathan Machta, Member

_____
Michael L. Williams, Department Head
Department of Geosciences

ACKNOWLEDGEMENTS

Lastly, thanks to Robert Gilbert who inspired me in this field many years ago. Thanks to my family for supporting me in my journey to a foreign country and for making it easy to follow my path. And thanks to Matt Menne for understanding, Lynn in Northampton, and to all my friends in Massachusetts and especially in Asheville who have been forced to listen to my frustrations!

ABSTRACT

THE IDENTIFICATION OF A SOLAR SIGNAL IN CLIMATE RECORDS OF THE LAST 500 YEARS USING PROXY AND MODEL-BASED ANALYSIS AND THE IMPLICATIONS FOR NATURAL CLIMATE VARIABILITY

SEPTEMBER 2006

ANNE M. WAPLE, B.A., UNIVERSITY OF WALES, SWANSEA.

PH.D., UNIVERSITY OF MASSACHUSETTS AMHERST

Directed by: Professor Raymond S. Bradley

There has been confirmation in the last two decades, through instrumental measurements onboard satellites, that the 'solar constant' does, as has long been hypothesized, vary. While there is no consensus as to the best method for estimating past variations in solar output, it seems likely that over the last 500 years, the sun has played a role in the changing climate. However, there is little evidence to suggest that changes in irradiance are having a large impact on the current warming trend.

A complementary approach of empirical and model-based analysis is used to determine if the climate effects of an estimated change in solar irradiance were significant in the pre-industrial era and what climate patterns emerge in response to reduced solar forcing at that time. Also investigated is the modification of solar-induced climate patterns by a hitherto underrepresented forcing - changes in Earth's orbit - and how solar and orbital forcing compare to that of increasing atmospheric greenhouse gas concentration. Finally

a brief analysis of the effects of a Maunder Minimum-like solar irradiance on a climate

forced by doubled CO_2 is undertaken.

Clear evidence is established herein for the ability of relatively small changes in solar

irradiance to impact the global climate. Both at the century scale and at shorter

periodicities, the variability of the solar 'constant' is influential in defining the global

mean climate and more importantly, the regional characterization of that climate.

Influencing the preferred mode of decadal variability, such as North Atlantic Oscillation,

solar variability alters the mean climate for northern Europe and the North Atlantic

region. The global response for temperature is found to be near-linear, while precipitation

is more complex. Excitation of important feedbacks, such as sea-ice, plays an important

role in determining the resulting pattern of response and ensures that even a much smaller

forcing (solar variability) can exert a similar fingerprint to that of a larger forcing

(greenhouse gases). Orbital forcing, typically excluded from model experiments for the

decadal-to-centennial scale, is found to provide important modification of regional

response and may be critical for determining a more accurate 'forecast' for future climate

TABLE OF CONTENTS

LIST OF TABLES

LIST OF FIGURES

Figure   Page

CHAPTER 1

INTRODUCTION

The aim of this dissertation is to assess the degree to which changes in solar irradiance impact the global climate on the decade-to-century time scale and their relative importance when compared with other possible forcing mechanisms. The hypothesis is that solar forcing does not exert significant influence on global climate on the decade-to-century scale.

The modern paradigm of 'change' as a means to investigate climatological principles necessitates a thorough understanding of the factors that combined to produce past, variations in climate. Of primary societal concern is the impact of global warming on our ecosystems and social systems. Global warming is simply the warming of the Earth's lower atmosphere without necessarily invoking cause. Nevertheless, it has become generally accepted that the principal reason for the observed late 20th and 21st century warming is the addition to the atmosphere of carbon dioxide and other 'greenhouse' gases as a result of industrial and domestic fossil-fuel use. It is important to be able to project the direction and magnitude of climate change, in order to plan for and/or mitigate anticipated effects. Despite the likely dominance of greenhouse gases in forcing future global climate change, this forcing (at both the global and regional scale) will be superimposed upon the naturally varying climate. The impacts of greenhouse gas forcing will therefore be tempered or augmented by these natural forcings and associated feedbacks. It is then of vital importance, in order to reduce uncertainty in projections of

future climate, to include a measure of both anthropogenically-induced and natural forcing.

At the decade-to-century scale, major contenders for external natural forcing are volcanic eruptions and solar irradiance variations (*e.g.* Mann *et al.*, 1998). These forcings likely played an important role in the Little Ice Age (LIA) cool period lasting from the 13th century to the mid 1800s as well as possibly the warm interval centered around 1000 AD. Although it has not been well-investigated, the relatively slow (low frequency) variations in the Earth's position relative to the sun (orbital parameters) also change the amount of solar energy the Earth receives at certain times of year and at different latitudes. There is therefore, a valid argument for the inclusion of small changes in orbital forcing that may contribute to decadal-to-centennial climate change, though this forcing has received little attention in climate attribution studies at this temporal scale. Since there is little evidence that volcanic eruptions in the observational period have affected global temperature for more than several consecutive years, this dissertation will not focus specifically on their overall influence. Some aspects of the modeling experiments will encompass the broad influence of internal oceanic processes – also a contributor to decade-to-century scale variability, though they will not be specifically addressed, except in reference to feedbacks associated with external forcing.

Intriguing correlations have been found to exist between global temperature and solar irradiance variations at the decade-to-century scale during the last several hundred years (*e.g.* Friis-Christensen and Lassen, 1991) and these will be described in more detail in the

literature review (chapter 2). Indeed, during the 20th and 21st centuries, during which time greenhouse gas forcing has increased exponentially, a positive global forcing from changes in total solar irradiance is also revealed and has been used in arguments against claims for the dominance of enhanced greenhouse gas forcing (*e.g.* Khandekar *et al.* 2005). For this reason, it has been difficult to separate out the relative effects of these influences. It is therefore important to determine if the global forcing of solar irradiance changes provides a spatial pattern of response distinct from that of greenhouse gas forcing and if so, what mechanisms are responsible.

This dissertation attempts to uncover the relative importance of solar irradiance for the pre-industrial climate up to the present, and for some possible future scenarios, both at the global mean and regional scale. Likely mechanisms to explain the resulting geographic patterns are examined. In addition, a brief examination of the effects of orbital forcing is undertaken. Its contribution has been assumed to be small and therefore largely ignored in decade-to-century scale climate studies. A combination of instrumental climate observations, proxy reconstructions of climate (necessary prior to the limit of reasonable accuracy in instrumental records), and general circulation model experiments has been used herein to attempt better quantification of the climate's response to likely decade-to-century-scale forcing. While proxy records show whether there is a spatial and time-varying response to specified forcing, the models provide greater insight into the climate dynamics associated with producing those patterns, and allow us to project into the future. Details of the data used in this dissertation are contained in chapter 3, while

methods are contained within the results chapters (4 and 5). Finally, conclusions are discussed in chapter 6.

Chapter 4 describes an empirical methodology to ascertain the likely impact of solar forcing during the pre-industrial era, and a comparison of results with model output enables a determination of likely mechanisms for the climate response. The influence of the changing sun is also compared to other possible forcing mechanisms over the last several hundred years (and into the future) in a series of sensitivity tests using a medium resolution general circulation model in equilibrium mode (chapter 5). This combination of analytical techniques reveals that the solar-forced patterns of global climate change likely resonate with established modes of climatic variability. All three forcing mechanisms investigated here (solar, greenhouse gases and orbital forcing) are detectable in changes in the North Atlantic Oscillation, indicating a high degree of sensitivity in this oscillatory mode to external forcing. This is of primary importance in determining the spatial pattern of response. Similar feedback mechanisms are excited by the different forcing scenarios, which includes sea-ice as a dominant feedback. While solar variability is the primary forcing prior to the industrial era, the dominance of greenhouse gases in the 20th century is established. These gases overwhelm the global equilibrium temperature effect of other forcing factors between the Maunder Minimum and present; they also dominate future climate based on projections of equivalent doubled CO_2. Nevertheless, if Maunder Minimum-like reductions in total solar irradiance were to occur under greenhouse gas-induced globally warmer conditions, they would have a significant global impact and produce regional modifications of climate patterns.

CHAPTER 2

LITERATURE REVIEW

2.1 Overview

Despite a recent resurgence of interest in the sun-climate relationship, much of it in the context of global warming, the study of the sun's influence on climate actually has a long history. There is much research and literature preceding this dissertation and leading to its inception. Though it is not possible to provide a fully comprehensive treatment of this literature, it is, however, appropriate to mention the most notable studies (both recent and historic) which give rise to the research contained herein, and to address the issue of context for this work.

It is well-established that the sun affects some of Earth's atmospheric processes, many of which are not considered important in studies of the surface climate (such as aurora and sprites), however there has also been a long tradition of attempts to link variations in the sun to changes in Earth's surface climate. While there is much quality literature analyzing the nature of the relationship, the field also suffered from frequent studies using dubious statistical practices and poor scientific method, especially in the early and mid-20th century. Consequently, progress in assessing the sun-climate relationship was slow as the science often lacked credibility and the significance of purported sun-climate relationships was not clearly demonstrated. There was a resurgence of interest in the late 20th century with new and rigorous investigations into the sun's role in terrestrial climate resulting, in part, from the need to address the issue of 'Global Warming', or the degree

to which human influence could affect the climate. The sun's inconstancy was deemed to be a possible alternative (or complementary) explanation for rapid 20th and 21st century warming. With the development of satellite-derived measurements of solar variability and the increased computing power available to produce mathematical models of global climate change and improved physical models of solar processes, recent progress in sun-climate research has been rapid.

This literature review begins by addressing key advances in our understanding of the sun and its processes. In order to assess the possible influence of a changing sun on Earth's climate, it is necessary to gain some appreciation for the envelope of solar change and the possible reasons behind it. Most of our understanding of the sun is based on observational evidence, albeit mostly from space in the modern era, as opposed to ground-based observations early in the 20th Century. This chapter is divided into two main parts – the history of solar observations and early attempts to link these to climate, and then some discussion of satellite-based observations of the sun, the derivation of solar proxies and more recent sun-climate research. Within this latter half, the chapter is further broken down into separate sections on solar observations followed by a summary of high and low-frequency climate variability linked to solar activity.

2.2 Solar variations and early links to climate

Observation of variations in the sun's appearance have been documented from as long ago as ~1200 BC during the Shang Dynasty in China (Shaefer, 1997), and a pupil of

Aristotle's (Theophrastus 370-290 BC) provides the earliest known reference to a sunspot (Coyne, 1991). Consistent observations of the sun have been possible since the beginning of the telescopic era (~ AD1610), Galileo perhaps being the first to observe a sunspot through a telescope (Coyne, 1991). The possibility of relationships between sunspots and weather was documented at least as early as the 1600s by Riccioli (1651 and 1653), as cited in (Schove, 1983).

Sunspots are dark areas seen on the 'photosphere' (the visible solar disk)(Figure 1.1), resulting from magnetic anomalies; as they increase in number, they reduce the sun's irradiance. The reduced irradiance due to sunspots is more than compensated for by corresponding bright areas on the photosphere (plages or faculae), at times of high solar activity (sunspot maxima) (Lean, 1991), and a more widespread granular network of bright areas across the disk. Therefore at times of high solar activity, the radiative output in the visible wavelengths (which dominate total solar irradiance (TSI), or spectrally integrated irradiance) is actually greater by a factor of 1.5, yielding an increase in net solar radiative output (Lean *et al.*, 1995). Since sunspots are easily visible on the solar disk and there is a record of their abundance extending back to the early 1600s, sunspots are therefore the most widely-used proxy for solar activity reconstructions.

The numbers of sunspots on the solar disk at any one time can easily be counted and recorded as an indicator of solar activity. However, in 1848, Rudolph Wolf at the Zurich observatory concluded that the activity of the sun could not be estimated well by simply

counting individual sunspots. He determined that the most accurate method of deriving

solar activity was to count the individual sunspots on any day and add them to 10 times

Figure 2.1. Image of sunspots and plages as seen on July 3rd 1991, Reproduced from
Charbonneau and White, 1995 from J. Harvey, National Solar Observatory.

the number of sunspot 'groups' or clusters. In this way he computed the daily 'Wolf

sunspot number', alternatively known as the Zurich sunspot number and as 'R' in

notation. Today, the sunspot number is computed much the same way, but a weighted

average of measurements from a number of cooperating observatories is used to

compensate for factors such as solar rotation and terrestrial atmospheric disturbance

(http://www.ngdc.noaa.gov/stp/stp.html). Hoyt *et al.* (1994) also determined that by

counting the number of sunspot groups only (as recorded by the Royal Greenwich

Observatory between 1874 and 1976), the Wolf sunspot number can be well simulated.

They termed this new index the 'Group Sunspot Number' and have used this to check the

earlier part of Wolf's record. It was found that Wolf's numbers prior to 1848 are generally higher than the Group Sunspot Number, so the secular trend in sunspot numbers from the Maunder Minimum (MM) (an historic period of reduced sunspot counts from ~1675-1715; further discussed below) to present is greater if only the Group Sunspot Number is used (Hoyt *et al.*, 1994).

An eleven-year cycle in sunspot activity was identified in 1843 by Heinrich Schwabe (and later confirmed by Wolf) (Figure 2.2), but a number of periodic variations in the sun's activity have been identified in addition to the now well known Schwabe cycle. Spectral analysis has shown that there are significant peaks not only at the 11-year Schwabe cycle, but also at 22 years (the Hale cycle), at 88 years (the Gleissberg cycle) and at still lower frequencies (e.g. Lean, 1991). Sunspots are most often grouped in pairs of opposite magnetic polarity and Hale and coworkers in the early 20th century indicated that from one sunspot cycle to the next, the magnetic polarities of sunspot pairs undergo a reversal (Charbonneau and White, 1995).This was subsequently discovered to be an expression of a global magnetic reversal on the sun every eleven years (Morfill *et al.*, 1991). Therefore, it actually takes 22 years to complete a true solar cycle (i.e the Hale Cycle), although generally, reference is still made to the '11-year solar cycle' (Charbonneau and White, 1995).

The lack of sunspots at the end of the 17th Century was noted by numerous academics, including Gustav Spörer, John Flamsteed, and arguably most importantly, Walter Maunder. Assuaging a concern that the period of diminished sunspots might actually be

due to a reduced number of observations, Spörer published two articles in 1889 indicating

that there were indeed sufficient observations to justify the conclusion that there had been

a sustained decrease in sunspot activity in the late 17th century. Maunder thought this
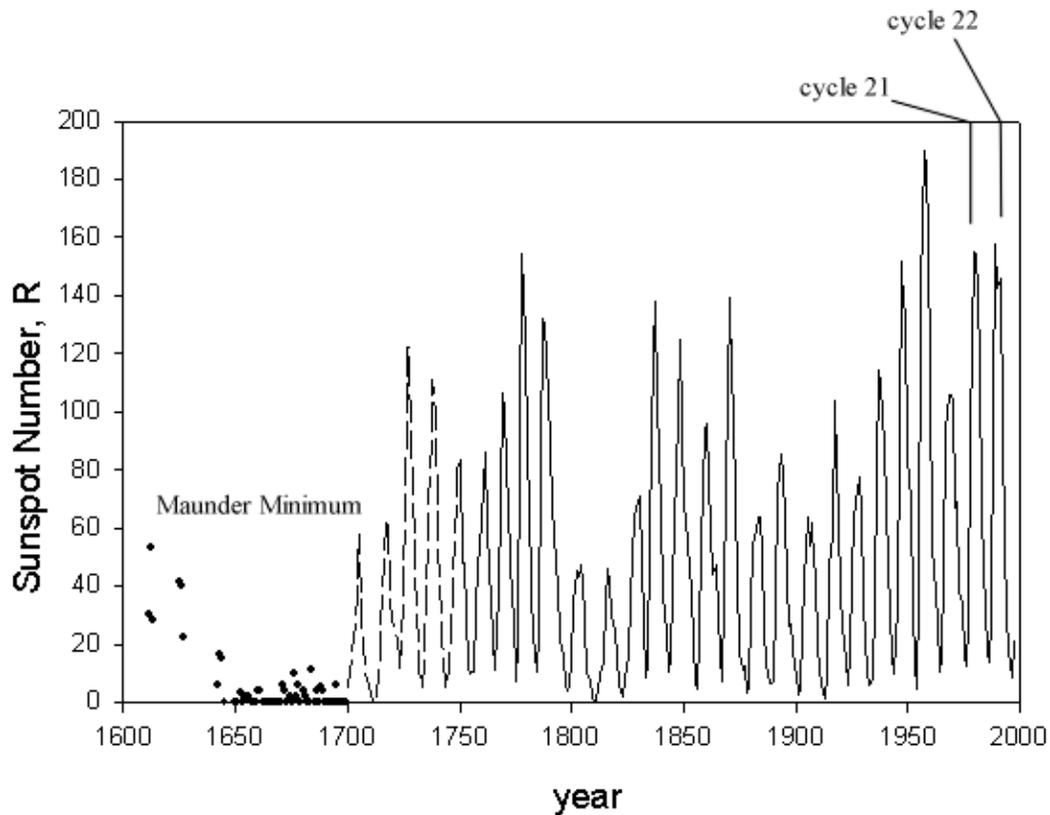
Figure 2.2. Estimated Annual Mean of Sunspot Number from 1610 to 1997.
(Data is taken from the Solar and Terrestrial Physics Division of the National
Geophysical Data Center - available at: http://www.ngdc.noaa.gov/stp/stp.html)

period of such great importance that he translated Spörer's German articles into English

and presented them in the Royal Astronomical Society's annual report in 1890, but they

attracted little attention. In 1922, Maunder again published an article on the period

suggesting a possible link to terrestrial weather, but it was not until 1976 and an article

from John (Jack) Eddy in Science, when he coined the term the 'Maunder Minimum',

that the academic community began to pay serious attention to the period (Hoyt and
Schatten, 1997).

Interest in solar-climate connections has waxed and waned over the last several centuries
with the first real surge in the late 1800s, spurred in part by William Herschel's
observations (as the Astronomer to the King in England) and Meldrum's paper in 1872
relating tropical cyclones to sunspot number. A decline in interest in the early 1900s was
followed by a steady increase in publications, peaking in the 1930s, then again in the
1950s and again in the 1970s (Hoyt and Schatten, 1997). Throughout the 20th Century,
the quality of publications linking solar activity to terrestrial climate has been variable,
occasionally spurring criticism of the whole field. Solar variations were linked to
everything from Earth's temperature, precipitation, droughts and floods, to economic
variations, wheat prices, insect populations, shipwrecks and wine vintages. Solid research
was mixed with careless statistical analysis and the field suffered from issues of
credibility (Hoyt and Schatten, 1997). This review will not address those articles which
are of dubious merit and will instead focus on the literature considered to have advanced
the field.

2.3 Satellites Observations and Recent sun-Climate Research

2.3.1 Satellite Observations
Although changes in solar activity, especially in the short-term do not necessarily result
in a change in irradiance, in recent decades, satellite-derived measurements of solar

activity have not only confirmed the existence of a 'variable sun', but have allowed

greater precision in solar irradiance measurements and better calibration of pre-satellite

era proxy indicators. Direct observational evidence confirming that the sun's output does

indeed vary came in the form of space-based measurements, as early as the 1960s.

Observations made from one of the Orbiting Solar Observatory (OSO) satellites enabled

greater understanding of the variations in the solar atmosphere, or the corona, for

example. The immensely high temperatures of the sun's corona control the solar wind,

driving electrically charged particles in all directions. Although not necessarily of prime

importance to climate, disturbances on the sun (or storms) disrupt the flow of the solar

wind and result in aurora and interruptions to radio communications on Earth. They also

cause variations in cosmogenic isotopes which can be used as proxies of solar activity

(see discussion in 2.3.2). In the early 1970s the Skylab mission took thousands of

photographs of the sun's corona during a quiet phase of the 11-year cycle and this was

arguably the most important mission to advance the study of the sun. The Solar

Maximum Mission (SMM), launched in 1980 enabled scientists to capture variations

during a more active phase of the sun and although this satellite failed after one year, it

was repaired in 1984 and continued to gather measurements (Phillips, 1992).

The SMM included a radiometer (Active Cavity Radiometer Irradiance Monitor -

ACRIM) designed to measure solar irradiance, which until the satellite era, was

understood to be constant, hence reference to the 'solar constant' as the sustaining force

of our climate (Benestad, 2002). A photometer aboard the SMM also measured changes

in visible light output of 0.1% to 0.3% over periods of days to months. It was then

recognized that radiative output integrated over longer time periods could be substantial, and more likely to impact terrestrial climate than daily-scale changes. There have since been numerous different satellite-borne instruments to improve our understanding of solar processes and their impacts on the Earth. Currently there are plans to fly a new radiometer on board the National Polar-orbiting Operational Environmental Satellite System (NPOESS) mission scheduled for launch sometime in the next 5 years.

A new problem has arisen within the satellite era with the intercomparison of space-based measurements. Figure 2.3 shows that during overlapping observation periods, different instruments do not show identical values of TSI. While they all illustrate similar temporal variations, indicating the existence of the 11-year cycle in TSI, the absolute average difference between the measurements from different instruments may be as much as 8 Wm^{-2} (Figure 2.3). Fröhlich and Lean (1998) merged these different measurements into a composite TSI and noted the clear expression of an 11-year cycle, but they found no discernable trend between the two observed cycle minima as had previously been suggested as a contributing factor to late 20th Century warming (Willson and Hudson, 1991).
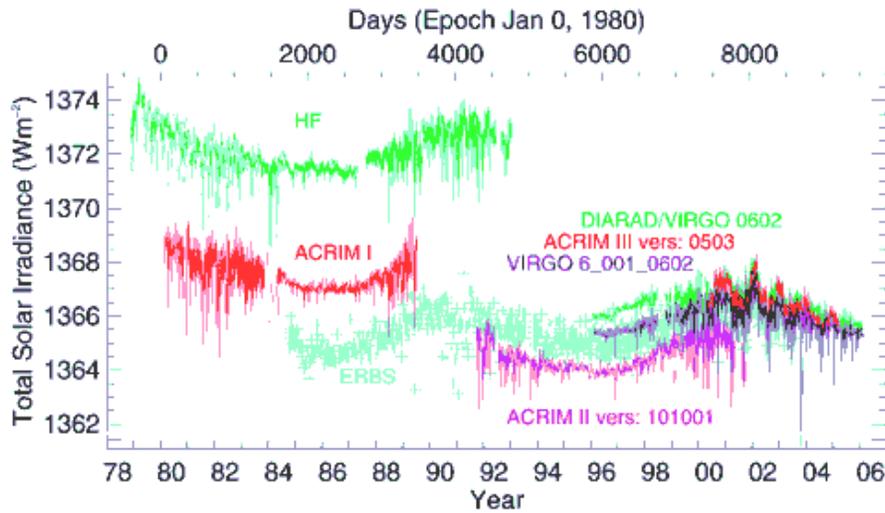
Figure 2.3. Daily averaged values of the sun's total irradiance TSI from radiometers on different space platforms since November 1978: HF on Nimbus7, ACRIM I on SMM, ERBE on ERBS, ACRIM II on UARS, VIRGO on SOHO, and ACRIM III on ACRIM-Sat. The data are plotted as published by the corresponding instrument teams (graph reprinted and modified by kind permission of Fröhlich and Lean, 1998)

In addition to total solar irradiance variations, the spectral irradiance is also important. Spectral irradiance refers to the proportion of irradiance changes that are in the ultraviolet (UV), visible and infrared (IR) portions of the electromagnetic spectrum. Variations in TSI from peak-to-trough of the 11-year cycle are only on the order of about 0.1%, (Fröhlich and Lean 2004), however, variations in the UV and extreme ultraviolet (EUV) can be as much as 10% over the Schwabe cycle. UV variations affect the thinner (upper) layers of the atmosphere and impact such processes as ozone production and destruction in the stratosphere (*e.g.* Haigh 1994). There is still much research to be done on how significant the cyclic variations in UV and EUV are for the near-surface climate, with studies such as Shindell *et al.* (2001) finding critical vertical coupling between the stratosphere and troposphere. However, recent research suggests that just such a coupling is less significant with respect to surface climate (*e.g.* Rind *et al.* 2004).

2.3.2 Solar 'proxies' and solar reconstructions

Vital contributions have been made to the field through determining additional solar 'proxies' that indicate solar variability over longer time scales. Without these proxies, we would be limited to the zero-bounded sunspot cycles and the short satellite record to infer solar variability. While both are invaluable in solar-climate studies, they are unable to tell the complete story with respect to the inconstancy of the sun's irradiance.

The two major proxy indicators of solar change are isotopes of carbon (^{14}C) and beryllium (^{10}Be). These isotopes are produced when cosmic rays enter the atmosphere and collide with atoms, creating sub-atomic particles of unstable isotopes (cosmogenic isotopes). Cosmic rays reaching the Earth and reduced when solar activity (solar wind) is strong. Thus higher solar activity leads to lower values of ^{14}C and ^{10}Be (Stuiver, 1961, McHargue and Damon, 1991) . Minze Stuiver in 1961 discovered evidence of solar variability in ^{14}C measured from annually resolved tree-rings. It was a turning point for sun-climate analysis, partly because tree-rings may also contain an annual record of temperature or precipitation variations that can be directly correlated to the solar activity. Both ^{14}C and ^{10}Be can also be recovered from ice cores (that also contain climate information) in both the Arctic and Antarctic, or at high-elevation, tropical locations, resulting in long annually-resolved records of these isotopes. Researchers such Beer (2000) and Bard *et al.* (2000) were able to produce time series of ^{14}C and ^{10}Be that showed both short and long-term variations in solar activity exhibiting similar temporal

characteristics to those suggested by observations of sunspots, including lower activity during the Maunder Minimum.

An additional proxy, the emission lines from ionized Ca, indicates solar (and by extension stellar) magnetic activity associated with the bright facular regions of the sun, and is most obvious in the visible portion of the spectrum (around 400nm) resulting from changes in temperature of the chromosphere.

Lean *et al.* (1992,1995) used a Ca index from non-cycling sun-like starts (i.e. those that appear to be in a Maunder Minimum-like state) to infer a solar irradiance reduction of approximately 0.24% during the MM compared to present (figure 2.4) The decadal variability from MM-to-present was then constrained by the monthly sunspot numbers. This reconstruction was compared to the time series of both ^{14}C and ^{10}Be to verify the method. While the cosmogenic isotopes were similar to the reconstruction of Lean *et al.* (1995), the time series varied considerably from a reconstruction based on solar cycle length, rather than amplitude as in Lean *et al.* (Hoyt and Schatten, 1993), (see also chapter 3 for more information). Lean and Rind (1998) and Fröhlich and Lean (2004) concluded that the resulting uncertainly in solar reconstructions based on different solar 'proxies' precludes a definitive estimate of historical irradiance, though there have been significant concerns over the methods of constructing accurate solar cycle length estimates, as used by Friis-Christensen and Lassen, 1991 for example (*e.g.* Damon and Peristykh, 2004; Laut, 2003).

More recently Wang *et al.* (2005), using modeled solar physics, concluded that the contribution of the secular, or background, solar variation is smaller than suggested in previous investigations. It is therefore likely, according to Wang *et al.* that the MM-to-present difference in TSI is also smaller, perhaps one third-to-one quarter smaller than that estimated by Lean *et al.* (1995). Chapter 3 describes Wang *et al.* (2005), Hoyt and Schatten (1993) and Lean *et al.*(1995) in more detail as their reconstructions are used in this investigation.
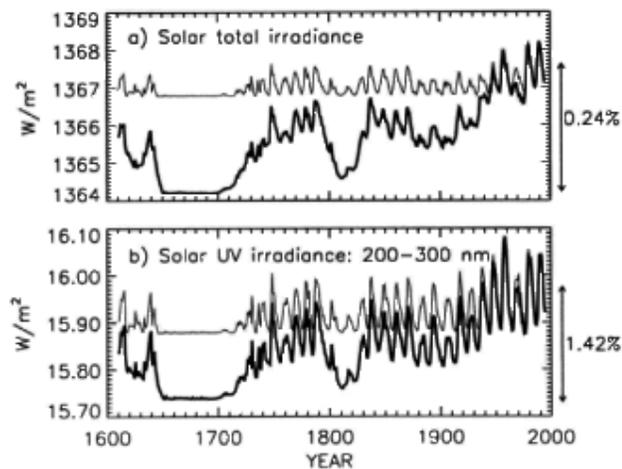
Figure 2.4 Reconstructed total solar irradiance - top, and UV irradiance (in the band between 200 and 300nm) - bottom. The thin line is the Schwabe cycle variability, and the thick line is the Schwabe cycle variability plus a longer-term variability component estimated from observations of sun-like stars (Lean *et al.*, 1995)

2.3.3 High Frequency (Decadal) Climate Variations Linked to the Sun

As mentioned in section 2.1, there have been a significant number of studies that have attempted to link the 11-year cycle to climate shifts on the same scale. Some appear to have merit and others less so. A substantial difficulty in detecting decadal-scale changes

in the climate that might be related to solar variability is that there is significant power in the decadal band frequency signal unrelated to solar variability, such as that produced by ENSO variations, volcanic activity and other modes of variability (such as the PDO). It is relatively easy, therefore to find correlations between the solar cycle and climate variations, though upon closer inspection, many of these relationships break down when longer datasets are used, or the phase of the correlation changes over time, usually indicating a lack of true coherence. In addition, physical mechanisms for producing noticeable surface climate changes at the decadal scale from solar changes on the order of 1 Wm^{-2} are elusive and/or hotly debated, and there is general recognition that any decadal sun-climate relationship would have to be augmented by positive feedback mechanisms in order to produce a signal that is detectable above the noise of the climate system. Nevertheless many studies appear to find intriguing relationships between solar variability and climate at this scale.

There is very clear evidence that the 11-year solar cycle does impact stratospheric temperatures, stratospheric ozone production and cosmogenic isotope production. The degree of coupling between the stratosphere and troposphere is a critical determinant in identifying tropospheric temperatures with a detectable solar signal. There is however, some evidence that both the troposphere and ocean temperatures respond to solar forcing at the decadal scale. While direct forcing of small irradiance changes is unlikely to produce an appreciable change in global-scale surface temperature, the dynamic coupling of the stratosphere (where we know the 11-year cycle has an effect) and the troposphere may lead to a redistribution of the energy already present in the atmosphere such that

large regional changes may result. For example, if the latitudinal pressure gradient is altered by differential heating in the stratosphere (induced by solar-forced changes in ozone), tropospheric redistribution of heat will likely occur (Shindell *et al.* 2001).

Using the GISS General Circulation Model and resolving more of the stratosphere than is typical in most GCMs, Shindell *et al.* (2001) determined that solar-induced circulation changes in the stratosphere also penetrated the troposphere, and resulting changes in model geopotential heights (and therefore column temperature) compared favorably to observations (outlined below). Critical in this model was the incorporation of a model stratopause (to allow realistic planetary wave propagation), and spectrally varying solar input, permitting a parameterization of wavelength-dependent stratospheric ozone response.

A series of studies by Harry van Loon and Karin Labitzke thoroughly examined the stratospheric response to solar forcing. Labitzke and Van Loon (1988, 1992, 1993, for example), examined the correlation between a ten-to-twelve-year oscillation in the stratosphere and the eleven-year solar cycle. They discovered that a correlation of 0.6 and above existed between the annual mean 30mb geopotential height (for 34 years) and the solar cycle in a geographic region between 20°N and 40°N from the mid-North Atlantic westward to the mid-North Pacific (Labitzke and van Loon, 1993). The correlations were highest in mid summer and lowest in January and February. The winter correlations also varied depending on the phase of the Quasi-biennial Oscillation (QBO) (Labitzke and van Loon, 1988). In addition, they found that there was a correlation between the eleven year

solar cycle and upper tropospheric temperature in two broad sections of the Northern

Hemisphere in the summer months (Labitzke and van Loon, 1992): one section extended

from 12-75°N across N. America, and the other was from 8-32°N from the Western

Pacific running eastward to the Western Atlantic. The most obvious temperature response

is between 500 and 100mb in both of the sections. The lower tropospheric geopotential

heights did not appear to show an eleven-year cycle clearly, however the response

increased with altitude.

The potential coupling of stratosphere-to-troposphere in relation to decadal solar forcing

was also examined by Haigh (1996). Through modeling the magnitude of irradiance

change including wavelength dependence of the solar variability, together with the

consequent effects on lower stratospheric ozone (using realistic assumptions of

irradiance), she found that there was a small poleward shift of the mid-latitude storm

tracks at solar maximum relative to the minimum of a solar cycle, indicating a

displacement of the position of the Westerly jet stream and therefore the meridional

extent of the Hadley Cells (Haigh, 1996).

An element of climate that has received relatively widespread attention in relation to

solar variability is drought and precipitation cycles. The Hale (22-year) cycle has for

some time been invoked as a possible reason for a bidecadal drought rhythm in the

Southwest USA and Great Plains. It is possible that this apparent cycle of drought could

be due to internal variability of the ocean-atmosphere system, but as Cook *et al.* (1997)

indicated, it is also not easy to eliminate the sun (and moon in this case) from the causal

hypotheses. It appears from Cook *et al.*'s findings, that since at least 1800, the lunar cycle (18.6 years) and the Hale cycle interact to modulate the drought cycle.

Drought may be a better indicator of a high frequency solar signal, in part because it may take only a small forcing to affect areas on the margin of meteorological aridity, leading to drought. For example, in a study of paleoclimate records from the GISP2 ice core from Greenland, there is clear evidence of a dust cycle of eleven years (Ram *et al.*, 1997). The Wisconsinan (the last glacial), with a much drier climate and higher dust loading of the atmosphere than today, exhibited particularly marked cycles. According to Ram *et al.* dust variation is most likely a measure of continental aridity rather than temperature and is therefore perhaps more sensitive to the small variations in solar flux. With only a small increase in precipitation amounts a dust source can cease to produce dust (Ram *et al.*, 1997).

High-frequency solar-related variations in upper ocean temperature have also been found for globally-averaged and basin-averaged ocean areas from 1955 to 1991. White *et al.* (1997), found a response to solar forcing at three different frequency bands including the decadal scale (White *et al.*'s multidecadal scale correlations are discussed in section 2.3.4). Filtering both the ocean temperature and the solar irradiance at the top of the atmosphere by using a bandpass filter and correlating the timeseries, reveals a correlation of 0.93 at 0 lag with 95% confidence. This translates to an average 0.04 K warming with a change of 0.5 Wm^{-2} at the top of the atmosphere from solar peak to trough in the bandpassed irradiance data. The correlations were in phase across three separate ocean

basins (Indian, Atlantic, Pacific) and penetrated the upper ocean to a depth of around 100

meters, but not below the pycnocline. White *et al.* find that the geographic pattern of

response in the extratropical oceans mirrors that of known modes of variability and

surmise that the anomalous heat exchange from the ocean to the atmosphere may help

drive these modes of variability to phase lock with the solar cycle. This is explored in

chapter 4 of the dissertation and further discussion of White *et al.* 1997 can be found

therein.

Svensmark and Friis-Christensen (1997) have proposed that clouds may also respond to

the eleven-year cycle. Using the cloud cover dataset of the International Satellite Cloud

Climatology Project (ISCCP), which runs from 1983 to 1990, they found a variation of

3%-4% in the cloud cover during this portion of the solar cycle. A cloud cover maximum

corresponded to the solar cycle minimum around 1986/87. The physical connection

suggested by Svensmark and Friis-Christensen for increased cloud cover at solar minima

is the variation in cosmic ray intensity. There is an inverse relationship between solar

activity and cosmic ray intensity due to a shielding of the Earth from cosmic rays during

high solar activity and they found very high correlations between the measured cosmic

ray flux and mid-latitude cloud cover changes. The authors proposed that the incidence of

cosmic rays affect cloud formation by changing the ion concentration in the atmosphere,

as ions act as cloud condensation nuclei. The temperature changes at the surface

associated with variations in cloud cover are not certain, but the net effect of a cloud

cover increase is believed to be a cooling. Sun and Bradley (2002) in a re-evaluation of

the proposed relationship used longer datasets as well as complementary ground-based

cloud observations and found the feedback to be negligible. Although the Svensmark and Friis-Christensen study has not stood up to further scrutiny (as have the other studies mentioned in this section), it has received a great deal of attention and is appropriate to summarize in the context of high frequency solar-climate relationships. A dataset of sufficient length is vital to establish the robustness of the relationship for a cyclic forcing.

2.3.4 Lower Frequency (Multidecadal) Variations

Lower frequency cyclic variations in solar activity have been identified at 88 years (the Gleissberg Cycle), 200 years (Seuss cycles or de Vries cycles) and a 2300-year Halstatt cycle as well as other quasi-periods in cosmogenic isotope data (see for example Damon and Sonnett, 1991). Studies investigating causal mechanisms for the warming of the last 150 years have often examined solar forcing as a possible contributor to the trend and to the multi-decadal variability. While the temperature trend of the last century or so can be explained by a combination of solar and greenhouse gas forcing, with greenhouse gas forcing becoming more dominant nearer the present, the non-linear nature of the trend is more difficult to associate with these gases, given the near linear increase in CO_2 for example.

Reid (1991) identified a correspondence between the 80-90 year Gleissberg period of sunspots and 20th century sea-surface temperatures. While the records are certainly not identical, as demonstrated by Figure 2.5, a minimum in the early decades of the 20th century, a rise towards the 1950s, a small drop in the 1960s, then a subsequent rise is

mirrored by similar features in the solar forcing. Friis-Christensen and Lassen (1991) using sunspot cycle length as an alternative proxy found a similar relationship with surface temperature. As Figure 2.5 demonstrates, there is an impressive agreement between solar cycle length and Northern Hemisphere land surface temperature for the 1860s to the mid 1980s outlined in Friis-Christensen and Lassen (1991). However, the relationship breaks down when the most recent decades are examined. Some further questions have also been raised as to Friis-Christensen and Lassen's methods (Laut, 2003). It is statistical correspondence such as in the studies above that have both given rise to a more concerted effort at understanding the solar-climate relationship and have at the same time have drawn some criticism for overinterpretation of a statistical correlation.
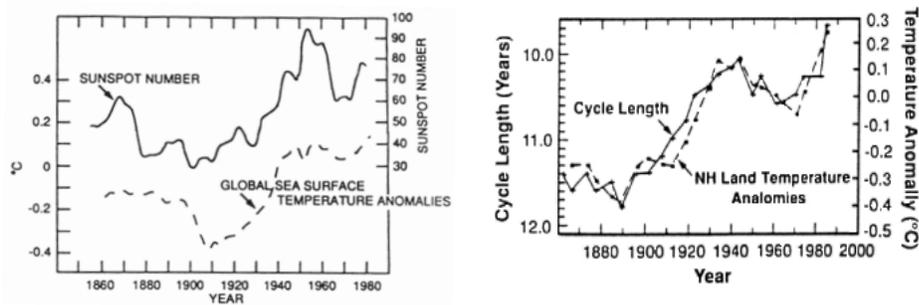
Figure 2.5. Left panel: Comparison of sunspot number (11-year running mean) with global sea-surface temperature anomalies (Withbroe and Kalkofen, 1994 after Reid, 1991); Right panel: The length of the sunspot cycle (from smoothed sunspot extrema) plotted against northern hemisphere temperature anomalies (Withbroe and Kalkofen, 1994 after Friis-Christensen and Lassen, 1991).

Schlesinger and Ramankutty (1994) also found an oscillation with a periodicity of around 65-70 years in a detrended global mean surface temperature series; they suggest this is a statistical expression of broader 50-88 year oscillations. However, they did not conclude

that solar variability is the major forcing, but predictable internal variability in the ocean-atmosphere system instead. Mahasenan *et al.* (1997) were also able to detect oscillations of 80 years in several long-term proxy climate records. While they acknowledged the possibility of a solar influence, the fact that they also found a more predominant 160-year oscillation suggested to them that ocean dynamics were the more likely culprit, since there is no identifiable 160-year solar cycle. Schlesinger and Ramankutty (1994) also reinforced their rejection of the solar hypothesis, suggesting that any solar response should be global in nature and the temperature differences they saw were regionally distinct. However, studies such as Haigh (1994, 1996) and Labitzke and van Loon (1988, 1992), White *et al.* (1997) (outlined above) suggest that a dismissal of solar forcing due to a supposition of a global response in the temperature, is probably not justified.

In addition to the high frequency signal that White *et al.* (1997) found in ocean temperatures (described in section 2.3.3), there was significant power at lower frequencies, >100 years and at 18-25 years, when filtered to isolate the multidecadal component. Using three different statistical techniques, the signal was found to be robust and in phase across three oceans and between two different datasets of ocean temperature. The temperature response was nearly twice that for the high frequency case with a maximum correlation of 0.81 at a lag of 3 years. While the oceans' temperature response appears to penetrate deeper below the sea surface at the multidecadal scale, significance is also harder to establish because of fewer cycles in the record.

Of more public interest than the decadal or interdecadal temperature variability in the last century or so, is the century-scale trend in temperature. Several notable studies, both observational and model-based have investigated the role of solar variability in the warming trend. The Maunder Minimum in sunspot activity coincides with a period of cooler temperatures, known as the Little Ice Age (LIA)(Bradley, 1999). Temperatures have increased through much of the subsequent period as estimated solar irradiance has also risen. Efforts to assess the likely contribution of that solar forcing to the trend in temperature have resulted in several approaches; empirical analysis, simple model experiments and more complex models have been used to investigate the relationship.

The Maunder Minimum decrease in solar activity, corresponding to a period of lower temperatures within the Little Ice Age has been estimated at 0.24% compared to present (Lean *et al.*, 1995). Wigley and Kelly (1990) used a simple energy balance climate model to estimate that a 0.22% -0.55% decrease in irradiance would have been necessary to cause the cooling estimated during the LIA, inferring a climate sensitivity of around $1^{\circ}C/Wm^{-2}$ forcing for a 0.22% decrease. At the time that Wigley and Kelly undertook that study, the only estimate of solar forcing for the Maunder Minimum was Lean and Foukal (1988), which was 0.14% below present day values. This was not enough to induce the LIA cooling that Wigley and Kelly estimated ($0.4^{\circ}C$-$0.6^{\circ}C$ for the globe), and they concluded that internal climate variability was at least partially responsible for the cooler period.

Since Lean *et al.* (1995) found a 0.24% reduction in solar irradiance for the Maunder

Minimum, Wigley and Kelly's conclusion may be modified to attribute more of the LIA

cooling (or MM-to-present warming) to solar forcing, however, even more recent solar

estimates (Wang *et al.* 2005) suggest a solar reduction similar to that of Lean and Foukal

(1988), implying that either the climate sensitivity is higher than previously thought or

that solar forcing may only be partly responsible for the cooler period. The global energy

balance model and the simplistic approach that Wigley and Kelly used is certainly useful

as a first order approximation of forcing and response, but it is now clear that a global

estimate of cooling for the Little Ice Age is perhaps less useful than regionally distinct

climate expressions for detection of external forcing. Much of the cooling during the LIA

appears to be focused on continental interiors and the North Atlantic region (Mann *et al.*

1998) and global estimates of cooling may have been exaggerated due to the

preponderance of proxy climate data in the North Atlantic region and a consequent bias

towards evidence for cooling during the period.

Studies such as Rind and Overpeck (1993), Cubasch *et al.* (1997), Rind *et al.* (2004) and

Shindell *et al.* (2001) as well as others use more sophisticated general circulation models

(GCMs) to examine the dynamical spatial response of the climate to estimated solar

forcing from the Maunder Minimum to present. Using either coupled or uncoupled ocean

components and different model resolutions, and focusing on different elements of the

climate system, most modeling studies based on GCMs conclude that solar variability can

and does have some impact on the global climate and produces distinct regional

responses. As with any modeling study, the sensitivity of the model and other model

specifics will determine the simulated climate response, yet there is remarkable

consistency in the conclusion that solar forcing of the LIA and subsequent warming is

non-negligible with an increasing dominance of greenhouse gases (and therefore

decreasing solar influence) towards the present. Many of these modeling studies are later

referred to and further explained in the context of the research contained in this study.

The model-based conclusions are largely supported by empirical evidence for significant

solar forcing. Without long-term records of upper air and ocean heat storage and other

elements of the climate system, our ability to determine causal mechanisms in empirical

studies is severely limited. Therefore many of these studies are confined in scope to

describing statistical correlations albeit far more sophisticated than simple linear

regression in many cases. Nevertheless, most rigorous and well-conducted empirical

studies are highly suggestive of a solar influence and in combination with modeled

studies, confirm the likely significant influence of solar variability on global climate.

Lean *et al.* (1995) for example, used a combination of the Schwabe cycle and a longer

term variability component to estimate total irradiance (explained in section 2.3.2) and

correlated this with the Bradley and Jones (1993) Northern Hemisphere temperature

series. They found that up to 74% of the temperature variation from 1610-1800, and 56%

of the variance from 1800 to the present could be attributable to changes in solar

irradiance. About half the observed warming (of 0.55°C) from 1860 to the present could

be accounted for by natural variability arising from solar radiative forcing according to

Lean *et al.* (1995). Correlations of temperature and solar irradiance decreased

significantly towards the present as the dominance of greenhouse gas influence is

established.

Mann *et al.* 1998 also used the Lean *et al.*(1995) solar reconstruction as well as volcanic

aerosol estimates and greenhouse gas concentrations to estimate the likely influence of

each since 1610. Using a 200-year moving window (to maximize signal-to-noise ratios),

they employed a multivariate regression method accounting for serial correlation and

used a Monte Carlo simulation to estimate the likelihood of spurious trends. Using this

method, they were able to detect a significant influence of solar variability during the 17th

and 18th century with greenhouse gases becoming much more dominant as the 200-year

window moves into the 20th century.
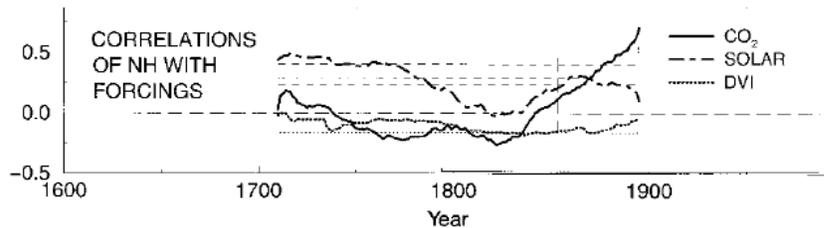
Figure 2.6 Evolving multivariate correlation of NH series with the three forcings NH, Solar, log CO_2 from Mann *et al.* 1998. The time axis denotes the center of a 200-year moving window. One-sided (positive) 90%, 95%, 99% significance levels (see Mann *et al.* 1998 for more details) for correlations with CO_2 and solar irradiance are shown by horizontal dashed lines, while the one-sided (negative) 90% significance threshold for correlations with the DVI series is shown by the horizontal dotted line.

Waple *et al.* (2002, and described in chapter 4) further analyzed the Mann *et al.* 1998

temperature reconstruction and empirically examined the regional expression of likely

solar influence gaining insight into the possible mechanisms for the forced response. Chapter 5 uses a suite of model experiments to further examine solar forcing compared to other possible forcing, including orbitally-induced irradiance changes, which have not received proper attention as a decade-to-century scale forcing.

In summary, the literature and research preceding this dissertation used multiple techniques to estimate solar irradiance for the last several hundred years and to examine its potential influence on the climate at the decadal-centennial scales. The precise time-history of solar forcing over the last several centuries is still a very active area of research and the solar physics community is continuing to make great strides in understanding how solar processes affect the amount of radiation we receive on Earth. Though uncertainty still remains regarding the solar irradiance for the Maunder Minimum and other pre-satellite periods, we have conclusive evidence that the 'solar constant' does indeed vary and is therefore a likely candidate for forcing global change. Using reasonable estimates of solar irradiance for the last several centuries we are able to gauge the envelope of likely climate sensitivity to changes in solar output. While the study of solar-induced climate changes suffered from issues of credibility from a multitude of poorly executed statistical analyses, it has regained stature with some notable rigorous studies using both empirical and model-based methods to establish a solar-climate relationship. This dissertation seeks to build on these analyses and examine empirical and modeled datasets to gauge the influence of the sun on both global mean and especially regional scale climate from the Maunder Minimum to present and into the next several decades.

CHAPTER 3

DATA DESCRIPTION

This dissertation is, in part, based on a range of data and models that have been
developed and researched by scientists acknowledged below. It would not be possible to
have completed my analysis without their integrity in producing these datasets as well as
their generosity in allowing these data and models to be available to me in this project.

In the various stages of this study, I have made use of proxy, instrumental and modeled
data. All of the sources are outlined below and a detailed description of the advantages
and drawbacks of the data are provided, along with reasons for inclusion of specific
datasets.

3.1 Instrumental and Proxy Climate Data

 In order to isolate the likely contribution of industrial greenhouse gases emissions to
climate change, it is necessary to gain an appreciation for the degree of natural climate
variability. To determine the full range of variability on the decade-to-century timescale
we must look at decades and centuries *prior* to the last century, before industrial
processes are thought to have been influential on our climate.

This presents challenges, since the industrial revolution brought with it a more
concentrated effort to record temperature and other climate parameters as well as more

reliable instruments. Hence, prior to the 1900s, the instrumental record of climate is geographically sparse, with large areas of the globe unsampled. Additionally, often meteorological instruments were misused or misread necessitating removal of some long records upon quality control investigations. It is necessary, under these circumstances, to resort to alternative measures of climate. Natural archives of climate information (including trees, ice sheets and corals) provide records of temperature and other climatic elements through a specific response to environmental change. For example, if a tree is stressed by drought, it will produce a smaller annual tree ring and tree ring records may be calibrated against the modern instrumental record to extend our understanding of climatic variations into pre-instrumental history. These proxy records can be combined with early instrumental or historical accounts of the climate, and a useful picture of the climate prior to the 20th century can be derived.

Until the early 1990s, most researchers had employed one indicator of climate in a particular location to infer that region's past climate. For example, tree-rings in the desert Southwest U.S. provide an annual record of precipitation for that region; ice cores from Greenland record that continent's annual snowfall and other climate parameters. However, until the early 1990s, few attempts had been made to combine these records into a more global picture of paleoclimate. It is difficult to achieve a 'multi-proxy' reconstruction due to several different factors: proxies may have different temporal resolutions (annual, interannual, decadal etc.); they may respond to different climatic parameters (precipitation, temperature, ocean salinity); and low frequency variations over the length of the record. However, if these issues can be overcome, the advantages of

using a network of indicators to reconstruct hemispheric or global climate are

tremendous. Bradley and Jones (1993) were the first to assess the possibilities of the

multi-proxy approach and this led to a northern hemisphere summer temperature decadal

reconstruction over the period 1400 to 1960. Since that time, several other studies have

tried to refine and further develop the techniques. The most notable of these and the one

that is used in this research is that of Mann *et al.* (1998) (henceforth MBH98).

Though there are still numerous problems with any reconstruction which relies on proxy

indicators, MBH98 provides rigorous calibration and verification (using the last century

of more reliable instrumental measurements), and the research not only results in global

or hemispheric annual values for temperature, but for the last several hundred years

provides estimates of regional-scale temperature change over time. Since a 'fingerprint'

of greenhouse gas-induced warming in the 20th and 21st century is a common detection

technique, it becomes increasingly important to look at the temperature patterns *before*

widespread industrialization. In this manner, we may establish a 'control' fingerprint or

series of fingerprints, from which to differentiate that resulting from greenhouse gases.

The MBH98 temperature reconstruction makes use of a widely distributed network of

seasonal or annual resolution proxy climate indicators (including ice cores, tree-rings and

coral - more details provided in the supplementary information of Mann *et al.*, 1998). The

individual indicators have been calibrated against the 20th century instrumental surface

temperature--represented in a reduced state in terms of its empirical orthogonal functions

(EOFs). This results in a reconstruction of global surface temperature patterns back in

time over the spatial domain governed by the coverage of 20th century instrumental record, based on the information in the proxy data network. The reconstructions are independently verified with the sparser instrumental surface temperature data available from 1854-1901 (and, in a few locations, with instrumental temperature records available more than two centuries back in time). The resolved spatial detail in the surface temperature reconstructions is dictated by the number of reconstructed surface temperature eigenvectors, which in turn is largely dictated by the coverage available from the proxy indicator network back in time. From 1820 to the present, based on the entire network of 112 indicators, 11 eigenvectors are skillfully resolved (approximately 70-80% of the variance), back to 1760, 9 eigenvectors are resolved, back to 1700 - 5 eigenvectors, and back to 1600, 4 eigenvectors are skillfully resolved equating to around 67% of the Northern Hemisphere temperature variance. (See Mann *et al.* 1998 for further details). Prior to 1450, by comparison, only 1 degree of freedom is resolved; just a single degree of freedom is adequate for estimating global or hemispheric mean temperatures [in fact, Mann *et al.*, 1999a extend the estimate of Northern Hemisphere mean temperature back to AD 1000 with evidence of significant reconstructive skill (Figure 3.1)], but not for any inferences into regional variability.

However, for the time period of interest here (1650 to 1850), the degree of spatial variance resolved in the instrumental record by the 4 to 11 eigenvectors retained in the reconstructions implies that coarse regional details, appropriate for comparison to the relatively low-resolution model simulation results that will be considered, are reasonably resolved. The time series of MBH98 temperature from 1650-1850 is shown in Figure 3.1

(inset). A period of cooler temperatures from around 1670-1720 is evident, and another from 1810-1830, followed by a brief warmer interval and then cooler-than-average temperatures from the mid 1800s to late 19th century. Temperatures then rose rapidly through the 20th century (Figure 3.1 top). The first cool period coincides with a depression in solar irradiance known as the Maunder Minimum (MM, described below) and the latter with the Dalton Minimum of solar irradiance. In the early 1800s there was also a brief increase in atmospheric turbidity from volcanic debris, particularly from a large eruption in 1815 (Tambora). A particular cold period can be seen around 1816-1820. However, the eruption of Tambora occurred in an already cool period, with the 4 years 1812-1815 having an average anomaly of -0.26 ºC, and those from 1816-1819 yielding an anomaly only five hundredths of a degree cooler at -0.31 ºC.

Results from the MBH98 investigation reveal a very significant and positive correlation (using a 200-year moving window) with solar irradiance (reconstructions of solar irradiance discussed below) in the global mean domain, from the mid-17th to early 18th century, corresponding to the cool period in their reconstruction and the MM in solar irradiance. Significant correlation is retained throughout the 19th century as generally increasing solar irradiance corresponds to a warming trend in MBH98, while correlations with greenhouse gases do not become significant until the moving window of correlation enters the 20th century. Correlations with the Dust Veil Index (DVI) indicating volume of atmospheric debris from volcanic eruptions, show some expected negative correlation in the window centered around 1830, the period containing the most explosive and significant eruptions. However, the significance of these correlations is marginal. Some

further discussion of potential forcing, other than solar irradiance, is also contained in chapters 1, 4 and especially 5.
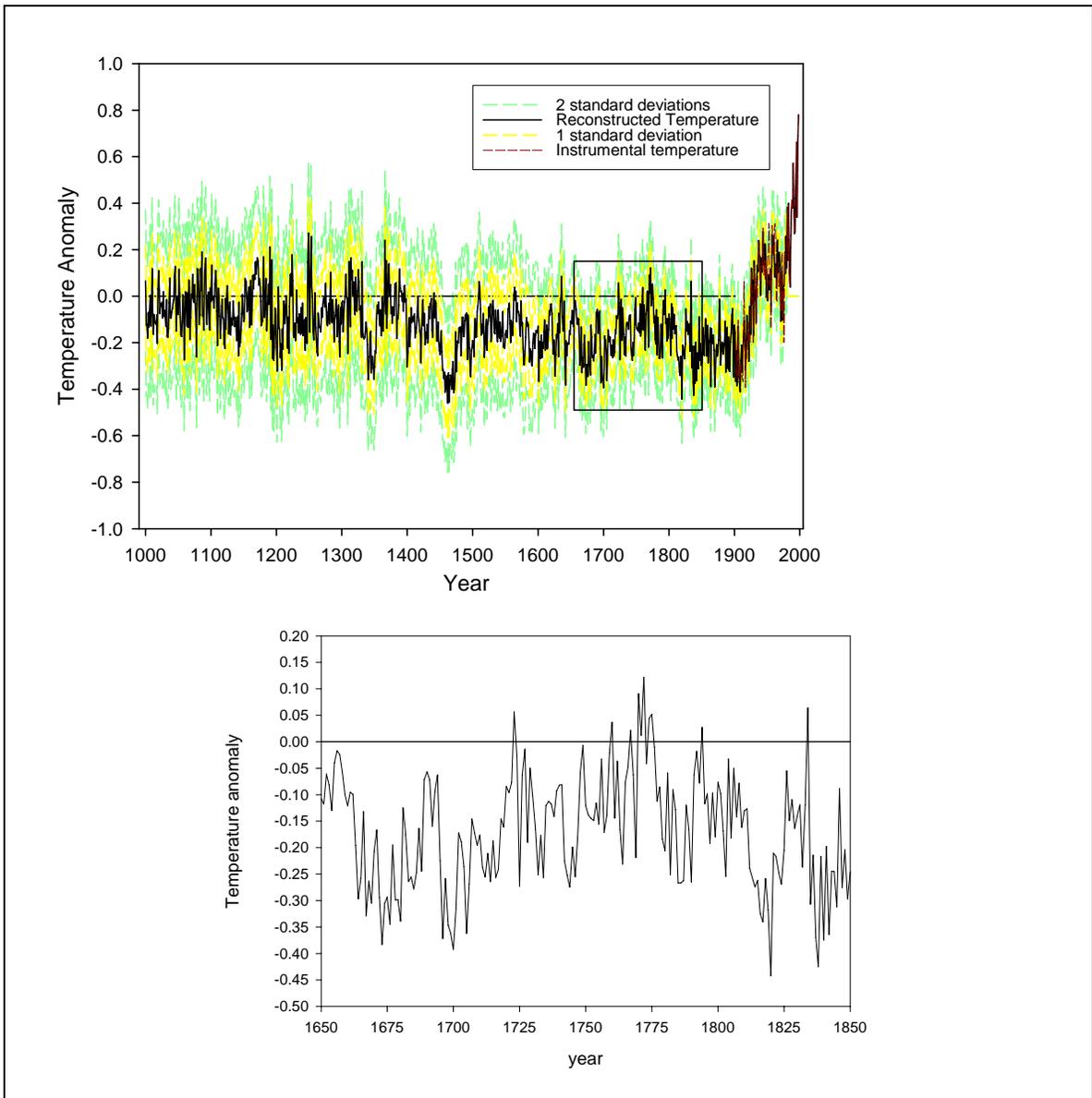
Figure 3.1 (a) 1,000-year reconstruction from Mann *et al.*, 1999 with 1 standard deviation error estimates (yellow) and 2 standard deviation error estimates (green). Dark red is the instrumental record. Square outline illustrates inset (b) reconstruction from 1650-1850.

3.2 Proxy-Based Solar Irradiance Reconstructions

There is a great deal of debate in the current solar physics literature regarding realistic estimates of long-term total solar irradiance (TSI) changes (see section 2.3.1 of TSI versus spectral irradiance). In this investigation, a reasonable upper boundary (Lean *et al.* 1995) and a lower boundary (Wang *et al.* 2005) long-term solar model will be analyzed.

The variation in TSI, as measured over the last two and a half decades by satellite-borne instruments is quite modest (~1-1.5 W/m^2 (or 0.1%) at the top of the atmosphere between peaks in the solar cycle (Willson, 1997, Fröhlich and Lean, 1998), fueling some uncertainty as to whether or not changes in solar irradiance are likely to have been sizeable enough to force significant climate variations. In order to answer this question, we must look at earlier records of solar variability so as to place these more recent measurements in some context. Since such direct measurements of solar variability are not available prior to the last 25 years, it is necessary to resort to indirect, less precise means of estimating solar irradiance variations prior to the recent era. Since the early 17th century, records of mean monthly sunspot numbers (as viewed from the Earth's surface through telescopes) are available as a proxy indicator of solar activity, and before these observations, cosmogenic isotopes trapped in ice cores can provide an alternative means of estimating changes in solar activity. Of interest in this study are three independent reconstructions of solar irradiance, which calibrate this information in different ways; the reconstructions of Lean *et al.* (1995), Hoyt and Schatten (1993) and Wang *et al.* (2005).

The Lean *et al.* (1995) (henceforth LBB95) reconstruction is the primary reconstruction for investigation in this analysis and combines several indicators of the sun's inconstancy to produce annual estimates of the solar irradiance back to 1610 (Figure 3.2, red line). The reconstruction parameterizes the effect of sunspot darkening and facular brightening during the 11-year Schwabe cycle and then calibrates this against the brief satellite record of direct irradiance measurements. (See section 2.1 for explanation of sunspots, faculae and solar cycles). LBB95 then extend this parameterization to 1610 using the longer observation history of sunspot activity. This yields a long-term change in irradiance of approximately 0.05% due to changing Schwabe Cycle amplitudes, with lower amplitudes during times of lower solar activity, including an absence of amplitude during the Maunder Minimum. Underlying the sun's 'active regions' or sunspot activity is a background network of 'ephemeral regions' or small bipoles, which arguably contributes substantially to solar irradiance variations. Through observations of other sun-like stars in apparently analogous states to Earth's 17th century non-cycling sun, LBB95 determined these stellar bodies appeared to have weaker overall emission than stars that are in cycling states and therefore a slowly varying, lower frequency component was also necessary. The reconstruction of this lower-frequency component was achieved by using measurements of ionized Ca emissions, a surrogate for magnetic variations in the sun. LBB95 interpret the Ca emissions from stellar bodies to suggest that during the Maunder Minimum (mid 17th Century), TSI may have been as much as 0.24% lower than the present mean. The LBB95 reconstruction is favorably compared to independent proxy measures of solar irradiance such as ^{10}Be and ^{14}C, but differs substantially from the solar

reconstruction of Hoyt and Schatten (1993) (described below), which is based on Schwabe cycle length rather than amplitude as in LBB95.

The solar reconstruction of Hoyt and Schatten (1993, henceforth HS93), used in the modeling study of Cubasch *et al.* (1997) discussed in chapter 4, uses the length (rather than the amplitude) of the solar-cycle as a proxy of solar irradiance variation. The resulting reconstruction of solar irradiance is greater in overall amplitude than the LBB95 estimate by approximately 20%, and lags the LBB95 reconstruction by ~20 years (Crowley and Kim, 1996). Doubts have been raised (Fröhlich and Lean, 1998) regarding the reliability of the latter means of estimating solar irradiance, due both to the underlying assumptions regarding solar physics, and the observation that the HS93 solar irradiance overestimates the actual irradiance increase recorded in calibrated satellite measurements. In this study, the alternative reconstruction of LBB95 is preferred given these concerns regarding a potential overestimation of irradiance.

Recent work by Wang *et al.* (2005) (henceforth WLS05) has argued for a smaller contribution from the background network of ephemeral regions, leading to a smaller Maunder Minimum-to-present change in solar irradiance. WLS05 do not rely on previous observations of non-cycling stars that indicated a lower overall emission, which they have been unable to reproduce, and instead employ a magnetic flux transport model to simulate the eruption, transport and accumulation of solar magnetic flux. The contribution of the background network results in a variation in overall solar irradiance (MM-to-present) that is only 27% of that of LBB95. Although this reconstruction does

not extend into the 17th century, WLS05's estimate is approximately one third the

magnitude of the LBB95 reconstruction with a post MM (1713 AD)-to-present change of
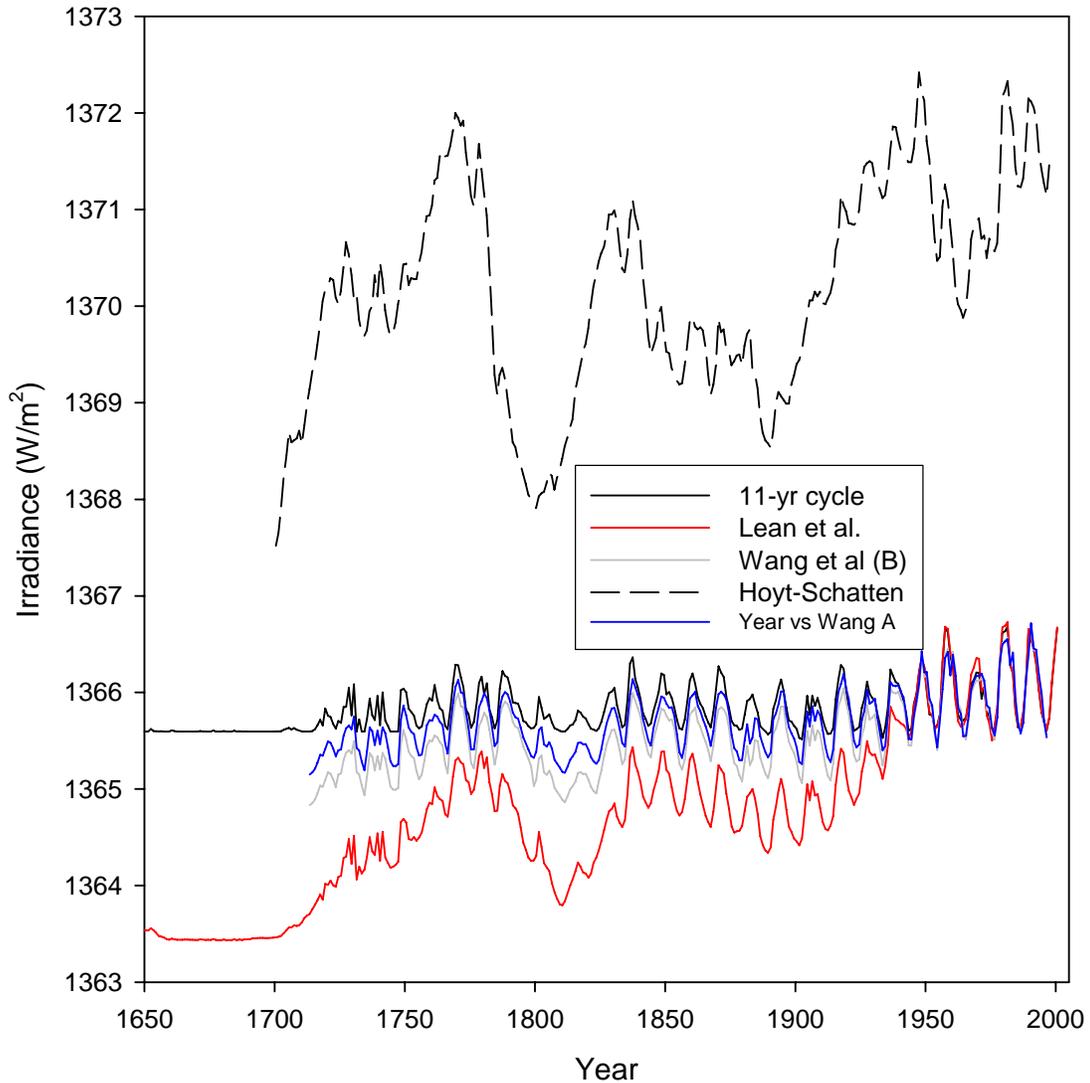
Figure 3.2 Comparison of various irradiance reconstructions used in this study. See text for more explanation on the different reconstructions. Wang *et al.* (A) refers to the reconstruction used herein. Wang *et al.* (B) is a reconstruction where an irradiance contribution from background ephemeral regions is included.

0.5Wm^{-2} compared to the around 1.5-2 Wm^{-2} for LBB95 over the same interval.

Although WLS05 also estimated some contribution from ephemeral regions (shown in

the gray line (Wang *et al.* (B)) in Figure 3.2), and the variance is somewhat larger than in

the 'no ephemeral region' case, the authors have less confidence in the fidelity of the

reconstruction when including the contribution from the background network. Therefore,

this analysis uses WLS05 without any estimated contribution of varying ephemeral

region output, and thus the variance can be considered a true lower bound estimate of

irradiance.

The most recent reconstruction of WLS05 produces the lowest estimate of long-term

solar irradiance variations and is likely based on more proven physical mechanisms,

though as recent as 2005, other reconstructions (i.e. Solanki and Krivova, 2005) indicate

a 2.2 Wm^{-2} increase in solar forcing from Maunder Minimum-to-present. Thus I have

chosen to use WLS05 as a lower bound estimate of solar change and LBB05 a reasonable

upper boundary to compare resulting climate sensitivity over the last several centuries.

3.3 General Circulation Model Simulations

Three distinct General Circulation Models (GCMs) of the climate are used in chapters 4

and 5 of this dissertation. Chapter 4 includes transient simulations from the Goddard

Institute of Space Studies (GISS) atmospheric GCM, model II (Hansen *et al.*, 1983) and

the Max Planck Institute (MPI) coupled ocean-atmosphere model (Maier-Reimer and

Mikolajewicz, 1992, DKRZ Modeling Group, 1993). Chapter 5 discusses results of the

GENESIS model 2.0 atmospheric GCM (Thompson and Pollard, 1995b).

3.3.1 Goddard Institute of Space Studies GCM

The Goddard Institute of Space Studies Atmospheric General Circulation Model is described in detail by Hansen *et al.* (1983). Both models I and II are described therein, however since only version II was used by Rind *et al.* (1999) in the experiments compared in chapter 4, the relevant specifications for that version are the only ones outlined here.

Transient experiments were run on the GISS AGCM version II, which has a horizontal surface resolution of 8°x10°. The top of the dynamical atmosphere is at 10mb, and the atmosphere has 9 levels. These are distributed with 2 layers in the stratosphere, 2 boundary layers and 5 in the remainder of the troposphere. The atmosphere is coupled to a mixed-layer 'Q-flux' ocean, indicating that heat transport is specified. Additionally, heat diffusion is allowed through the base of the mixed layer parameterizing heat uptake by the ocean. This atmospheric-only version of the model was used to avoid 'climatic drift' which must be corrected in most coupled models. It also eliminates confounding the climate response from solar forcing with North Atlantic Deep Water formation variations, which have also been cited as a possible reason for the temperature depression during the Little Ice Age (Rind and Overpeck, 1994). However, the lack of a coupled ocean limits any inferences into possible ocean dynamical responses or feedbacks to radiative forcing. The sensitivity of the GISS model is considered at the high end of the IPCC range of estimated sensitivities (IPCC 1996) at ~1°C per Wm^{-2}. It was determined by Hansen *et al.* (1983) that many of the climatologic features of the 4°x 5° surface resolution are

reproduced well in the coarser 8°x10° resolution, therefore it is more computationally efficient to employ the coarser surface grid while producing much the same result. Rind *et al.* (1999) notes that a newer version of the model with finer resolution slightly reduces sensitivity (~0.85°C per Wm^{-2}) and may therefore produce a slightly smaller climate response. Again, this newer version was not used, so as to maximize the computational efficiency permitting several 400-500-year long simulations in a reasonable time frame.

Model year 1 is the year 1500AD in the experiments discussed in chapter 4, minimizing the impact of model spin-up on the period of interest, beginning in the 17th century. When the model is started later, the cooling in the Maunder Minimum is smaller due to the inability of the model to spin-up sufficiently quickly. Rind *et al.* (1999) extended the irradiance reconstruction of LBB95 to 1500 AD by calibration with ^{10}Be and ^{14}C cosmogenic isotope data. Estimates of heat diffusion through the base of the mixed layer are also critical in this model. If heat diffusion is eliminated, the cooling response to the reduction in irradiance during the Maunder Minimum is twice as large (Rind *et al.* 1999).

3.3.2 Max Planck Institute GCM

The second model analyzed in chapter 4 is the MPI/Hamburg coupled ocean-atmosphere GCM (Maier-Reimer and Mikolajewicz, 1992; DKRZ, modeling group, 1993, Voss *et al.* 1997). The atmospheric portion of the model is the ECHAM3 model, which is based on the European Centre for Medium Range Weather Forecasting (ECMWF) model, with some necessary changes in the parameterization schemes to account for longer, climate simulations. The Ocean is the LSG (Large Scale Geostrophic) ocean circulation model.

The resulting coupled model is also fairly coarse in resolution (T21 truncation, giving an average resolution of about 5.5 degrees in latitude and longitude) with 19 levels in the atmosphere and 11 in the ocean. The equilibrium sensitivity to radiative forcing in this model is ~0.6°C/Wm^{-2}. A control run (integrated for 700 years) with fixed solar irradiance at 1365 W/m^{-2} showed that a drift correction needed to be applied to the model which artificially enhances the variability. It was therefore decided that two solar-forced model runs, using initial conditions 160 years apart in the control experiment, ought to be run to better isolate the solar signal from the increased noise (Cubasch *et al.* 1997). The solar-forced runs were begun in 1700 and integrated to 1992 using the solar irradiance estimates of HS93 scaled so that the average value of irradiance agreed with the fixed value of solar forcing for the control run. The model also employs a 20-year spin-up period to gradually reduce irradiance to the 1700 value since, the irradiance at 1700 is lower than the 'average'.

In comparison of these two models, both with each other and with the empirical data, we have focused only on the period since 1650 for which the most reliable data, both solar and temperature, are available and for which one or more of the model runs are available for comparison. It is unfortunate that the different model experiments employ two different estimates of irradiance (TSI) and the author acknowledges that this makes direct comparison between the model outputs difficult. However, since the models are based on internally consistent relationships between forcing and response, this still enables us to make a comparison between the models for the *sensitivity* of climate to solar forcing.

3.3.3 GENESIS

The GENESIS (Global ENvironmental and Ecological Simulation of Interactive Systems) model version 2.0 (Thompson and Pollard, 1995b), used in chapter 5, was developed at the Interdisciplinary Climate Systems (ICS) section of the Global and Climate Dynamics Division at NCAR. It is an atmospheric GCM with a horizontal surface grid resolution of 2°x 2° though this is independent of the horizontal resolution of the atmosphere, which is T31 (translating into 3.75° in latitude and longitude). The atmosphere is coupled to the land surface by a Land-Surface-Transfer (LSX) Scheme, which allows computation for the exchange of water mass, thermal energy and momentum. It has 18 vertical atmospheric layers and is coupled to a mixed layer 50m slab ocean and a dynamical sea-ice model. Sensitivity of the GENESIS is approximately 0.6ºC/Wm^{-2}, or in the middle of a range of model sensitivities estimated by the IPCC (1996).

Despite large improvements in version 2 versus previous iterations, some biases still exist in GENESIS, including cold biases in surface temperature over the Himalayan Plateau, possibly due to wintertime dynamical effects. Much of the Antarctic interior is also too warm in model 2.0 (up to 10ºC), though snow and ice budgets remain unaffected by this erroneous warmth due to the temperature remaining below the melting point throughout the year. Antarctic precipitation is realistic. Temperatures, after an elevation correction is applied, are still around 3ºC too warm over Greenland in both seasons. Zonal mean precipitation agrees well with present-day observations as does Northern Hemisphere

winter snow depth and fractional snow cover. In boreal summer, all snow cover melts

except on Greenland and trace amounts on sea ice and in the central Himalayas.

Arctic sea-ice is an important feedback mechanism in the experiments in chapter 5, and is

well-represented in the model, close to present day observations. As in modern

observations, circulation in the Arctic Ocean creates larger ice-thicknesses on the western

(Greenland-Canada) side of the basin and realistic ice advection occurs down the east

coast of Greenland. Given the prescribed ocean heat flux, and therefore warm water

advection northeastwards across the northern Atlantic, the Norwegian Sea area is

maintained as an ice-free region.

The specific experiments undertaken with the GENESIS model are described in chapter

5.

CHAPTER 4

CORRELATION AND SENSITIVITY OF TEMPERATURE TO SOLAR
IRRADIANCE: EMPIRICAL AND MODELED RESULTS

4.1 Introduction

As previously mentioned, the approximately 120-year long global instrumental climate

record is too brief to adequately capture the full range of variability in climate trends and

extremes. In this chapter, proxy reconstructions of climate and solar irradiance are used,

with the aim of empirically determining the sensitivity of global temperature to changes

in solar irradiance. Though a brief description is given here, further details of the climate

reconstruction are outlined in chapter 3, as are details of the reconstructions of solar

irradiance employed in this analysis, as well as discussion of rationale for their inclusion.

This empirical analysis is then compared to two transient GCM experiments, both of

which were forced with changes in solar irradiance. Details of the models used are also

available in chapter 3.

The multiproxy temperature reconstruction of Mann *et al.* 1998 (MBH98) and the solar

irradiance reconstructions of Lean *et al.* 1995 (LBB95) and Wang *et al.* 2005 (WLS05)

(details in chapter 3) are the proxy reconstructions used here. Integrations of two distinct

GCMs are also compared to the empirical analysis – the Goddard Institute of Space

Studies AGCM (Hansen *et al.* 1983, Rind *et al.* 1999) and the Max Planck Institute

AOGCM (Maier-Reimer and Mikolajewicz, 1992, DKRZ Modeling Group, 1993,

Cubasch *et al.*, 1997). The MPI model is forced by a third solar reconstruction published

by Hoyt and Schatten, (1993) (HS93), while the GISS experiment employs the LBB95 solar model.

The period of analysis for this investigation is the 201 years from 1650-1850. This period precedes any apparent anthropogenic influence on the climate and encompasses a considerable range of estimated solar output (approximately 4 Wm^{-2}) including the Maunder and Dalton Minima in solar irradiance. It is important to prevent the analysis period encroaching into the interval of potential anthropogenic interference in the climate signal in order to empirically fully separate the climate responses. Detection of solar influence in the 20th century is hampered by the similarity of its temporal trend to that of increasing greenhouse gases. Modeled sensitivity experiments comparing greenhouse-gas induced climate change to the response from solar irradiance changes are described in chapter 5. This chapter focuses only on the period prior to the industrial revolution and post-1650 for which the most reliable empirical data, both solar irradiance and climate, are available and for which one or more of the model simulations are available for comparison.

The focus of this analysis is not just on the global and hemispheric mean sensitivities to solar forcing, but the study will examine in some detail the regional patterns of response and their timescale dependence, and in so doing gain insight into the possible underlying dynamical mechanisms associated with the response of the climate to solar forcing. Description of the empirical data (solar irradiance and surface temperature reconstructions) used in the study is undertaken in chapter 3, as well as the model

simulations to which we compare empirical results. In section 4.2, there is discussion

regarding the empirical analysis and model simulations for the integrated spectrum of

forcing (or across all timescales), section 4.3 deals with similar analysis at the low

frequency (multidecadal-centennial) portion of the spectrum and 4.4 discusses the higher

frequency (decadal) response. In section 4.5, there is a summary and concluding

comments.

4.2 Correlation and integrated sensitivity

In MBH98 a significant relationship was established between the estimated Northern

Hemisphere mean surface temperature variations and the LBB95 solar irradiance

reconstruction during the past few centuries, including a significant relationship between

solar irradiance increases and the warming of the early 20th century, and a significant

warming from the MM to post-MM period. From the latter transition, MBH98 estimated

an approximate increase of 0.4°C in response to an approximate $4Wm^{-2}$ increase in total

solar irradiance, giving an approximate sensitivity of 0.4°C/W/m^2 (taking into account

the earth's cross-sectional surface area), similar to the global-mean response cited by

Cubasch *et al.* (1997). Here the MBH98 analysis is expanded considerably, considering

the patterns as well as hemispheric and global mean relationships between the empirical

(LBB95) solar irradiance forcing and MBH98 temperature reconstructions, examining the

timescale dependence of the spatial patterns of response and mean sensitivities, and

explicitly comparing empirical and model-based results. Since the publication of LBB95,

49

a new solar reconstruction (WLS05) has become available and has a significantly lower

estimate of irradiance variability from the termination of the MM to present. The

relationship between this WLS05 solar reconstruction and MBH98 is also compared,

though given that the solar reconstruction does not begin until 1713, compared to a 1650

inception for LBB95, and at least one of the model simulations was forced with LBB95

irradiance, LBB95 is the main focus of this analysis. To date no model experiment has

been undertaken using WLS05.

It is useful to use the more physically interpretable diagnostic of "sensitivity", rather than

just correlation statistics, to guide our interpretation of solar-climate relationships. The

sensitivity, *s*, as in Cubasch *et al.* (1997) can be estimated by linear regression,

$$s = cov(T,F)/var(F) \qquad (1)$$

Where *T* is the model or observed surface temperature (either global mean, or for a

particular spatial region or gridpoint), *F* is the forcing, and *s* has units of $°C/Wm^{-2}$. In the

case of solar forcing, we take $F = S * 0.7/4$ where *S* is the integrated total solar irradiance

(e.g., the "Solar Constant"), while *F* represents the associated average radiative forcing

incident upon the earth's surface, dividing through a factor of four accounting for the

earth's surface geometry and the half of the earth not receiving sunlight, and multiplying

by a factor of 0.7 accounts for the incoming short-wave radiation reflected back to space

from the earth's surface [assuming an albedo of 30%; note that Cubasch *et al.* (1997)

employ a somewhat high value of 36% albedo in their calculations. We here use a more

standard 30% albedo in all cases, including our assessment of the results of Cubasch *et al.* (1997) to provide a comparable sensitivity measure.

It is important to keep in mind that "sensitivity" defined in this fashion is an inherently linear concept, and becomes less applicable as non-linear dynamical feedbacks and processes become important. For the sake of our foregoing discussions, we will make the conventional assumption that the large-scale response of the climate system to radiative forcing can reasonably be approximated, at least to first order, by the behavior of the linearized system. It is also important to note that the sensitivity is based on correlation with global mean values of irradiance. It may be argued that a more appropriate correlation is one based on a latitudinally-weighted value of irradiance. If this were to be approximated via an acknowledged weighting convention (*i.e.* something closer to $\Delta S \cos \phi (1-A)/4$), the correlation is however the same. This is due to the correlation being independent of the amplitude of the curves.

Equation (1), allowing for lag between T and F in the covariance estimation is in fact a physically consistent means of estimated linear sensitivity to forcing under certain assumptions. It can be readily shown from energy balance considerations (White *et al.*, 1998 provide an especially lucid treatment) that the linear response of a thermodynamically diffusive medium (e.g. either the ocean or the land surface, averaged over some appropriate depth) to an oscillatory variation in solar radiative forcing incident at the Earth's surface,

$S = S_0 \cos (\omega t)$ *(2)*

is simply,

$$T = T_0 \cos (\omega t - \phi) \quad (3)$$

where,

$$T_o = S_0 \; \alpha \, (K^2 + \omega^2)^{-1/2} \quad (4)$$

with α depending only on properties (density, heat capacity, and skin depth) of the

medium, and the delay,

$$\phi = \tan^{-1} (\omega/K) \quad (5)$$

depends only on the frequency of the forcing ω and the dissipation timescale K^{-1}

In such a case, the sensitivity to the associated forcing,

$$s_S = T_0 / S_0 \quad (6)$$

is correctly yielded by (1), where the covariance of T and S is evaluated at its maximum

value with T lagging S by $\omega \Delta t = \phi$. While the sensitivity to an arbitrary solar forcing can

be expressed in terms of an integral over frequency of the frequency-dependent response

(4), it is instructive, as discussed below, to examine the frequency dependence of the

sensitivity.

Under further approximation (assuming that the periodicity of the forcing is very long

compared to the dissipitation timescale of the surface or near-surface response, and the

forced variations in temperature are small compared to the global mean surface

temperature of approximate 288K), the Stefan-Boltzmann relationship can be used to

yield the equilibrium ("blackbody") approximation $s_S = 0.3$ K/Wm^{-2} for the sensitivity

(see White *et al.*, 1998). Because this represents an equilibrium response, it will

overestimate the sensitivity if the timescale of the forcing is comparable to the dissipitation timescale of the system. It should also be kept in mind that the true sensitivity will be either greater than or less than this value if positive or negative dynamical feedbacks, respectively, are important at the global-mean scale of response. Cubasch *et al.* (1997) for example, using a coupled ocean-atmosphere model, estimate a global sensitivity s_S=0.4 K/Wm^{-2} , modestly greater than the blackbody response. Cane *et al.* (1997) argue that dynamical feedbacks involving tropical Pacific coupled ocean-atmosphere processes are not adequately represented in coarse-resolution coupled models, leading to a potential overestimation of the true sensitivity to radiative forcing in such models.

Alternatively, the low-frequency limit of (4) can be equated with the blackbody sensitivity, to yield an upper limit on the dissipation timescale K^{-1}. This value can then be used in (4) to estimate the frequency-dependent sensitivities semi-empirically, using estimated forcing amplitudes in different frequency bands. Applying the latter analysis to global (20°S-60°N) depth-averaged ocean temperature estimates during roughly the past 40 years, White *et al.* (1998) estimate a maximum dissipation timescale of $K^{-1} = 2.8$ years, implying sensitivity values s_S=0.22 K/Wm^2 on interdecadal (15-30 year periods), and s_S=0.15 K/Wm^{-2} on decadal (8-14 year) periods that are somewhat below the theoretical Blackbody value (s_S=0.30 K/Wm^{-2}). Applying linear regression of estimated irradiance and the same ocean temperature estimates (e.g., application of eq.1), on the other hand, they calculate sensitivities very close to the blackbody value (see Table 4.1). Both methods yield estimates of lags of 0-2 years, on decadal and bidecadal timescales.

I favor here the purely empirical approach (1) to estimating sensitivities, and subsequently apply this approach to both proxy-based surface temperature reconstructions and model simulation results. However, several caveats are essential to keep in mind in applying (1) to the estimation of sensitivity. Particularly, in the case of the empirical analysis, the regression estimates are more likely to provide a lower-bound approximation. Such caveats are discussed in more detail in Appendix A.

4.2.1 Correlations and significance

The significance of the domain-averaged (global mean) relationship between the empirical MBH98 temperature estimates and the LBB95 solar irradiance series during the 1650-1850 period and also between MBH98 and WLS05 is established. It should be noted that 'global mean' in the MBH98 series is dominated by the Northern Hemisphere due to the sparseness of data in the Southern Hemisphere. The lack of grid squares containing data at the highest northern and southern latitudes is however, not as problematic, since areal weighting affords them less importance as contributors to global or hemispheric means. Where there is a large discrepancy between the Northern and Southern Hemisphere, it is noted in Table 4.1. This only occurs in one circumstance. The correlation between the global mean temperature series and the LBB95 series over this interval is 0.26 at lag 0 which is significant at the 99% level based on a one-sided test, taking serial correlation into account. The value increases to a maximum of 0.35 at a lag of 14 years. For comparison, MBH98 estimated a correlation r=0.4 between the Mann *et*

al. (1998) Northern Hemisphere mean temperature series and the LBB95 solar irradiance series over the same interval, significant at the 99% level. This correlation was found to increase very modestly (by 0.03) to a maximum with temperatures lagging irradiance by 10 years (Mann *et al.*, 2000b). For a global mean correlation between WLS05 and MBH98, over the period 1713-1850, the result was 0.07, compared to 0.09 for LBB95 and MBH98 over the same interval. Maximum correlation was 0.13 at a lag of 3 years for WLS05 and MBH98. Significance over this interval was 80% at lag 0 and 94% for lag 3. The lower correlations as well as the marginal significance can be attributed to the shorter interval over which the analysis was undertaken. Though it is preferable to consider WLS05 further, given its probable improvement over LBB95 for the fidelity of its reconstruction, and indeed pattern correlations and sensitivity have been calculated (discussed shortly), yielding interesting results, the brevity of the reconstruction does not permit as thorough an investigation as is possible with LBB95, therefore the frequency analysis in section 4.2 is feasible using only LBB95 as the available irradiance reconstruction. Additionally, results from the sensitivity analysis between LBB95 and MBH98 (below) can be considered a conservative estimate compared to WLS05. As discussed in chapter 3, much of the difference between WLS05 and LBB95 is based on the amplitude of the reconstruction rather than the time history of variation. This will lead to a higher estimate of linear sensitivity with WLS05 compared to LBB95 (over the same period) given the larger effective response in the climate system, to a smaller overall forcing. Therefore, the analysis with LBB95 can serve as a lower bound estimate of global temperature sensitivity to solar forcing.

Patterns of significant response were estimated by correlating each grid point in a map of the reconstructed surface temperatures with the LBB95 solar irradiance reconstruction during the same (1650-1850) interval of time, and with WLS05 over the 1713-1850 period. Significance must in this case be established by a two-sided test since, unlike hemispheric or global mean temperatures for which a positive response can be required based on *a priori* physical considerations, the sign of the response spatially can in fact take on both negative and positive values (see e.g. Cubasch *et al.*, 1997; White *et al.*, 1998). Even with this more conservative criterion, the resulting LBB95/MBH98 correlation map exhibits broad coherent spatial regions of significant response, as shown in Figure 4.1 at zero lag, as well as at 14-year lag corresponding to the maximum correlation with global mean temperatures. The same is shown for WLS05 at lag0 and lag3 over the 1713-1850 period in Figure 4.2. Particularly in Figure 4.1, over the longer period, the patterns emphasize substantial positive correlations with continental interiors and large portions of the tropics, and low correlation (and even significant negative correlation) over substantial regions of the extratropical oceans. The potential significance of such regional variations is discussed later. Remarkably similar patterns can be seen in Figures 4.1 and 4.2, with the correlations in 4.2, over the shorter interval, having less power and significance, due in part to the fewer degrees of freedom and the absence of the known strong temperature-irradiance correlation during the termination phase of the Maunder Minimum, not available in the WLS05 solar reconstruction. Other differences include the absence of a negatively correlated area in the eastern Mediterranean and weak positive rather than negative correlations for western Greenland. The Equatorial Pacific also displays near zero correlation in the WSL05 analysis

compared to a generally positive correlation in the LBB95 results. Further discussion of these patterns is continued below.

Having established broad areas of significant apparent response of surface temperatures to solar forcing, focus is now instead on the more easily interpreted diagnostic of "sensitivity", as discussed earlier.
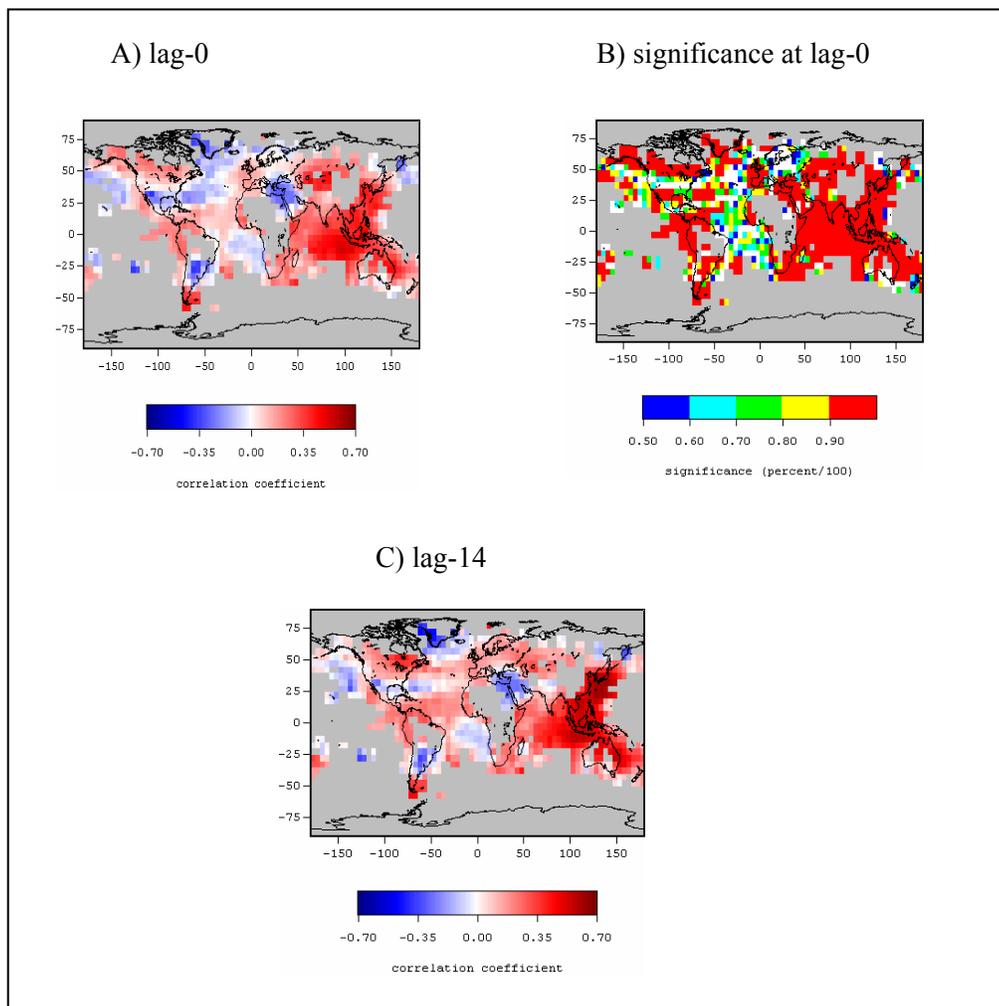
Figure 4.1. Correlation pattern between Mann *et al.* (1998) proxy-reconstructed surface temperature patterns and Lean *et al.* (1995) solar irradiance reconstruction for the period 1650-1850. Significance levels are shown at the 50-60% level (dark blue), 60-70% level (cyan), 70-80% in green, 80-90% in yellow and and >90% (red) based on a two-sided test taking into account serial correlation into account. Shown are both (a) correlation pattern

for lag=0 and (b) correlation pattern for lag=14 corresponding to maximum global-mean correlation. Missing data is masked with a gray background.

A) Lag-0 Wang

B) Significance at lag-0

C) Lag-3
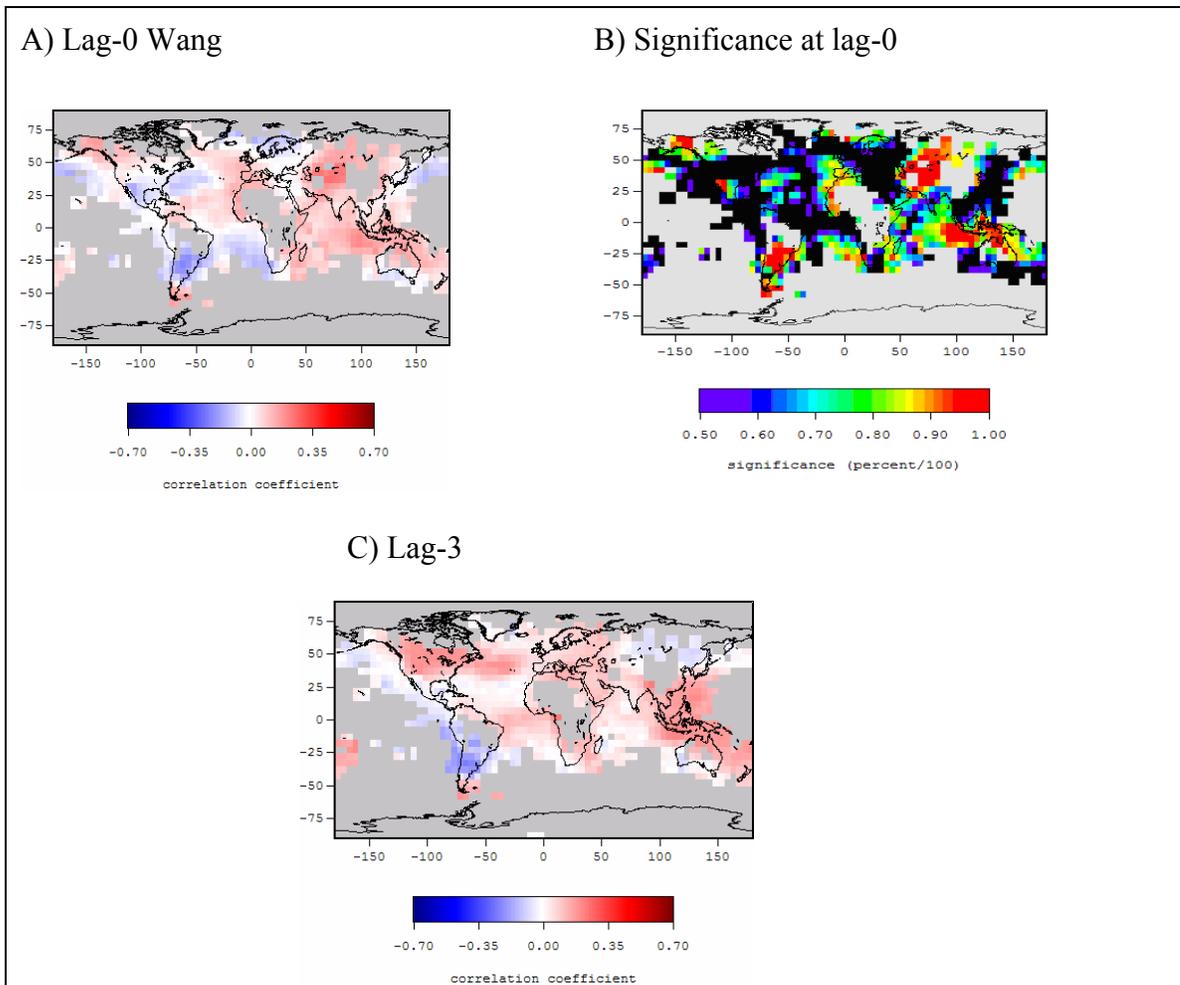
Figure 4.2. Correlation pattern between Mann (1998) proxy-reconstructed surface temperature patterns and Wang *et al.* (2005) solar irradiance reconstruction, for the period 1713-1850. Significance levels are shown at the <50% level (black), 50-60% level (dark blue), 60-70% level (cyan), 70-80% in green, 80-90% in yellow and and >90% (red) based on a two-sided test taking into account serial correlation into account. Shown are both (a) correlation pattern for lag-0 and (c) correlation pattern corresponding to maximum global-mean correlation (*i.e.* 3 years). Missing data is masked with a gray background.

Table 4.1 Empirical and model-based estimates of global mean sensitivity to Solar Irradiance Forcing for both integrated spectrum of forcing, and individual frequency bands. Indicated are (top) peak sensitivity over all possible delay or "lag" with respect to forcing and (bottom) value of delay (in years) at which maximum response is achieved

Maximum Sensitivity in degrees C/Wm^{-2}

	integrated	>40yr	9-25yr	8-15 yr	15-30yr
This study (1650-1850)	0.24 nh 0.25 sh 0.22	0.25 nh 0.26 sh 0.24	0.17** nh 0.19 sh 0.13		
CUB97	0.39	0.41	0.21		
RLH99	1.13	1.10	0.36		
WCL98			0.19*	0.15	0.22
WCL98[2]			0.28*	0.27	0.29
BBDY	0.30				
MBH99c	0.40				
This study (1713-1850 with WSL05)	0.15				

Lag corresponding to maximum sensitivity (in years)

	integrated	>40yr	9-25yr	8-15 yr	15-30y
This study (1650-1850)	10-14	15	1.5+/-1.5		
CUB97	1	1-2	6		
RLH99	10-15	0-15	3		
WCL98			2.2*	2	2.4
WCL98[2]			0.5+/-2.5*	0+/-2	1+/-3
BBDY	0				
MBH99c	10				
This study (1713-1850 with WSL05)	3				

CUB97 Cubasch *et al.* (1997) ECHAM coupled ocean-atmosphere model experiment
RLH99 Rind *et al.* (1999) GISS atmospheric model w/ specified ocean heat flux
WCL98[1] White *et al.* (1998) modern semiempirical [inverse energy balance calculation]
WCL98[2] White *et al.* (1998) modern empirical [linear regression of observations]
MBH98 Mann *et al.* (1998) - estimate of peak/trough Maunder Minimum change
MBH99a Mann *et al.* (1999a) - estimate of lag for maximum solar-temp correlation
BBDY Blackbody equilibrium estimate.

_____
*approximated by the average of estimates in the 8-15 and 15-30 year bands.
** Greater discrepancy between northern and southern hemisphere means

4.2.2 Global Mean Sensitivity

Empirical and model-estimated global mean sensitivities were estimated from linear

regression (i.e., application of eq. 1) of the Mann *et al.* (1998) empirical temperature

reconstructions and the Rind *et al.* (1999) GISS model temperatures against the LBB95

solar irradiance reconstruction, the MBH98 temperature and the WLS05 irradiance

reconstruction, and the Cubasch *et al.* (1997) MPI coupled model results against the

HS93 solar irradiance reconstruction, each as a function of lag. It is worth noting that

this quantity can be calculated either through an areally-weighted sum over the individual

gridpoint sensitivities, or, based on the global mean temperature series alone, owing to

the linearity of the regression (eq. 1) with respect to temperature. The global-mean

sensitivities for both model and proxy-based observations (including the "integrated

spectrum" and distinct multidecadal/century-scale and decadal bands, see subsequent

sections) are summarized in tabular form (Table 4.1)

The estimated global mean sensitivity at lag 0 is $s=0.17°C/Wm^{-2}$ for the empirical

analysis with LBB95, $s=0.36°C/Wm^{-2}$ for the MPI coupled model, and $s=1.06°C/Wm^{-2}$

for the GISS model. The sensitivity is $0.15°C/Wm^{-2}$ for WLS05 over the 1713-1850

period, more than twice the sensitivity of MBH98 and LBB95 over the same period,

indicating the lower variance of the Wang *et al.* irradiance reconstruction and therefore a

greater overall global sensitivity. In the case of the empirical analysis with LBB95, the

global-mean sensitivities take on their maximum value at a 14-year lag, the GISS model

at a 10-year lag and the MPI coupled model's maximum global mean sensitivity is at a lag of one year (see Table 4.1) relative to forcing, with a value s=0.24° C/Wm^{-2} for the empirical sensitivity, s=0.39°C/Wm^{-2} for the MPI coupled model, and s=1.13°C/Wm^{-2} for the GISS model. For the shorter analysis period, 1713-1850, the empirical result for LBB95 and MBH98 has a maximum value at a lag of 18 years (0.17°C/Wm^{-2}) versus 3 years (0.28°C/Wm^{-2}) for WLS05 and MBH98.

The sensitivity determined by the empirical estimate over the 1650-1850 time interval is remarkably similar to the empirical estimates of White *et al.* (1998) which are based on an entirely different (depth-averaged rather than surface temperature) dataset and a distinct, modern interval of time. It should nonetheless be kept in mind that the latter estimates are based on only decadal timescale relationships, rather than the long-term variations implicit in the former. We might thus (e.g., through equation (4)) expect less attenuation, and a modestly higher sensitivity at the longer multidecadal and century timescales. In fact, given the tendency of the empirical approach to underestimate sensitivity from the application of (1) due to the uncertainty in the actual forcing history (see discussion in Appendix A), our empirical sensitivity should not be considered inconsistent with the slightly higher value (0.4°C/Wm^{-2}) found in both the MPI coupled model experiment, and cited by Mann *et al.* (1998) based on the observed mean temperature change from the period encompassing the Maunder Minimum (late 1600s) to the late 1700s (a moderate solar maximum). The GISS model, however, exhibits a sensitivity that is substantially greater than any of the other model or empirical estimates.

This is discussed in more detail below. Figure 4.3 compares the empirical and two model global mean temperature variations during the 1650-1850 interval.
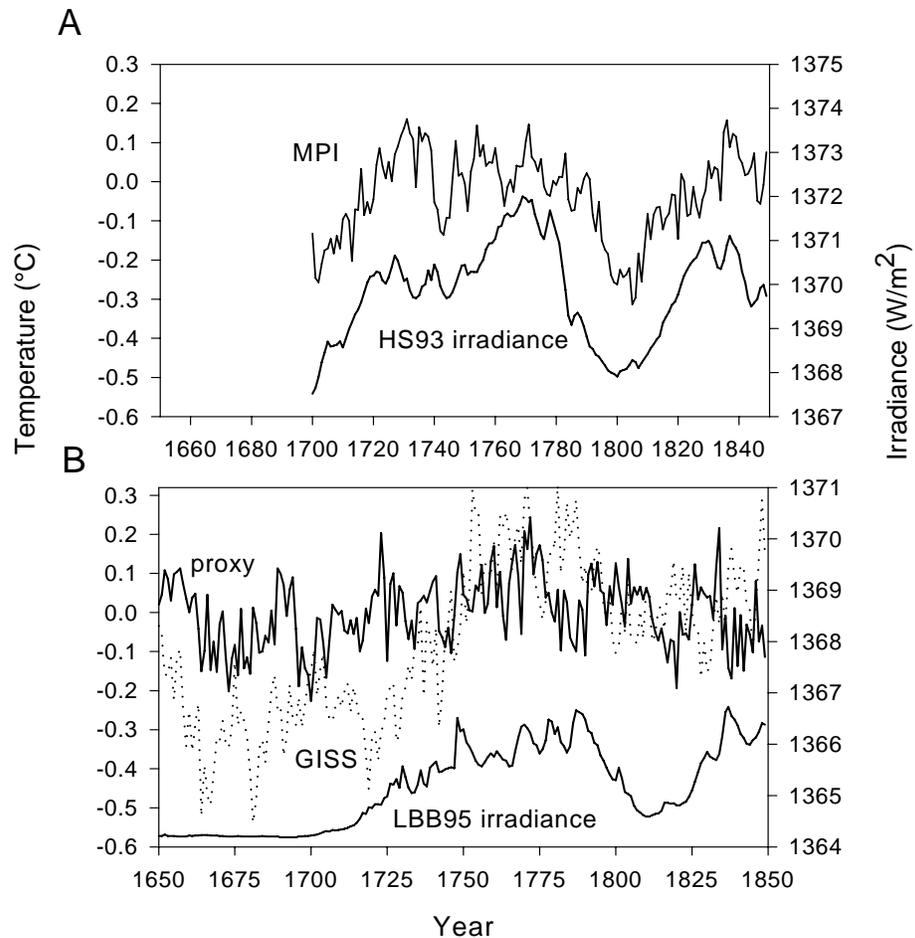
Figure 4.3. Temperature and solar irradiance time series. a) global mean temperature output of from the MPI model integration (average over the 2 independent integrations performed by Cubasch *et al.*, 1997) and Hoyt and Shatten (1993) irradiance reconstruction, with which the model was forced. b) proxy-reconstructed global mean surface temperature (solid line) (Mann *et al.* 1998), GISS simulated global mean temperature (dotted line) (Rind *et al.*, 1999) shown along with the Lean *et al.* (1995) irradiance reconstruction used in the GISS model simulation to calculate the empirical forcing relationships.

4.2.3 Spatial Patterns of Sensitivity

The spatial patterns of sensitivity provide greater insight into potentially important regional dynamics and feedbacks. Notable in the empirical sensitivity pattern over the full interval (1650-1850) (Figure 4.4, panel a) are the large regions of positive sensitivity in the extratropical continental interiors, and very small or even sizeable negative sensitivities in the North Atlantic and northern North Pacific (giving rise to a strong land-ocean contrast to the sensitivity pattern), as well as greater sensitivity in the tropical vs. extratropical oceanic regions. These features are remarkably mirrored in the solar "fingerprint" provided by the MPI coupled model experiment (Figure 4.4, panel b). The similarities are even more evident when the pattern of the low-frequency component of the response is isolated, and the time-evolving patterns of low-frequency response are examined (see section 4.3). Negative sensitivities in the subtropical South Atlantic found in the empirical pattern are not observed in the MPI model pattern.

Significantly, the relatively enhanced positive sensitivity in the western tropical Pacific `Warm Pool' (relative to the eastern and central Tropical Pacific) observed in the empirical pattern is not evident in the MPI model pattern. This latter feature may be associated with a feedback mechanism outlined by Cane *et al.* (1997) and Clement *et al.* (1996). These studies suggest that the imposition of a uniform external positive radiative forcing should reinforce the negative temperature gradient across the Pacific basin through the Bjerknes feedbacks; since the source of cool upwelled waters in the Eastern Pacific suppresses any initial warming, the negative temperature gradient is initially

enhanced. Once this enhanced gradient is established across the Pacific, an increase in trade wind strength exacerbates the gradient by enhanced upwelling in the east and a further increase in thermocline slope. Thus, according to these studies, we might expect the western Pacific to exhibit enhanced positive sensitivity to solar radiative forcing relative to the eastern tropical Pacific. Cane *et al.* (1997) suggest that such a feedback is not adequately represented in most coupled ocean-atmosphere models due to a dynamic coupling between the equatorial ocean and atmosphere which is too weak in such coarse resolution models, and thus presumably absent in both of the model simulations we have analyzed here. It is at least a plausible explanation for the observed discrepancy between the models and the empirical pattern. Further analysis is required before we can suggest this consistency with the Cane *et al.* argument is based on observable physical processes. It is also worth noting that this enhanced tropical sensitivity is found in a region which does not, in longer paleoclimate records (Holocene, Quaternary and Cenozoic), exhibit a great deal of sensitivity to external forcing. It is possible in this case that there are biases in the Mann *et al.* reconstruction. However, It is *also* possible, that the more recent past exhibits more variability in this region through such processes as ENSO, and that the boundary conditions of the last several hundred years allow a greater sensitivity than those prior to the last millennium. This apparent feature of the empirical sensitivity pattern at the very least, highlights the potential importance of tropical Pacific ocean-atmosphere dynamics in the climate response to radiative forcing, even if the true nature of that response is not readily yet agreed upon (e.g., Meehl and Washington, 1996; Cane *et al.*, 1997).

In contrast to the MPI model, the GISS model pattern (Figure 4.4, panel C) shows very

little regional distinction in the exhibited spatial pattern of sensitivity, but rather displays

ubiquitous positive sensitivity, except for a small area of the northern North Atlantic. The

GISS model also exhibits very little evidence of any significant evolution in the pattern of

response over time. The lack of a dynamical ocean in this case (see discussion in section

4.3) is almost certainly a limitation to any favorable comparison with observed patterns

of response.

A) lag-0 empirical sensitivity
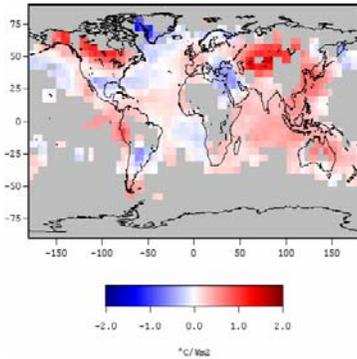
B) lag-0 MPI sensitivity
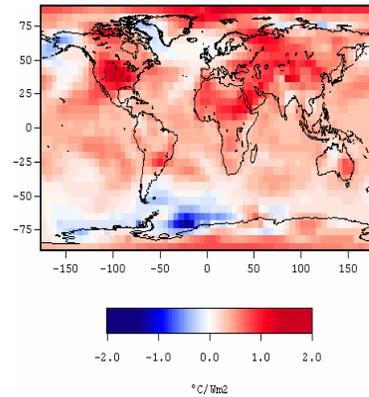
C) lag-0 GISS sensitivity
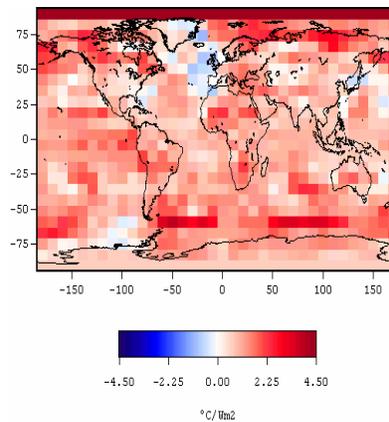
Figure 4.4. Maps of sensitivity of surface temperature with respect to solar irradiance forcing for the integrated spectrum of solar irradiance forcing at zero lag. a) empirical sensitivity pattern of Mann *et al.* (1998) surface temperature reconstructions against the Lean *et al.* (1995) solar irradiance series for the period 1650-1850. b) MPI simulated temperature sensitivity (Cubasch *et al.* 1997) relative to the Hoyt and Schatten (1993) irradiance reconstruction over the period of 1700-1992. c) GISS simulated temperature sensitivity relative to the Lean *et al.* (1995) solar irradiance reconstruction, over the same period (1650-1850) as in (a). As in similar following plots, regions without data are masked by a gray background, and the amplitude of the sensitivity is indicated by the color-scale provided.

Explicit comparisons of regionally-averaged surface temperature time series from the

MBH98 reconstructions with the LBB95 solar irradiance reconstruction (Figure 4.5) help

to illustrate some important regional relationships, and emphasize the apparent

enhancement of sensitivity at multidecadal and longer timescales (see section 4.3).

Shown are regional series of the western tropical Pacific (Figure 4.5, dashed line) which, as discussed above, exhibits a particularly large-amplitude apparent response to forcing, and of the tropical North Atlantic (Figure 4.5, solid line) which exhibits a response to the forcing that may be related (see discussion in section "B" below) to the resonance of solar forcing with an intrinsic multidecadal mode of the Atlantic that has been discussed elsewhere (Folland *et al.*, 1986; Delworth *et al.*, 1993;1997; Kushnir, 1994; Schlesinger and Ramankutty, 1994; Mann and Park, 1994; 1996; Mann *et al.*, 1995a; Mann *et al.*, 1998; Timmermann *et al.*, 1998; Delworth and Mann, 2000). The variations in this multidecadal mode of climate variability most strongly impacting the subtropical North Atlantic are well represented by the time series of one of the reconstructed eigenvectors (the 5th EOF) of the MBH98 reconstructions (also shown in Figure 4.5 (dotted line) for comparison) which can be thought of as representing one standing component of this evolving multidecadal signal (see Delworth and Mann, 2000).
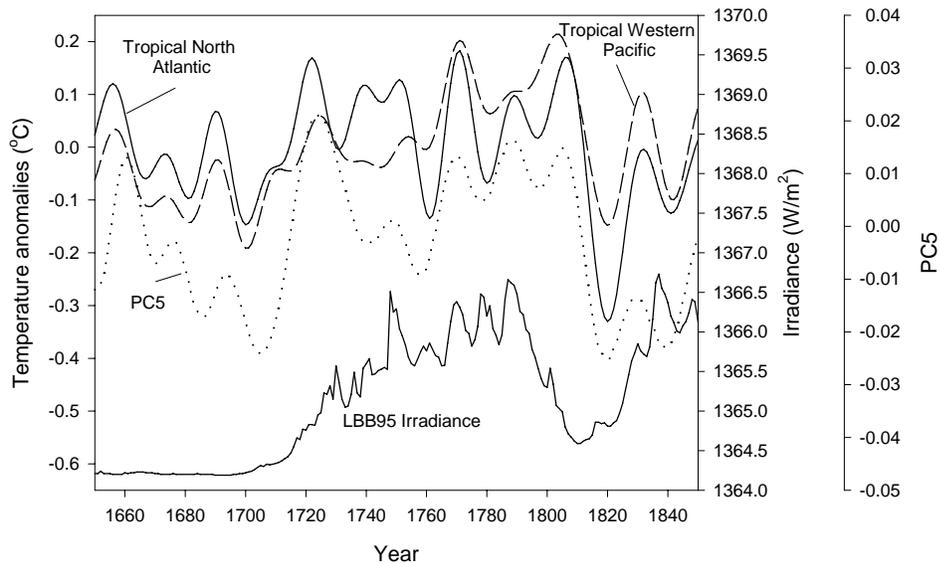
Figure 4.5. Comparisons of time series of Mann *et al.* (1998) reconstructed regional temperature variations (15-year lowpassed data are shown) and Lean *et al.* (1995) solar irradiance series. Temperature averaged over a selected area of the tropical western Pacific (dashed line) (112.5° x 137.5°lon by 22.5°N to12.5°S) and temperature average over a selected area of the tropical North Atlantic (solid line) (-67.5° x -27.5°lon by 22.5°N to 12.5°N). Also shown (dotted line) is the time-series of the 5th EOF identified in the Mann *et al.* (1998) study as representing the principal mode of multidecadal variability.

Figure 4.6 shows the pattern comparison between the calculated sensitivity of MBH98 to

the more recent solar reconstruction of WLS05 , and MBH98 to LBB95 over the period

1713-1850. Interestingly, the pattern depicted in LBB and MBH over the 1650-1850

period appears to remain quite robust despite the removal of the largest change in solar

irradiance (1650-1720) during the 1650-1850 period. This would seem to indicate that the

sensitivity over the 1650-1850 period is not dependent only on the depth of the Maunder

Minimum-to-present variation, but rather there is resonance with the climate at decadal-

to-multidecadal scales. Major differences between the full interval and the shorter period
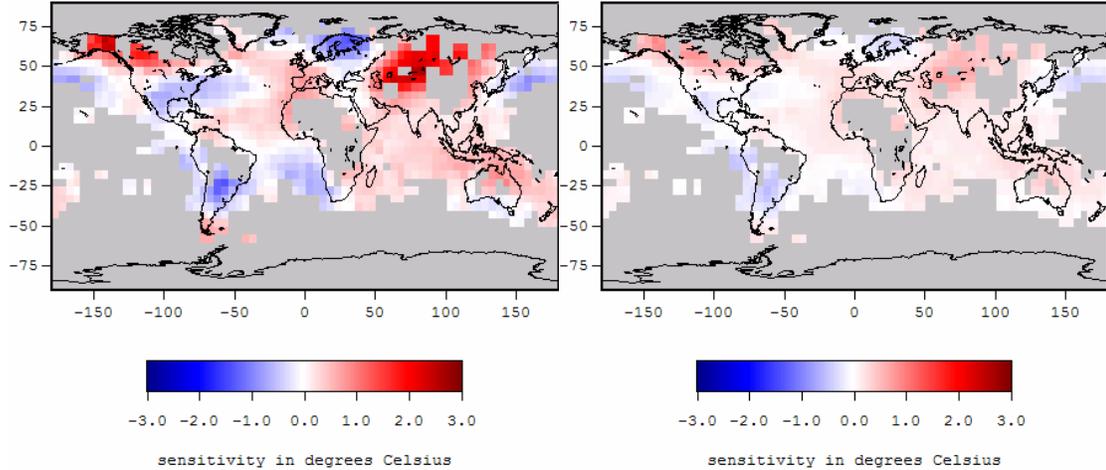
Figure 4.6. Maps of sensitivity of surface temperature with respect to solar irradiance forcing for the integrated spectrum of solar irradiance forcing at zero lag. Left panel: empirical sensitivity pattern of Mann *et al.* (1998) surface temperature reconstructions against the Wang *et al.* (2005) solar irradiance series for the period 1713-1850; right panel: empirical sensitivity pattern of Mann *et al.* (1998) surface temperature reconstructions against the Lean *et al.* (1995) solar irradiance series for the period 1713-1850.

for the LBB95 sensitivity analysis include a disappearance of the negative anomalies around Greenland and the eastern Mediterranean, a larger negative sensitivity in the western Atlantic and greater negative sensitivities through the eastern pacific. Overall, the sensitivity is somewhat diminished for the shorter period as would be expected. However, inspection of the Wang *et al.* solar reconstruction sensitivity calculations reveals a more intense pattern of sensitivity both compared to the same interval, and over the longer time period using LBB95. The land-sea contrast is relatively enhanced and negative sensitivities in the southern Atlantic, South America and the eastern and North Pacific are greater, along with a region of intense negative sensitivities in Scandinavia.

Positive sensitivities in the western Pacific are moderately reduced compared to the longer interval, but are still greater than in the shortened LBB95/MBH98 analysis.

A general increase in sensitivity for WLS05 compared to LBB95 over the same interval is to be expected given the reduced variance in the solar forcing but the same response in the climate. Additionally, the similarity of the patterns over the shorter period indicates the similar time history of forcing in the two irradiance reconstructions. The intensity and modification of the pattern from the shorter period relative to the longer interval is more similar to the lag0 pattern derived from filtering the time series and isolating the higher-frequency variations (see section 4.4 and Figure 4.9). This indicates the greater relative importance of decadal scale variability in the shorter time frame (given that much of the long-term trend has been removed, and the lower frequency variations thus attenuated) and its greater approximation to the dissipation timescale. Like the high frequency pattern evolution in Figure 4.9, the pattern is somewhat more spatially heterogeneous and temporally more variable as is indicated by the maximum lag at year 3, and therefore also indicative of a response to more time-evolving features. See section 4.3 for a more detailed discussion.

4.3 Low frequency (multidecadal-century scale) band

4.3.1 Global mean sensitivity

An analogous set of calculations to those described in section 4.2 was performed, instead focusing on sensitivity in the multidecadal/century-scale period band (timescales > 40 years). Equation (1) was applied using the 40-year low-pass versions of the temperature reconstructions and LBB95 solar irradiance series (the lowpass filtering was performed with a Hamming weights filter, favored for long, relatively stationary time series (see Stearns and David, 1988)). The global-mean low-pass-filtered series from the Mann *et al.* 1998 temperature reconstructions, MPI, and GISS simulations are shown in Figure 4.7. As discussed earlier, the GISS model exhibits clearly higher-amplitude variability in response to the specified low-frequency solar irradiance variations suggested by either the empirical or MPI model results. The GISS model's higher temperature variance can be attributed to the high equilibrium sensitivity of the model. The greater amplitude of the MPI model temperature variations relative to the empirical temperature estimates (see Figure 4.7), is in large part related to the use of the HS93 solar irradiance series to force the MPI model, rather than the lower-amplitude LBB95 series. Note (e.g. Table 4.1) that the sensitivities, for example, are reasonably similar. Signal-to-noise considerations may explain the small discrepancies between the actual low-frequency sensitivities. For example, the average of an ensemble of two realizations used by Cubasch *et al.* (1997) should increase the expected signal-to-noise ratio by a factor of $2^{1/2}$, leading to smaller expected random departures from the true sensitivity in the estimates (see Appendix A)

More significantly, unlike the empirical estimates, the solar-only forced runs are not influenced by other external climate forcings. For example, MBH98 show that explosive volcanism leads to significant cooling during the early 19th century which is not accounted for in the solar-only forced model runs, but clearly plays a role in early 19th century evident in the low-passed empirical temperature series. In contrast, the solar-forced model temperatures increase during the early 19th century in response to solar-only forcing. Mean global sensitivities (see Table 4.1) in this low-frequency band are , for the empirical case, 0.21 at zero lag, reaching a maximum value at a 15-year lag (0.25), and declining thereafter. For the MPI model lag-0 sensitivity at this frequency is 0.40, reaching a maximum lag at 1-2 years (0.41), while the GISS model experiment shows a lag-0 sensitivity value of 1.10 which changes barely at all over 15 years of lag, but which is actually highest at lag-0.
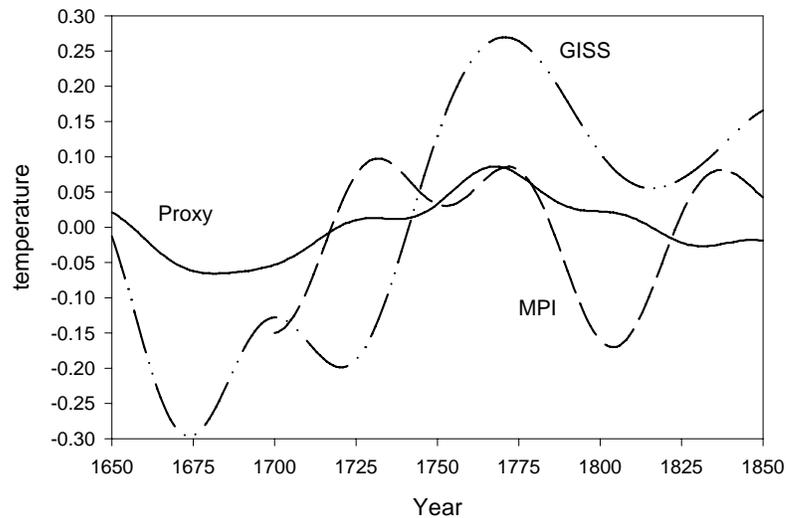
Figure 4.7. The 40-year lowpassed filtered global mean temperatures of the proxy reconstructed temperature (Mann *et al.* 1998), the MPI simulated temperature (Cubasch *et al.* 1997), and the GISS simulated temperature (Rind *et al.*, 1999). For the MPI temperature, an mean of the two runs was calculated, then filtered.

4.3.2 Spatial Patterns of Sensitivity

Figure 4.8 shows the empirical pattern of sensitivity at varying lag (0, 10, 20, 30) relative to forcing, spanning roughly one half period of the dominant timescale (about 90 years, i.e., the "Gleissberg Cycle") of low frequency solar forcing. As these lower-frequency variations appear to dominate the global-mean sensitivities (see Table 4.1), it should not be considered surprising that the pattern at zero lag is, by-and-large, similar to that determined (Figure 4.4) for the frequency-integrated response. It is worth noting, however, that the low-frequency band, dominated by timescales that are large compared

73

to the dissipation timescale of approximately 3 years (see earlier discussion), more

effectively captures the equilibrium or near equilibrium response of the system. Indeed,

the broad-scale features of enhanced land-sea contrast, and enhanced tropical SST

response are more clearly captured (Figure 4.8), while some of the more regionally-

heterogeneous features (e.g., the tropical south Atlantic negative sensitivities) present in

the integrated pattern of response, are far less evident in the low-frequency pattern of

response. The former lower-frequency features appear to be fundamental aspects of the

equilibrium response to solar forcing (e.g., as in Cubasch *et al.*, 1997), while these latter

higher-frequency features appear to be related to the resonance of solar forcing with the

intrinsic decadal modes of the climate system (see e.g. White *et al.*, 1998, and the

detailed discussion of the higher-frequency patterns of response in section "D", see also

Drijfhout *et al.* 1999 for further indications of solar forcing of internal climate

variability).

Both the warming of the continental interiors and the enhancement of the tropical Pacific

warm region become maximized, as does the global-mean sensitivity, between a lag of 10

and 20 years. After a lag of 20 years, the sensitivities in most regions of the globe begin

to decrease. The evolving features of the North Atlantic are particularly interesting, as

they appear to relate to a coupling of the forcing to internal multidecadal ocean-

atmosphere variability centered in the basin. Especially notable is the appearance of

negative anomalies in the North Atlantic through the evolution of the sensitivity pattern

(see e.g., Figure 4.8d), though negative sensitivities in the very northernmost parts of the

region (i.e., near Greenland) remain throughout the evolution of the forced pattern.
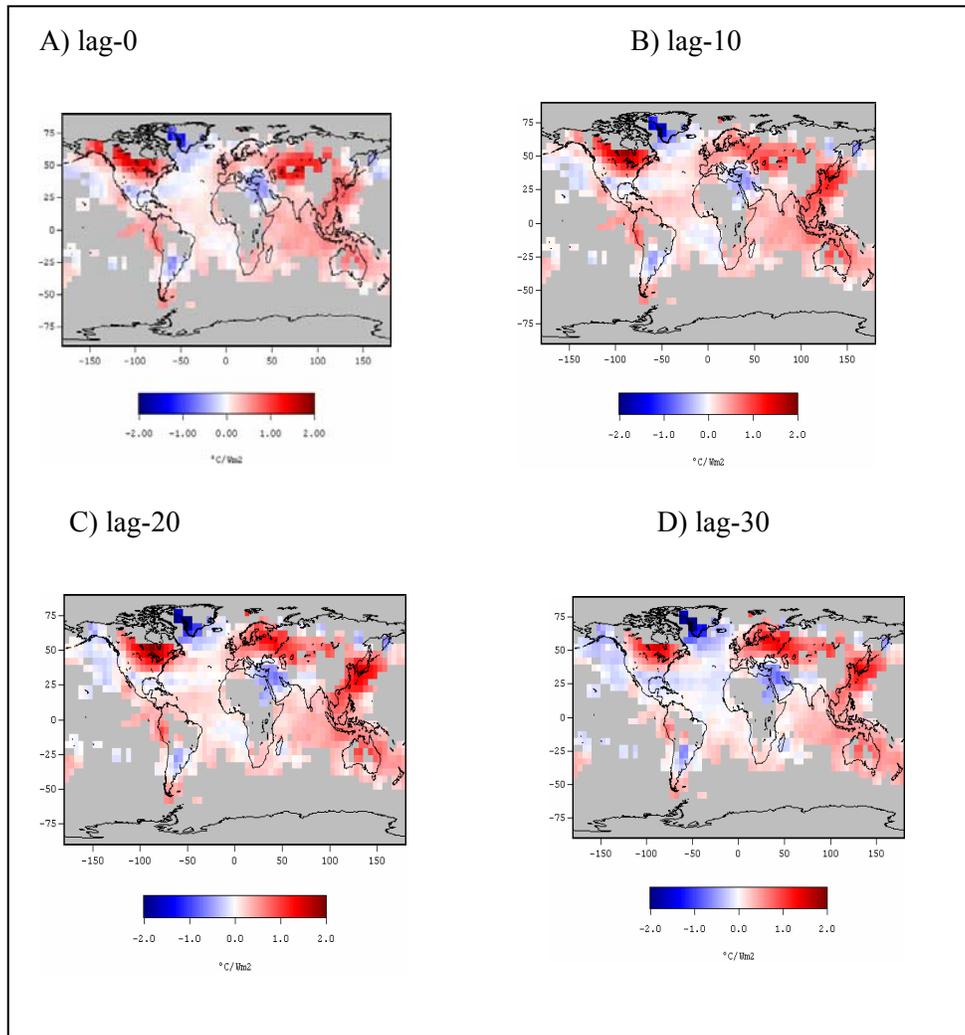
Figure 4.8. Sensitivity of Mann *et al.* (1998) reconstructed temperature with respect to Lean *et al.* (1995) estimated solar irradiance in the multidecadal/century-scale (>40 year period) band, at lags of (a) 0, (b), 10 year, (c) 20 year (d) 30 year. The temperature and solar irradiance series were filtered using a Hamming-weights lowpass filter with half-power cutoff centered at frequency 0.025 cycles/yr.

Cubasch *et al.* (1997) attribute such negative sensitivities to solar forcing in the North Atlantic at lags of 25-30 years directly to an anticorrelation (-0.8) of the meridional overturning of the thermohaline circulation with irradiance. During the strongest change in irradiance in the HS93 reconstruction (between 1770 and 1830), the overturning of the

thermohaline circulation (THC) was reduced by as much as 10% (Cubasch *et al.*, 1997), leading to a decrease in the Northward oceanic heat transport in the Atlantic, and a consequent reduction in sea-surface temperatures. These changes are associated with a negative sensitivity (about -0.4) in the northern mid-latitude temperature that is maximum at a lag of 25 years in the MPI coupled model, and is closely mirrored in the empirical pattern at a lag of 30 years (Figure 4.8, panel D). This scenario is, in certain respects, similar to scenarios that have been suggested under conditions of greenhouse-induced warming (Manabe and Stouffer, 1994; Stocker and Schmittner, 1997). This same model (see Timmermann *et al.*, 1998), as other models (e.g., the GFDL coupled model--see Delworth *et al.*, 1993;1997; Delworth and Mann, 2000) appear to exhibit variability in the North Atlantic thermohaline circulation at multidecadal timescales due to intrinsic ocean-atmosphere processes, excited from stochastic forcing alone without the need of any external pacing.

The evolution in the North Atlantic exhibited by the empirical low-frequency sensitivity pattern to solar radiative forcing suggests a scenario in which this intrinsic multidecadal mode of variability may indeed resonate with solar radiative forcing. The pattern at lag 30 years, closely resembles a particular phase (the reverse of the "120 degree" phase pattern shown in their Figure 4.5 and Figure 4.8) of both the empirical (as isolated in the MBH98 surface temperature pattern reconstructions) and modeled (as observed in long integrations of the GFDL low-resolution coupled ocean-atmosphere model) 60-70 year timescale signal discussed by Delworth and Mann (2000) (for comparison, this represents roughly 90 degrees in phase, or 15 years, subsequent to the peak warmth in the

subtropical North Atlantic as shown in Figure 4.4). In the model, this phase of the signal

is indeed associated with a minimum in the THC index. These observations thus suggest

a resonance scenario in which solar forcing may impose this favored phase of the natural

multidecadal pattern and, in doing so, phase-lock the near-term evolution of the signal, at

least during those (e.g., late 18th century and early 19th century) during which the

multidecadal solar variations are particularly pronounced. In the absence of such high-

amplitude forcing, we would expect the multidecadal pattern to nevertheless exhibit free

oscillatory behavior (see Delworth *et al.*, 1993;1997; Timmermann *et al.*, 1998; Delworth

and Mann, 2000). Such a scenario is consistent with the apparent partial phase-locking of

the solar variations and multidecadal Atlantic SST variations shown in Figure 4.5

(bottom).

The somewhat weaker negative sensitivities in the North Pacific evident in both the

empirical and MPI coupled model sensitivity pattern could also be associated with the

dynamical mechanisms outline above. Timmerman *et al.* (1998), using the MPI coupled

model, argue that there is a direct atmospheric teleconnection between multidecadal

North Atlantic SST anomalies, arising from changes in the strength of the thermohaline

circulation, and atmospheric circulation patterns influencing SSTs in the North Pacific.

Delworth and Mann (2000) confirm a similar, though substantially weaker,

teleconnection into the North Pacific in the GFDL model and argue (as in Mann *et al.*,

1995a) for a significant Pacific expression of multidecadal variability over the past few

centuries based on long-term proxy data and proxy-reconstructed temperature patterns.

The observational study of Minobe (1997) confirms the existence of such multidecadal

oscillatory behavior in the Pacific region and western North America. Some of the

enhanced warmth in Europe and the United States, and cold anomalies in Greenland and

in the Middle East, appearing to peak at 30-year lag in Figure 4.5, are consistent with the

observation of multidecadal/century-scale variations in the NAO (see e.g., Appenzeller,

1998), that appear to be tied, at least in part, to the multidecadal North Atlantic signal

discussed above (Delworth and Mann, 2000).

4.4 High-Frequency (Decadal) Band

4.4.1 Global-Mean Sensitivity:

In order to isolate the surface temperature sensitivity to solar irradiance forcing at decadal

timescales, the temperature and irradiance were bandpassed in the 9-25 year period range

(using, as in section 4.2 a Hamming weights filter), and the sensitivity estimated through

equation (1). The moderately lower sensitivities in the decadal band ($s=0.17$), are

consistent with an attenuated response relative to the lower-frequency sensitivities

established in section 4.2, expected from equation (4) since the timescale of forcing is in

this case more comparable to the dissipitation timescale. The resulting sensitivity is quite

close to that obtained by White *et al.* (1998) by their semi-empirical approach, averaged

over a similar range of decadal-to-bidecadal timescales (see Table 4.1). The amplitude of

the empirical sensitivity is nearly constant from lag 0 years (0.17) to lag 3 years (0.13)

constraining the lag of the response to between 0 and 3 years (e.g., 1.5 +/- 1.5 years), again consistent with the results of White *et al.* (1998).

4.4.2 Spatial Patterns of Sensitivity:

Figure 4.9 shows the empirical pattern of sensitivity at varying lag (0, 3, 6, 9, and 12 years) relative to forcing, spanning roughly one-half period of the lower-frequency (22 year) timescale that dominates the 9-25 year period band. The pattern is far less dominated by the broad patterns evident at multidecadal timescales, which resemble the expected equilibrium patterns of response. Instead, more spatially heterogeneous patterns of negative and positive sensitivities are evident. At zero lag, for example, substantial negative sensitivities are evident over Europe, the southeastern U.S./subtropical North Atlantic, and tropical South Atlantic (leading, in part, to the expression of similar features in the integrated pattern of response shown in Figure 4.4), while substantial positive sensitivities are observed in the tropical North Atlantic, tropical Pacific, and central Eurasia. The pattern of response is, in fact, characterized by strongly time-evolving features (compare panels A,B,C,D,and E in Figure 4.9) that are quite reminiscent of established decadal modes of the climate, including in the Atlantic region, the North Atlantic Oscillation (NAO) (Deser and Blackmon, 1993; Hurrell and van Loon, 1997) and tropical Atlantic Dipole (Tourre *et al.*, 1999 and references therein) patterns dominated by quasidecadal timescales, and in the Pacific region, ENSO-like tropical and extratropical patterns (e.g., the Pacific North American or "PNA" pattern) of variability (see e.g., Trenberth, 1990; Mann and Park, 1993;1994;1996; Trenberth and Hurrell,

1994; Graham, 1994; Latif and Barnett, 1994; Zhang *et al.*, 1997; Miller *et al.*, 1998; White and Cayan, 1998) dominated by roughly bidecadal timescales. It is notable that the decadal Atlantic variability in the reconstructed temperature patterns are largely described by the pattern of the 3rd eigenvector (see MBH98), while the interdecadal ENSO-like variability in the MBH98 reconstructions are discussed in detail by Mann *et al.*, 2000a. The finer decomposition into quasidecadal and bidecadal components of response is clearly of value, and the reader is referred to White *et al.* (1998) for such an analysis in the context of the modern climate record.

Quite analogous to the discussion in section 4.2 of a possible resonance between low-frequency solar forcing and a natural multidecadal mode of the climate system, it would thus appear that the regional patterns of sensitivity to decadal timescale solar forcing (which often appear far more impressive than the modest global-mean response) may in fact result from the resonance of the forcing with the internal decadal modes of the climate system. This observation has indeed been made with regard to the instrumental record. Mann *et al.* (1995b, see also Mann and Park, 1996) find evidence that intrinsic large-scale quasidecadal patterns of climate variability appear to resonate with the 11-year solar cycle during periods of unusually high solar cycle amplitude (e.g., the past few decades), but not during periods of lower-amplitude variability (e.g., the earlier decades of the 19th century) during which the same mode may exhibit largely stochastically excited internal variability. White *et al.* (1998) in fact observe a strong relationship between solar variability and the intrinsic decadal modes of the climate system during the past few decades. Cook *et al.* (1997) review, and demonstrate strengthened new

dendroclimatic evidence, for a phase locking of 22-year timescale solar variations, and large-scale atmospheric patterns of continental drought in North America, during the past few centuries. Evidence thus appears to be mounting for the notion that decadal timescale solar forcing excites a response of the climate largely through such a resonance with internal modes of variability. It is possible, (see discussion in Mann and Park, 1999) though far from certain, that this is caused by the stratospheric modulation of ozone concentrations (Haigh, 1996) or cloud-electrification processes (Tinsley, 1988) associated with solar variability. Significantly, however, such feedbacks do *not* appear to be significant at the global-scale since, as discussed above, the spatial patterns of sensitivity average out to global-mean sensitivities in the 9-25 year band that appear to fall short of the (no-feedback) blackbody estimates.
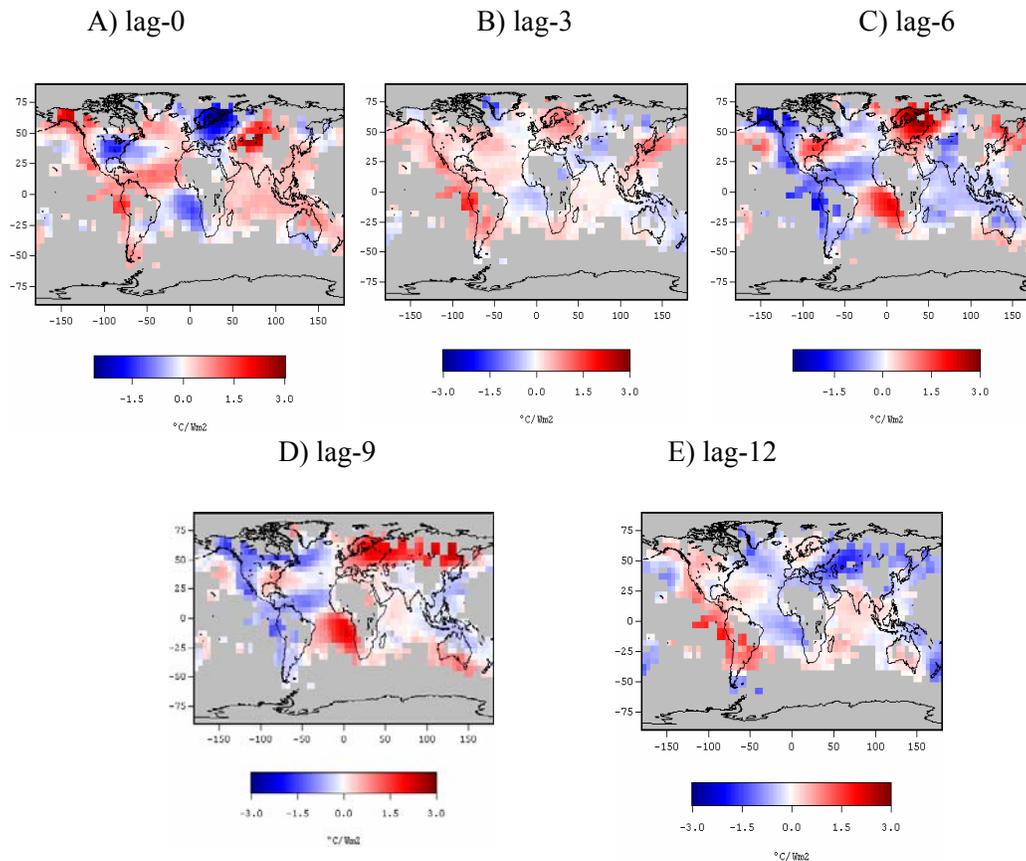
Figure 4.9. Sensitivity of Mann *et al.* (1998) reconstructed temperature with respect to Lean *et al.* (1995) estimated solar irradiance in the decadal (9-25 year) period band, at lags of (a) 0, (b) 3 year, (c) 6 year, (d) 9 year, and (e) 12. The temperature and solar irradiance series were filtered using a Hamming-weights bandpass filter with half-power boundaries centered at frequencies of 0.04 and 0.11 cycles/yr.

4.5 Summary and Discussion

Empirical inferences into solar irradiance forcing are possible during an extended interval of time prior to widespread industrialization, 1650-1850, using indirect information to reconstruct both large-scale surface temperatures and solar irradiance forcing estimates. Comparisons of these empirical estimates of climate variability and forcing provide insights into solar influence on climate which, though not without their sources of

uncertainty and limitations, are essentially immune from the typical contamination by anthropogenic influences. This latter feature makes such estimates an important independent check on any empirical inferences based on modern solar-climate relationships. These empirical results lead to an estimate of global-mean sensitivity to solar radiative forcing very close to the Blackbody value (approximately 0.3 K/Wm^{-2}), but certainly not inconsistent with the moderately higher values (approximately 0.4 K/Wm^{-2}) of sensitivity estimated in the MPI coupled ocean-atmosphere solar-forcing experiment analyzed, taking into account the likelihood that the sensitivity is underestimated due to uncertainties in the empirical long-term solar forcing estimates.

Regional patterns of response in the observations, moreover, match in many respects, those isolated in the coupled model response to solar forcing, particularly with regard to the low-frequency variations. This includes the basic signatures of enhanced positive sensitivity in extratropical continental interiors, low/negative sensitivity in oceanic regions (together constituting a pattern of strong land-ocean contrast), and relatively enhanced SST sensitivity in the tropics. The complex and delayed empirical pattern of response of the North Atlantic to solar forcing appears to be mirrored in the coupled model response, resulting from a spinning-down of the thermohaline circulation (and consequent decrease in Northward oceanic heat flux) in response to positive radiative forcing. There appears to be a relationship between this response, and possible resonance with an internal mode of variability in the North Atlantic that results from multidecadal timescale coupled ocean-atmosphere mechanisms. There is less similarity in both the mean estimates and spatial patterns of empirical sensitivity in the case of model

experiments employing specified ocean heat transport, emphasizing the apparent importance of ocean dynamical processes in explaining observed patterns of sensitivity, although model coarseness may limit inferences in this case. In contrast to the low-frequency patterns, the pattern of response at decadal timescales appears to be dominated by a resonance of known modes of decadal climate variability with solar forcing, with relatively modest sensitivities at the global-mean scale.

Finally, there is some evidence in the empirical patterns of response of a dynamical feedback in the tropical Pacific which has been hypothesized as a potentially important negative feedback to positive radiative forcing (Cane *et al.*, 1997), not captured in current generation coupled models. Accounting for the absence of such a feedback in the model could potentially bring both the global mean and pattern of the model sensitivities even more closely in line with the empirical estimates.

CHAPTER 5

GLOBAL CLIMATE SENSITIVITY TO SOLAR IRRADIANCE IN
COMPARISON TO OTHER POSSIBLE FORCING MECHANISMS: A SUITE
OF MODEL SENSITIVITY TESTS.

5.1 Control simulations and experiment design

Following the conclusions of chapter 4, (discussed also in chapter 6), it is appropriate to

consider how the climate sensitivity to solar forcing compares to that of other probable

forcing mechanisms over the last several centuries. Of particular interest is whether

significant solar influence is sustained in the industrial era, wherein increased

atmospheric greenhouse gases are known to have impacted climate behavior (*e.g.*. IPCC,

2001, Mann *et al.* 1998).

Differentiating between solar and greenhouse gas forcing of the surface climate in the

modern period poses a particular problem of detection. Both solar and greenhouse gas

forcing is globally distributed and of the same sign, thus having no *a priori* regionally

distinguishing features. Although the magnitude of the forcing is different, the likelihood

of exacting similar feedback mechanisms is substantial.

One approach to investigating the relative climatic influence of these and other forcings,

includes controlled simulations of the climate. Numerical climate models provide the

ability to analyze the manner in which the various features of the climate system respond

to specified changes in boundary conditions and/or forcings. The results of complex

interactions of climate system processes can be compared among different experiments

with different forcing mechanisms, leading to a more thorough understanding of climate behavior under specified conditions.

In this chapter, several equilibrium sensitivity experiments are compared. Rather than attempting to recreate the exact time history or 'transient' response to forcing, these experiments are designed to capture the sensitivity of the climate, or the strength and direction of response to a particular stimulus, in this case, globally-distributed external climate forcing. Rarely, if ever, is the observed climate able to reach complete equilibrium, given the multiple time frequencies over which forcing occurs and the dissipative timescale of the climate system. In chapter 4, the frequency dependence of sensitivity to solar forcing was discussed and results showed that more power existed at the lower frequency portion of the spectrum (>40 years). Given that the empirical global mean response to solar forcing is dominated by the low-frequency portion of the spectrum, which is dictated by timescales that are large compared to the dissipation timescale of approximately 3 years (see discussion in section 4.2), an equilibrium response to solar forcing is adequately approximated in the climate system prior to the 20th century. It is therefore not unreasonable to draw conclusions regarding the actual climate history from equilibrium experiments forced by changes in solar irradiance. However, this is not true with respect to the rapidly changing concentration of greenhouse gases in the atmosphere. Primary focus here will be on internally consistent sensitivity comparisons between solar and other realistic specified forcing.

The model employed in this study is the GENESIS Atmospheric General Circulation Model (described in detail in chapter 3). It is a high resolution model, compared to many GCMs, with a 2º x 2º horizontal surface resolution, allowing a more reasonable surface topography and 3.75º x 3.75º atmospheric resolution. Its sensitivity is approximately 0.6ºC/Wm^{-2}, or in the middle of a range of IPCC estimates (IPCC, 2001).

There are several caveats that are important to consider for the GENESIS model in this analysis. The absence of a fully coupled dynamical ocean prevents conclusions being drawn about ocean dynamical responses or feedbacks as a result of specified forcing. While the inclusion of a fully coupled ocean would be ideal, the computational expense of running a high resolution model (such as GENESIS) in a fully coupled mode would hinder the completion of the suite of model experiments here described. The main priority in these experiments is the self-consistent intercomparison of atmospheric sensitivity of separate and integrated forcing mechanisms. However, a fully coupled sea-ice model, allowing for dynamic sea-ice response, accounts for an important feedback mechanism often absent in AGCM sensitivity tests.

Furthermore, possible feedbacks that have been ignored in these experiments include ozone-related changes in the lower stratosphere cited as a possible influence on tropospheric temperatures (Haigh, 1994, 1996), though more recently, Rind *et al.*, (2004) have concluded that the ozone indirect forcing is small. In order to incorporate this feedback, a spectrally varying solar irradiance forcing must be included (since ozone responds to the UV portion of the spectrum) and the complex photochemical response of

ozone concentration must be parameterized or treated explicitly. It was decided that due

to the likely small effect of ozone feedbacks on radiative forcing (*e.g.*. Larkin *et al.*

2000), and the potential for parameterizations of the ozone effect to fail to fully capture

the dynamic response, as well as recent disagreement concerning the overall magnitude

of irradiance changes (and therefore the magnitude of UV changes, which have increased

more than three times as much as the visible portion of the total spectral irradiance since

the Maunder Minimum (Lean 2000)), a more simplistic irradiance estimate was adequate.

Svensmark and Friis-Christensen (1997) have suggested that there is also a global cloud

feedback due to modulation of cosmic rays by changes in solar activity, in phase with the

solar cycle (increased solar activity reduces the cosmic ray flux, and is speculated to

reduce ions in the atmosphere and hence cloud droplet formation, diminishing global

cloudiness). This would also lead to a positive feedback enhancing the effect of increased

solar irradiance. Sun and Bradley (2002) in a re-evaluation of the proposed relationship

used longer datasets and found the feedback to be questionable. Nevertheless, by ignoring

both of these potential positive feedback mechanisms, we may consider our global mean

temperature to be a lower bound estimate of the solar-climate response. Dynamically,

these feedbacks may result in modifications of regional patterns, though in light of recent

research suggesting a lesser impact than previously considered, this is probably of less

significance than model uncertainty as a source for error.

Table 5.1 indicates the suite of model runs performed and their abbreviations used in this

chapter. Each run, including the control run was integrated over 30 model years with the

first 20 years allowing for spin-up of the model and the last 10 averaged to produce

equilibrium estimates. Average global temperatures of the latter 5 years of the 30 year control integration were not significantly different to years 21-25, indicating that an assumption of equilibrium was satisfied.

Table 5.1. The key features of each model experiment

Experiment Name/abbreviation	Description of key experiment forcing changes
CONT	"present day" (c. 1985). CO_2 - 345 ppm, solar - 1365 Wm^{-2}. F11 – 0.238 ppb, F12 0.408 ppb, CH_4 – 1.653 N_2O – 0.306
SOL	solar irradiance is reduced to Maunder Minimum (c. 1675) estimated values. Solar irradiance is reduced by $4Wm^{-2}$ at the top of the atmosphere relative to present. Solar irradiance: 1361 wm^{-2}. Other parameters as for Control
SOLORB	As for SOL, but introducing the linearly interpolated values of orbital parameters as for 1675 (interpolation from calculated values of Berger and Loutre,1991) Eccentricity – 0.016862 Obliquity – 23.482 Precession – 82.827 Other parameters as for SOL
SOLORBC	As for SOLORB but reducing greenhouse gases to pre-industrial levels (as per IPCC, 1990). CO_2 – 280 ppm CH_4 – 0.8ppm N_2O – 0.288 ppm F11 – 0 F12 – 0
2060	Conditions as projected for ~2060AD from IPCC, 1996. This is approximately the year that equivalent CO_2 is expected to double from 'present' values (present model year - c.1985). CO_2 – 600ppm, CH_4 – 3.48 N_20 – 0.369 F11 – 0.280 ppb (1990 value – assumes no increase and no significant decline since 'present day' values) F12 – 0.484 (1990 value) Present-day solar irradiance
2060SOL	As for 2060, but with values of irradiance estimated for Maunder Minimum (1361 Wm^{-2}).

Each experiment was examined and compared to the control run for a number of key climatic elements and processes. To isolate the climate response to specific forcing mechanisms, each model run was compared to the others. For example, in order to examine the effects of orbital parameters in 1675 relative to present, the output files for various climate elements of the SOL run were subtracted from SOLORB.

An important assumption in this methodology is that the linear combination of forcings is equivalent to the sum of the linear response to each forcing individually. This linear additivity is shown to be a valid assumption in many model-based temperature analyses, including Rind *et al.* (2004) and Meehl *et al.*, (2004). This is important too, in that it implies that the climatic effect of solar irradiance does not change with varying background states (*i.e.* sensitivity remains relatively constant for pre-industrial climate to present day).

Section 5.2 will compare the equilibrium effect of greenhouse gases to that of solar irradiance changes, both in the global mean and considering regional patterns, over the pre-industrial to present period. Section 5.3 will address the modifying feedbacks (from the pre-industrial-to-present time period) associated with orbital forcing – a factor not generally considered in GCM experiments examining century-scale changes due to its assumed insignificance. Section 5.4 will summarize the equilibrium effects of assuming a MM-like solar irradiance change on doubled CO_2. A summary of the chapter will be provided in section 5.5

5.2 Maunder Minimum compared to present: solar forcing versus greenhouse gases.

5.2.1 Global mean response

As mentioned in section 3.2, Lean *et al* .(1995) estimated total solar irradiance changes from MM to present of approximately 0.24% or around 3 Wm^{-2} (at most) at the top of the atmosphere. Accounting for albedo (approximately 30% attenuation), and the geometry of the Earth (where the sunlit disk is receiving energy equal to Πr^2, or ¼ of the surface of the Earth), the surface change in energy would be approximately 0.5 Wm^{-2}. If we were to take the Hoyt and Schatten (1993) estimate (or Fligge and Solanki, 2000), this would be slightly larger than 4 Wm^{-2} at the top of the atmosphere, or 0.7 Wm^{-2} at the surface. Over the same period, greenhouse gas forcing is equivalent to a little less than 2.5 Wm^{-2} at the surface (IPCC, 2001). In an attempt to give as much possible weight to solar change as is reasonable, the *a priori* assumption is made that the equilibrium greenhouse gas response will dominate the combined climate response, and a change of 4 Wm^{-2} from MM-present was chosen, slightly larger than the LBB95 estimate and consistent with HS93 and Fligge and Solanki, 2000. Based on more recent research (*e.g.* Wang *et al.*, 2005), it is possible that the magnitude of solar irradiance change has not been as large (see discussion in 3.2). Therefore, in choosing an estimate at the high end of the spectrum, it can be considered an upper bound estimate to the effect of solar forcing when compared to greenhouse forcing. However, while it may be reasonable to assume that the climate system may reach an approximate equilibrium in response to solar forcing (see discussion

5.1 and Lean and Rind, 1998, Waple *et al.* 2002, chapter 4), an equilibrium response to rapidly changing greenhouse gases is likely unapproachable in the near future, nor has it likely been attained over the last 100 years. This more than offsets a relatively large solar irradiance estimate, since here, we are comparing equilibrium climates and the effect of greenhouse gases will be larger than for equivalent transient simulations with present day conditions.

As expected for the SOL experiment, equilibrium model temperatures are reduced relative to present (Figure 5.1). Globally averaged temperature is 0.46ºC lower than CONT and is in the middle of a range of estimated MM-to-present transient model simulations investigating irradiance–only effects (*e.g.*, Rind and Overpeck, 1994, Rind *et al.* 1999, Cubasch *et al.* 1997), suggesting that the assumption that equilibrium response approximates the transient response is satisfied. Isolating the response of greenhouse gases (SOLORBC-SOLORB), the model temperature reduction is -1.44ºC, or more than three times the magnitude of global mean response for SOL-CONT. Transient experiments (*e.g.* Rind *et al.*, 2004) have found the greenhouse gas response to be double that of solar-forced MM-to-present climate. However, in not allowing the climate in transient models to reach equilibrium, the greenhouse-gas effect is likely to be underestimated, relative to this analysis. Considering expectations that the magnitude of forcing might be equivalent to that of the response (IPCC, 2001), calculations indicate that this is indeed reproduced. CO_2 forcing is 3.38 times that of solar, while the global temperature increase as a result of increased greenhouse gases is 3.13 times that of the

increase induced by irradiance changes, resulting in a slightly higher global climate

sensitivity to irradiance when comparing the Maunder Minimum to present.

Despite the near linearity in forcing and response for the annual mean condition, there is

a seasonal bias in global mean temperature effects. For the boreal summer months, the

June-August (JJA) mean response is -0.19ºC for SOL-CONT and -0.52ºC for greenhouse

gases alone, or 2.7 times greater. Comparing this to the boreal winter response (Dec-Feb),

the change in response to greenhouse gases is much larger with a global cooling of

-1.61ºC relative to only -0.06ºC for solar. A reduction in greenhouse gases alone

therefore also causes three times as much cooling in Northern Hemisphere (NH) winter

as it does in summer. Obviously, solar forcing is generally reduced in the NH in winter

due to the development of polar night in response to a lower angle of solar incidence

across the mid- and high-latitudes. Given the greater sensitivity of northern high latitudes

(Arctic Climate Impact Assessment, 2005), the heterogeneity of circulation and the larger

amount of land in the NH affected by changing length of day, it is not surprising that the

boreal winter global response is dominated by greenhouse gases. Regional patterns of this

effect are outlined in section 5.2

As expected with reduced temperature, the hydrological cycle is suppressed and global

precipitation reduced, both for solar-only and CO_2-only changes. With a reduction of

0.04 mm/day, SOL-CONT is moderately wetter than for a CO_2 reduction only, which

yields a 0.08 mm/day decrease. These are both moderate reductions given that the model

annual average precipitation is 3.2 mm/day in CONT. It also illustrates that an

assumption of simple linearity with respect to proportional response for precipitation is
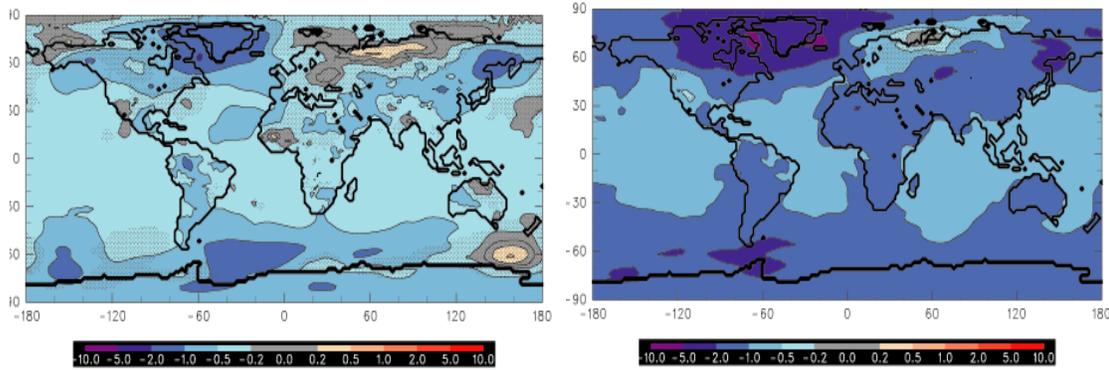
A

B
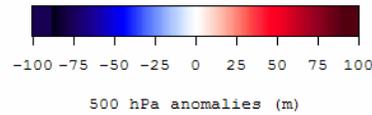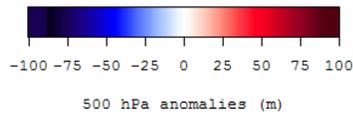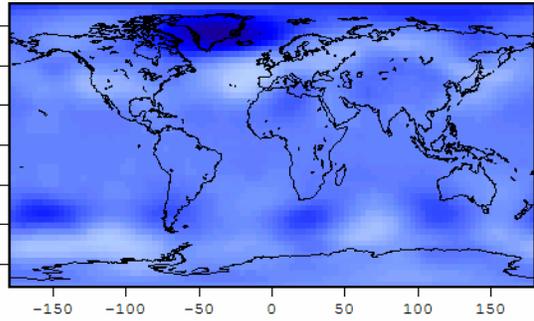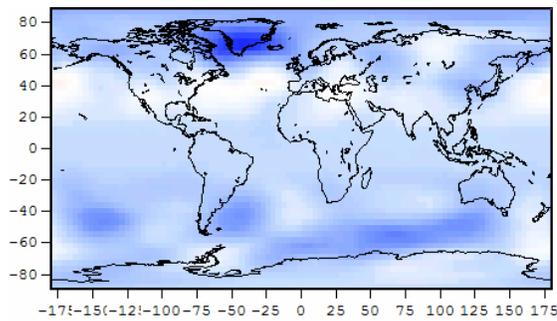
C

D
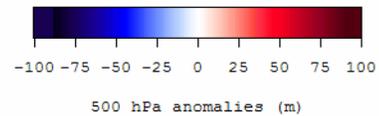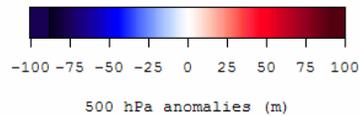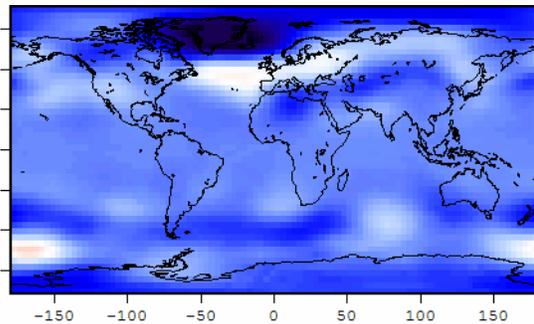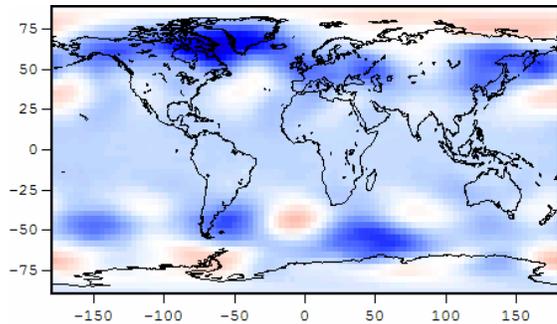
E

F

Figure 5.1 Annual model temperature response (degrees C) for (a) SOL-CONT, and (b) SOLORBC-SOLORB. Hatched areas are statistically insignificant at 95% according to the student's t-test. Model 500 hPa height (meters) for (c) SOL-CONT, and (d)

SOLORBC-SOLORB. (e) and (f) are as for (c) and (d) but for boreal winter (DJF) conditions.

not met. Large interannual variability of tropical precipitation in GCMS, even when average over 10 years, is likely to bias precipitation results. The sensitivity of precipitation changes are twice as large for solar than for greenhouse gases, indicating that, unsurprisingly with a drying trend, there is an asymptotic relationship with forcing. As precipitation decreases (i.e. reaches values closer to zero), the forcing needed to further decrease precipitation becomes greater. The reduction in forcing of 2.4 Wm^{-2} (0.2%) imposed by reducing greenhouse gases to pre-industrial values forces a global drying of 2.5% compared to a drying of 1.3% for a small negative forcing of solar irradiance of 0.7 Wm^{-2} or 0.05%. However, overall, CO_2 does have a larger absolute impact on precipitation. Simulated precipitation is significantly improved in GENESIS version 2 (the version used here), compared with previous iterations of the model, yielding a lower global annual average than for version 1.02 (Thompson and Pollard, 1997). Zonal means also agree well with average observations and illustrate well the larger effect of reduced CO_2 relative to solar variability (figure 5.2).
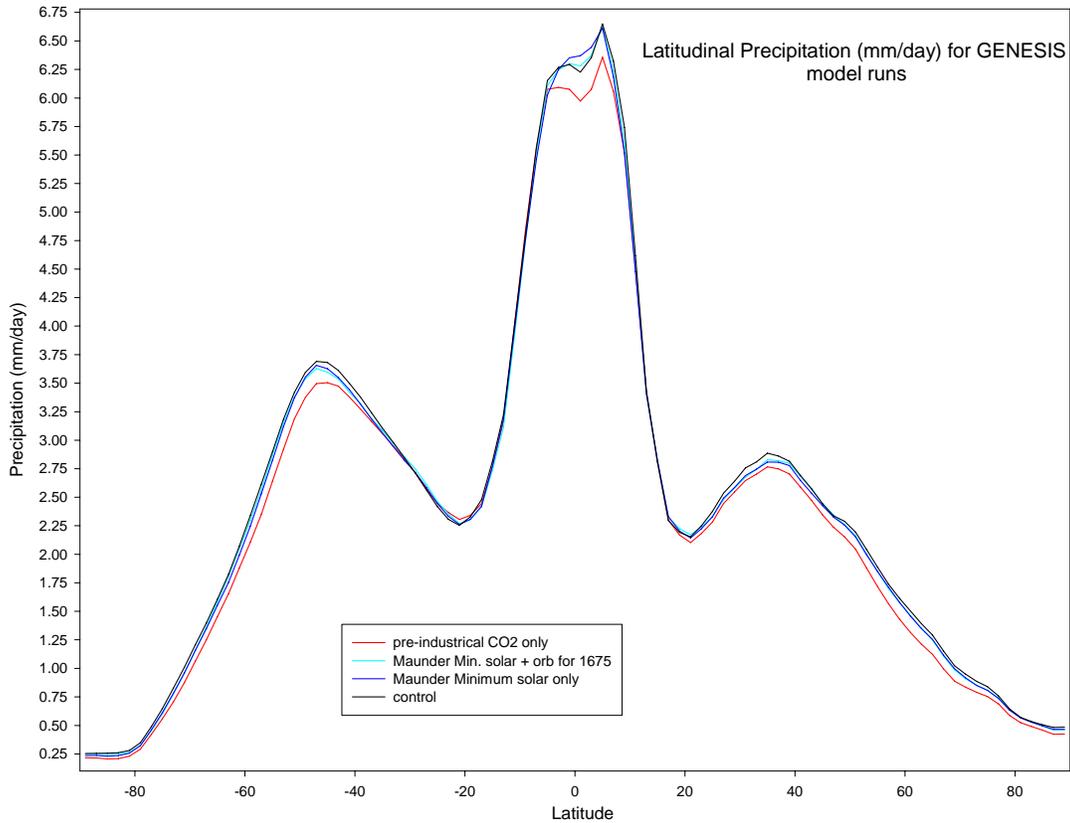
Figure 5.2 Latitudinal profile of precipitation with each model run.

The largest influence of MM-greenhouse gas forcing on precipitation, apart from a consistent global mean reduction, is in the equatorial region, where differences are as much as 0.44 mm/day between the greenhouse gas-forced run and that of SOL. This is not surprising given the high annual rainfall totals of the tropics and high interannual variability of the models. In the desert regions of the sub-tropics, where rainfall is at its global minimum, the magnitude of forcing is relatively unimportant as overall effects are minimal. SOL-CONT and SOLORB-SOL (discussed in section 5.3) are a much closer approximation of CONT zonal mean values. Greenhouse gases clearly have also the

greatest influence across the mid-latitudes. Simulations begin to diverge at around 20ºN in the Northern Hemisphere with reductions of CO_2 showing the greatest influence, while in the southern hemisphere, there is no significant difference between the runs until approximately 30-35º South. It is likely that the monsoonal systems of the Northern Hemisphere influence the lower latitude differences. Further differences in precipitation regimes will be discussed in section 5.22.

5.2.2 Regional Response

The spatial pattern of temperature comparing the annual response from solar and greenhouse forcing is shown in figure 5.1. As discussed above, the overall temperature response from greenhouse gas forcing alone is approximately three times greater than that of solar forcing. While the magnitude of the response is, in general, proportional to the forcing (i.e. greenhouse gases exert more overall change than solar forcing), the regional patterns of the annual mean temperature response are also notable for their similarity. A dominant land-sea contrast is a signature of both patterns, with a maximum response (of negative sign) around Greenland. A strong negative response is also evident surrounding Antarctica, and a robust, but less obvious node of maximum (negative) response exists around the Sea of Okhotsk.

In the pattern produced by solar forcing alone, some warm anomalies are apparent in northwestern Russia and south of Australia in the Southern Ocean. An area of positive

anomalies is also present on the north slope of Alaska. Although there are no positive

anomalies in the greenhouse-gas only case, a small area of reduced negative response

also occurs in northwestern Russia. In figure 5.1(c) and (d), the pattern of 500 hPa height

anomalies show that in both SOL-CONT and SOLORBC-SOLORB, there is an enhanced

positive NAO-like pattern (Hurrell 1995). The sub-tropical high pressure center, located

close to the Azores, is relatively enhanced compared with a depressed Icelandic low. This

gradient results in cold air advection from the Arctic across northern Canada and

Greenland, while relatively warmer air is pulled northeastwards from the Atlantic across

northern Europe and northern and western Russia. This is particularly evident in the

boreal winter temperature patterns (figure 5.1, a,b), the season during which NAO would

likely be at its peak intensity as is the case for present-day.

During the December-February period (DJF), despite widespread cooling across the

Atlantic in the SOLORBC-SOLORB case, there are warm anomalies in the eastern

Norwegian Sea/Barents Sea, north and east of Scandinavia – areas cited (Hurrell, 1995)

as having higher temperatures during positive NAO winters. For the winter 500 hPa

pattern (5.1, e,f), the area of lower heights is greater in extent for the SOLORBC-

SOLORB case allowing more widespread cool air advection from the north. Since the

Atlantic is cooler in general, warm air advection across Europe and northern Russia is

moderately reduced compared with the SOL-CONT pattern. The greatest pressure

difference between the low pressure center of action in the Icelandic area and the Azores

High is found in the winter greenhouse-gas-only case with a difference of 101.1 meters.

In the global mean case for greenhouse gases alone, it is 49.8, partially reflecting a lack

of NAO signature in the summer. For SOL-CONT, a maximum pressure difference is also found in the winter with a value of 56.9 m. However, this is much more equivalent to the global annual mean, with summer conditions reflecting a much more intense Azores High and thus an equivalent pressure difference as for winter, though the Icelandic low is much less intense and extensive.

Figure 5.3 shows DJF precipitation patterns for SOL-CONT and SOLORBC-SOLORB. As is evident from the figure, significance at the 95% level is not achieved for the vast majority of the globe. Modeled interannual variability is relatively high for precipitation preventing the establishment of significance for all but the largest anomalies (*e.g.* Western Greenland and isolated other areas). Nevertheless, the model's tendency is for precipitation patterns to be consistent with identifiable modes of the atmosphere. For the case of greenhouse gases only, the winter precipitation pattern is consistent with a positive NAO state (identified for the temperature patterns), with marginally wetter conditions across Scandinavia and in the Norwegian/Barents/Greenland Sea area contrasting drier conditions to the south across southern Europe (figure 5.3b). For the SOL-CONT pattern (fig 5.3a), no signal is apparent, except generally slightly increased precipitation across Europe. Since the magnitude of forcing is around 3 times lower in the solar only case, compared with SOLORBC-SOLORB, it is reasonable to assume that although the forcing exerts a similar dynamic response to that of reduced CO_2, (*i.e.* crossing a threshold necessary to initiate similar feedbacks and a sustained dynamic result), that the expression of that response might be slightly reduced. In this case, this is true for precipitation though not for temperature. For greenhouse gases, the global

temperature reduction is greater than for solar alone, leading to a *less* well expressed

temperature signature of NAO (*i.e.*, warm air advection is reduced across northern

Europe due to generally depressed temperatures across the Atlantic). So despite a greater

magnitude of forcing, the NAO temperature signature is less obvious, even with a clearly

stronger pressure pattern for greenhouse gases. For precipitation, the opposite is true,

with the greater pressure difference in the greenhouse gas-only case leading to enhanced

storminess relative to the SOL-CONT case (Figure 5.1e and f).
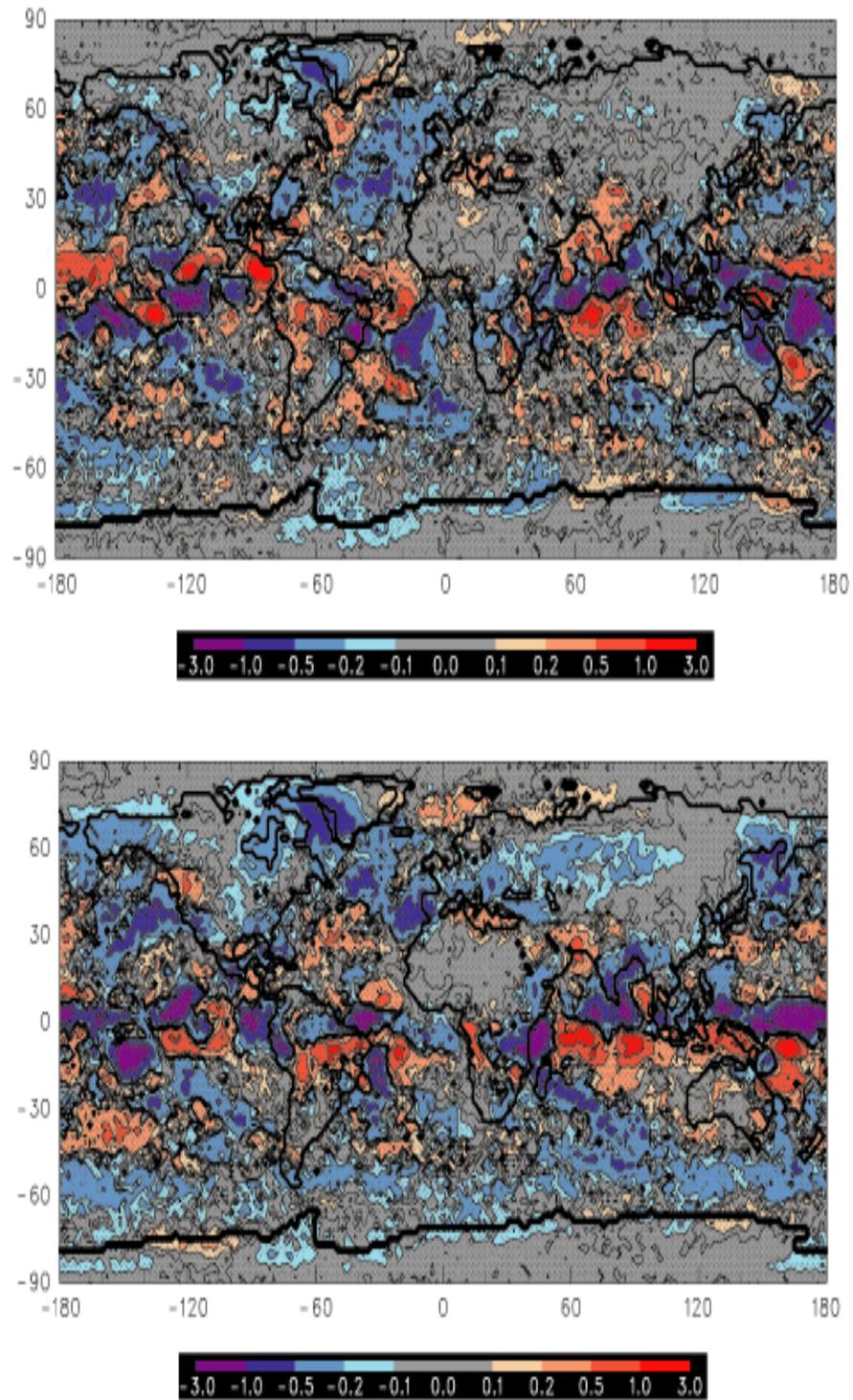
Figure 5.3 DJF precipitation patterns for top: SOL minus CONT (effect of solar reduction only), and bottom: SOLORBC minus SOLORB (effect of greenhouse gases only). Hatched areas are not significant at the 95% level.

The existence of a positive NAO fingerprint is in direct contrast to empirical and alternative modeling studies indicating that a more negative NAO pattern emerged during the Maunder Minimum. Waple *et al.* (2002, also described in chapter 4) and Shindell *et al.* (2001) illustrate that negative sensitivity develops in the North Atlantic in response to increasing solar irradiance (see figure 4.4a *i.e.* cooler temperatures result from increased forcing), which, should in this analysis, yield the opposite result – positive sensitivity to decreased solar irradiance, and areas corresponding to the North Atlantic Oscillation reflect a negative phase. Instead, here we see a profound negative temperature response to decreasing TSI and a distinctive positive NAO pressure pattern. There are several possible explanations for this apparent divergence of response. As previously mentioned, GENESIS does not incorporate a dynamic coupled ocean and cannot resolve variations in the meridional overturning of the ocean, which, if enhanced relative to present (as in Cubasch *et al.* 1997), could yield positive temperatures in the North Atlantic in response to a negative forcing. This is cited as a cause for a generalized negative sensitivity in the region forced by increasing solar irradiance in Cubasch *et al.* (1997). However, the specific NAO-like pattern (rather than a more general North Atlantic cooling) is also reproduced in its negative phase during the Maunder Minimum in the GISS AGCM (*i.e.* a model with no dynamic coupled ocean). Rind *et al.* (2004) ran a series of transient experiments incorporating the various effects of spectral solar irradiance, total solar irradiance and anthropogenic forcing and found that a negative NAO phase was present in all experiments. GENESIS does not incorporate dynamic feedbacks associated with stratospheric ozone and while Shindell *et al.* (2001) cite these ozone feedbacks as a strong factor in the development of a negative NAO, Rind *et al.* (2004) noted that the

inclusion of ozone feedbacks was less important than full resolution of the model's stratosphere. They contend that the negative NAO phase likely arises, for the most part, from reduced tropical warmth in the upper troposphere and a corresponding change in relative refraction of the Eliassen-Palm (EP) flux at around 100 mb. The net dynamic result in Rind *et al.* (2004) is rising air (and low pressure) at mid-latitudes and sinking air (high pressure) at higher latitudes giving rise to a more negative NAO phase during the Maunder Minimum.

Considering the lack of any transient experiment with the GENESIS model, it is impossible to compare the temporal sequence of feedbacks, but given the much higher sensitivity in the GISS model as compared to GENESIS (1.2ºC vs 0.6ºC) and the associated increased cooling in the tropics relative to GENESIS, the threshold necessary to invoke substantial E-P flux changes is likely not initiated in GENESIS. Nevertheless, the results of Waple *et al.* (2002) are cause for further investigation regarding the different phases of the NAO during the Maunder Minimum. Clearly, the annular mode of the Northern Hemisphere is extremely sensitive to relatively small changes in global forcing with both solar and greenhouse invoking the same dynamic response. Although, it is likely that the empirical study of Waple *et al.* (2002) approximates an equilibrium response in the climate from solar variability (see discussion in chapter 4), some differences may exist in phase locking when using a transient experiment compared to the equilibrium experiments described here.

Furthermore, the Waple *et al.* (2002) empirical experiments implicitly include some influence of volcanism during the 1650-1850 time period, though this is unlikely to be a cause of the phase difference. Neither Rind *et al.* (2004) nor Shindell *et al.* (2001) or Cubasch *et al.* (1997) incorporated the effects of volcanism and results were more similar to the empirical result for the phase of the North Atlantic annular mode than in the GENESIS experiments. In addition, consideration of century-scale orbital forcing substantially alters the pressure and temperature patterns of the Northern Hemisphere in the GENESIS model and will be discussed in section 5.3

As discussed below, it is equally plausible that the dynamic sea-ice model in GENESIS is oversensitive and forces a more negative temperature response in the area surrounding Greenland and Iceland, leading to dynamics supporting a more negative NAO. While empirical observations (*e.g.* Ogilvie, 1992) include significant interannual variability during the Maunder Minimum, this is not reproducible in an equilibrium model and only the more general increase in sea-ice extent during the 17th to 19th centuries around Iceland and Greenland is captured. Figure 5.4 shows the change in sea-ice fraction for both solar and CO_2 forcing, and illustrates the increased sea ice to the east and west of Greenland and across the Arctic north of the North Atlantic. It is worth noting that sea ice around the margin of Greenland appears to be especially susceptible to external forcing, and given that the recent decrease in Arctic sea-ice in response to increasing global temperatures has shown particularly large changes around Greenland during that portion of the year when average sea ice concentrations exist in the region (i.e. all months but summer), this indicates that the region is indeed sensitive to external forcing (images available at

www.nsidc.org). Sea ice around Antarctica also has greater fractional coverage as a
result of reduced greenhouse gas and solar forcing in the annual mean.
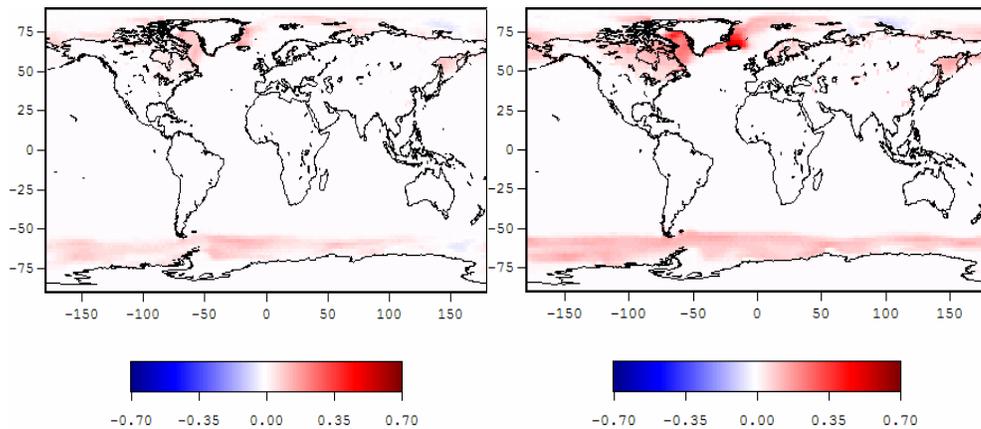
Figure 5.4 (a) Change in Sea-ice fraction for SOL-CONT, and (b) for SOLORBC-
SOLORB.

Up to a 20% increase in sea-ice fraction was calculated in isolated grid squares around
Greenland for the annual mean equilibrium condition in SOL-CONT and more than a
50% for the case of greenhouse gas reduction, though the patterns of increase are very
similar. A relationship of NAO to sea-ice has been well documented in the literature,
though almost exclusively with respect to the NAO's (or Arctic Oscillation's) influence
on decadal-scale sea-ice distribution and extent (e.g. Deser *et al.*,2000, Rigor *et al.*,
2002). It should be noted that it is equally plausible, in this scenario (i.e. equilibrium
climate response to reduced radiative forcing), that a persistent NAO phase is sustained
due to an overall cooler NH and resulting increased sea ice. Honda *et al.* (1996, 1999)
examine the effects of increased sea ice in the Sea of Okhotsk (an area that also displays

sensitivity of sea ice in these experiments) on atmospheric dynamics and conclude that circulation anomalies can result. In their model, large scale atmospheric effects include the development of a stationary wave train forced by varying surface heat fluxes developed in response to anomalous ice cover. While it is not possible to examine the temporal development of feedbacks in an equilibrium climate simulation, evidence does exist to support the hypothesis that increased sea-ice would likely further promote a sustained single or preferred mode NAO.

5.3 Contribution of Orbital Forcing at the decade-century scale

Changes in the Earth's position relative to the sun are known to impact the global temperature on scales of millennia. Due to the relatively small changes in our orbital location on the decade-to-century scale, it is typically not considered as a forcing element in equivalent temporal scale climate change modeling studies, and has received relatively little attention as a comparable scale forcing to variations in the sun's acitivity (Bradley, 1999). However, it is reasonable to assume that if small changes in solar irradiance as a result of the sun's magnetic shifts can induce climatic adjustments, it is also feasible that fluctuations in Earth's position relative to the sun may lead to modulations in climate response. The combined forcing may result in a significantly different interpretation of recent regional climate change.

Three elements of orbital forcing – obliquity (~41, 000 yr periodicity), precession, (~21,000 yr) and eccentricity (~100,000 yr periodicity) interact to influence climate

(Berger, 1978). Eccentricity, or the ellipse of the Earth's orbit, is the only parameter that

changes the total annual insolation received at the top of the atmosphere. Considering that

over a 100,000 year cycle, the ellipse of the orbit varies by only 6% (Berger *et al.* 1993),

the change in receipt over the several hundred years analyzed in these experiments will

be negligible. More important is the change in precession (the importance of which relies

on eccentricity to some degree), and tends to dominate obliquity at all latitudes, though

less so at high latitudes (Berger *et al.*, 1993). To ascertain their relative impact over the

century-scale, climate models are a useful tool. As for section 5.2, here, we deal with

only relative sensitivity for equilibrium climate and compare to forcing from solar

irradiance.

Calculations have been made for orbital parameters at 1000-year intervals (Loutre and

Berger, 1991) as differences from present (~1950 AD). It is reasonable, on the century

time scale to use a linear interpolation to derive annual values (Loutre pers. Comm.) in

order to force the GENESIS model. Annual orbital values were calculated for 1675 AD

(to coincide with minimum solar irradiance during the Maunder Minimum), and run as an

additional experiment (SOLORB).

JAN

FEB

MAR

APR

MAY

JUNE

109

JUL

AUG

SEP

OCT

NOV

DEC
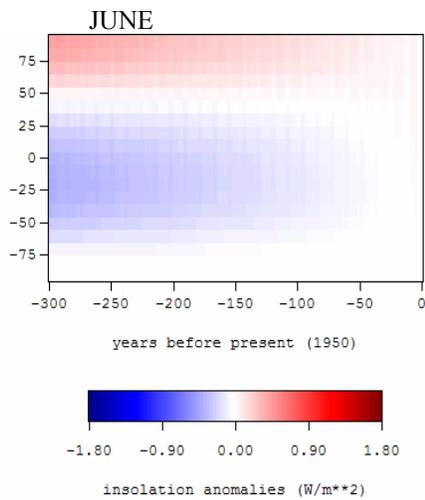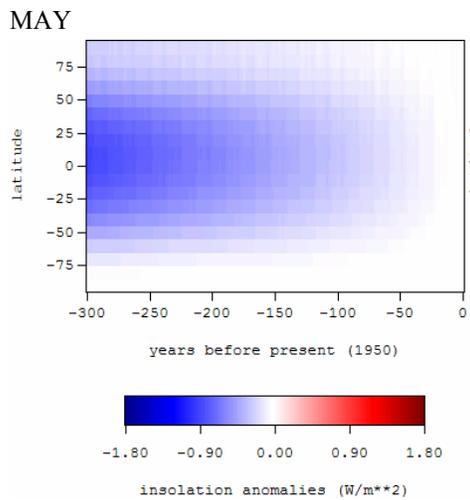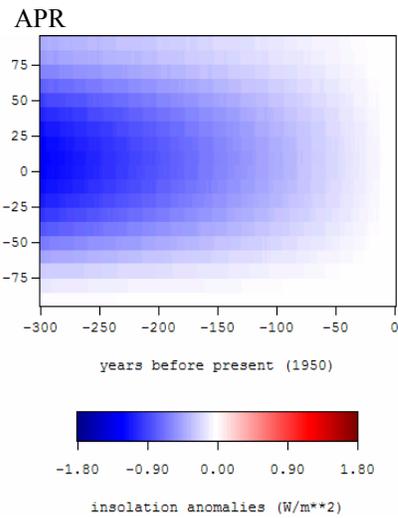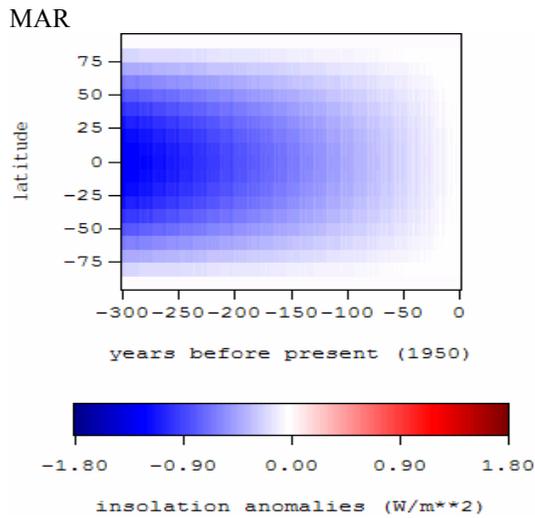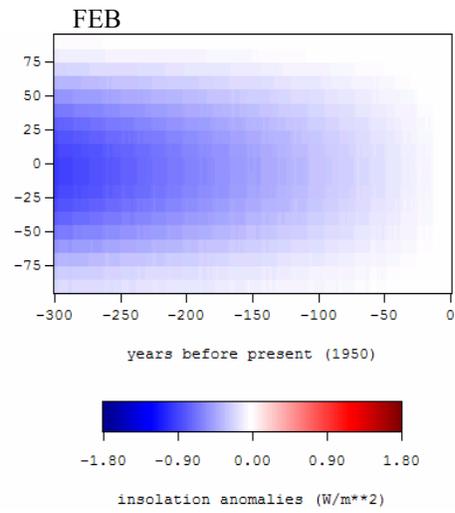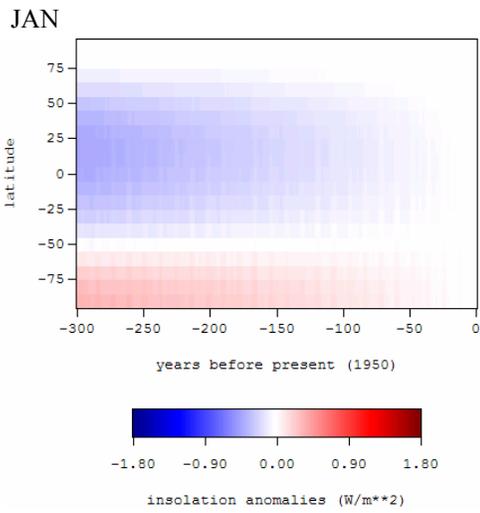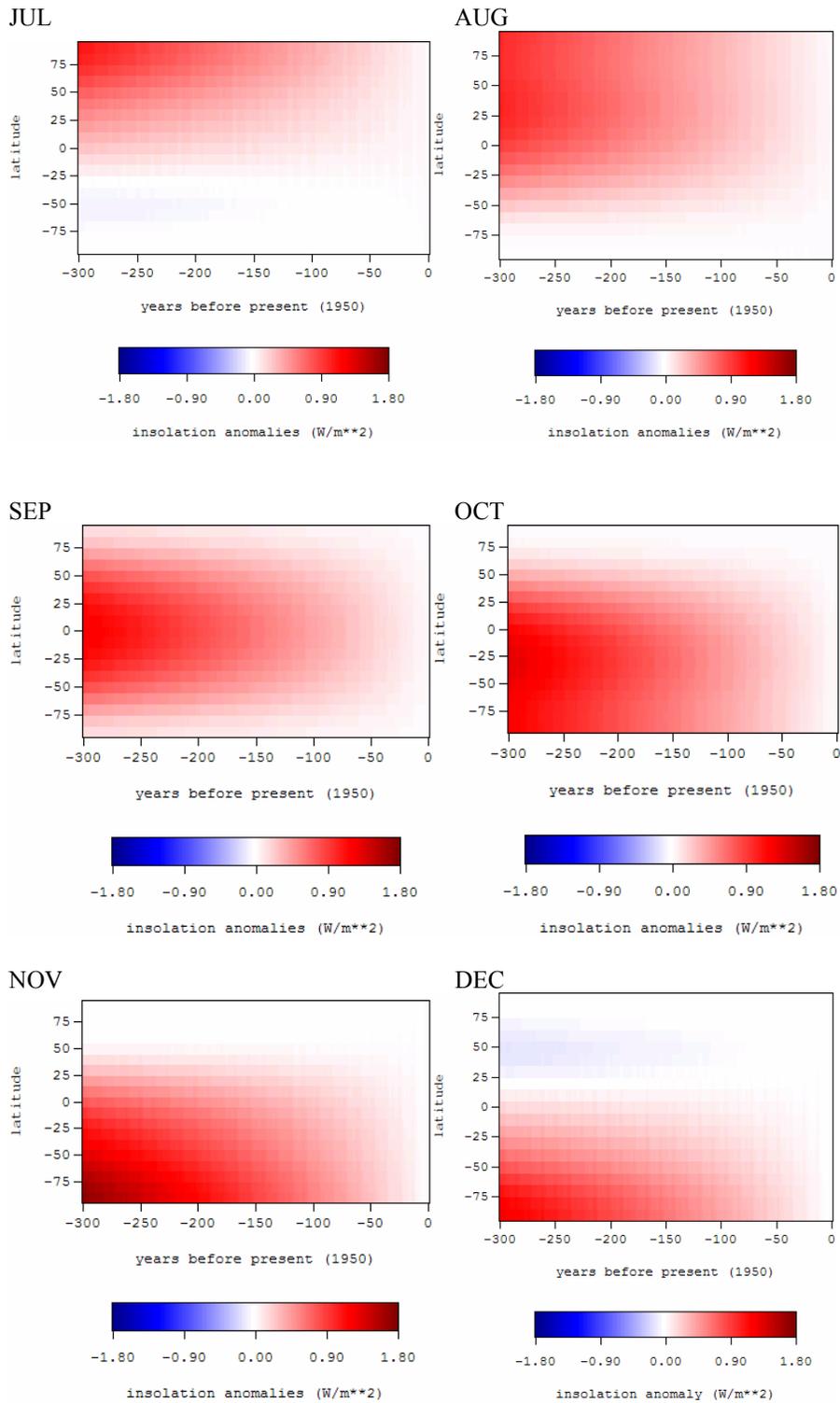
Figure 5.5 Insolation anomalies, relative to 1950, for each month of the year over the last 300 years (1650-1950).

Surface temperature for SOLORB-SOL (*i.e.* the influence of orbital forcing only in 1675 AD compared to present) is shown for annual mean, boreal winter and boreal summer in figure 5.6. Of note is the large positive anomaly for DJF around Greenland and Arctic North America contrasting the negative anomalies around Scandinavia and northwestern Russia. Conditions in JJA are also warmer over Arctic North America relative to present. Cooling across Africa is a dominant orbital signature in boreal summer, along with large anomalies (both positive and negative) along the margin of polar night for JJA.
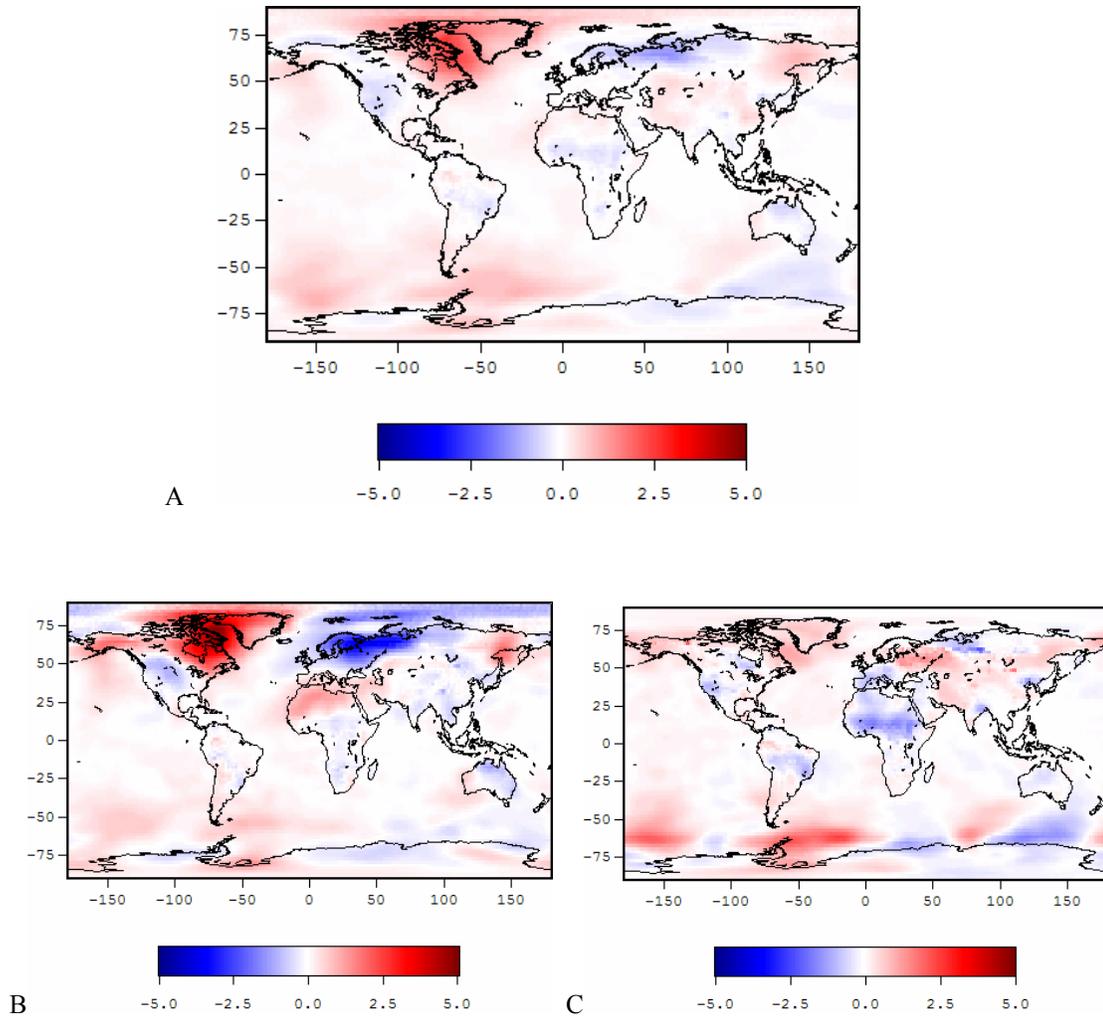
Figure 5.6 Surface temperature for SOLORB-SOL (*i.e.* the effect of orbital forcing only between 1675 and present), for A) annual mean, B) DJF and C) JJA.

As previously noted, the precipitation signal is not statistically significant due to high model interannual variability. However, the summer decrease in temperature for northern tropical Africa coincides with a clear tendency towards increased precipitation due to a northward shift in ITCZ-related rainfall (fig 5.7). This relationship is in accordance with studies examining millennial scale effects of orbital forcing during the Holocene (*e.g.* deMenocal *et al.*, 2000, Kutzbach and Liu, 1997).
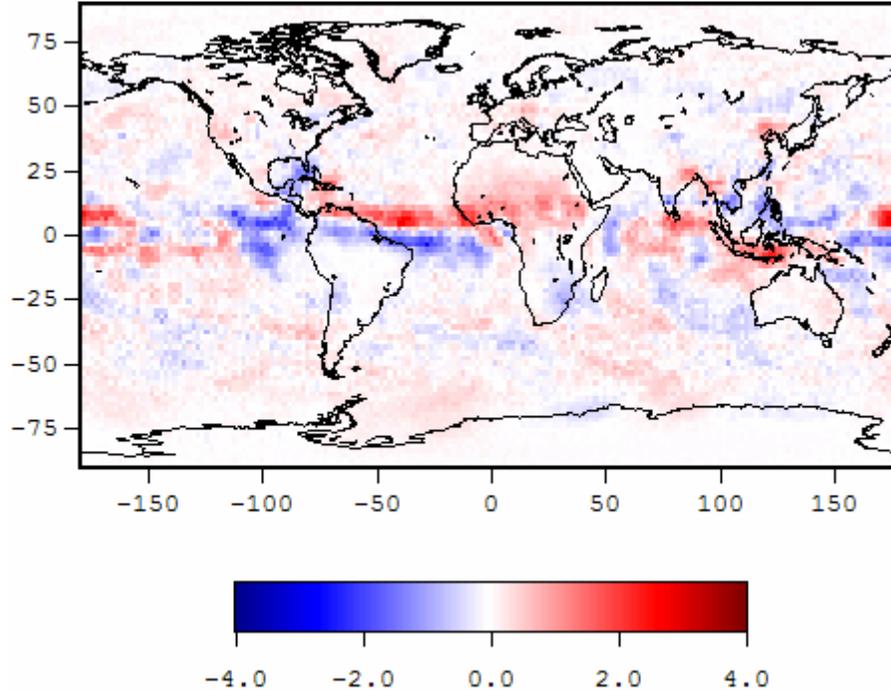
Figure 5.7 Precipitation change for JJA for the SOLORB-SOL experiment (*i.e.* The effect of orbital forcing from 1675 to present).

Northern Africa was much wetter during the mid-Holocene (5-6,000 yrs bp) due to increased insolation relative to present in the Northern Hemisphere. This heats the Saharan land surface leading to increased precipitation from increased monsoonal flow into the region. In addition, an increased north-south temperature gradient across the tropical Atlantic further enhances the process (Hastenrath, 1990). As precession-related insolation decreases across the NH, (as it does towards the present), then the dynamics producing north African precipitation are diminished and a threshold crossed allowing a desert environment to emerge (as seen today). It is interesting to note that many models under-represent north African wetness compared to paleo-evidence for rainfall during the mid-Holocene (*e.g.* Brostrom *et al.* 1998), and the incorporation of the enhancement

generated from north Atlantic SSTs is necessary in some studies. While vegetation

changes also appeared to be a major feedback in previous analyses of millennial-scale

orbital forcing (Claussen *et al.*, 1999), in the GENESIS model, the orbitally-forced

response is much larger than one might expect for the small changes imposed and no

vegetation feedback. This suggests that it may not require a large change in precession to

cross a threshold necessary for climate effects to occur. Furthermore, DeMenocal *et al.*

(2000) find that a transition from a wet to dry regime (and vice versa) across northern

Africa may occur in only decades to centuries. However, a caution must be used with this

conclusion due to the consideration of equilibrium. It is possible that this experiment will

overstate the influence of a small perturbation in orbital forcing due to the expression of

an equilibrium climate only, and therefore more easily approximate the wetter conditions

of the mid-Holocene.

Overall boreal summer temperatures are slightly higher (0.1ºC), as expected with

increased NH insolation for 300 years before present (fig 5.5), though the warming is not

uniform. Those areas displaying a cooling signature in the boreal summer tend to

coincide with areas of increased precipitation (figure 5.6c and fig 5.7). This is consistent

with other studies (e.g. Joussame *et al.* 1999) that suggest the hydrological cycle was

enhanced earlier in the Holocene as a result of increased convection over land. The more

persistent cloud cover from frequent convective storms prevents the temperatures rising

as much as in other areas, especially in the boreal summer. Generally, the air temperature

over the oceans for the GENESIS experiment show more uniform warming.

The boreal winter temperatures shown in figure 5.6b are again indicative of a resonance

with, or modulation of the North Atlantic Oscillation. When western Greenland is warm,

northern Europe tends to be cold as the Icelandic low is shifted west of its 'average'

position. This conclusion is supported by a greatly enhanced pressure gradient from

Greenland to the Azores (fig 5.8a), with pressure associated with the Icelandic Low being

higher than CONT and vice versa for the Azores High – a typical signature of a negative

NAO. Furthermore, rainfall and total cloudiness (not shown) are both increased across

Europe, again indicative of a negative NAO, and the combination of cooler than average

temperatures across northern Europe and wetter conditions across the majority of Europe

promotes increased snowfall in the winter across eastern Europe and southern

Scandinavia, while diminishing snowfall in the areas surrounding Greenland (figure

5.8b). It has also been argued that an NAO pattern existed in the mid-Holocene with a

modulation of the phases on a 900-year cycle (Schultz and Paul, 2002). A possible

contributing factor to these periodic modulations in the mid Holocene is the timing of

orbital forcing. Equally plausible according to Schultz and Paul (2002) is that the

oscillations result from internal perturbations and feedbacks.
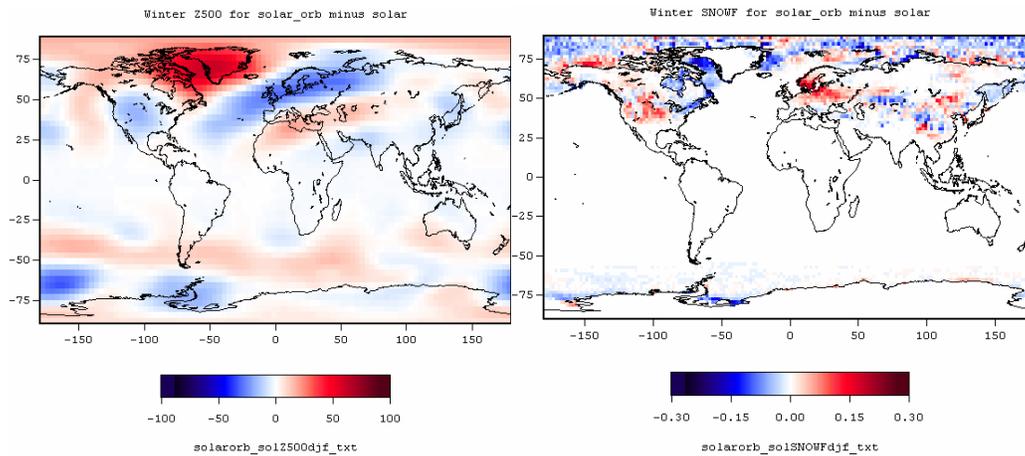
Figure 5.8. A) DJF 500hPa heights for SOLORB minus SOL, and b) DJF snowfall for SOLORB minus SOL.

In this experiment where a perturbation is allowed to occur only for orbital forcing, a reasonable conclusion is that a change in insolation in the Northern Hemisphere forces modulation of the major circulation mode of the NH – the North Atlantic Oscillation. A more persistent negative condition is forced to occur as annual radiative forcing is increased for the NH. While most of the increase in insolation occurs in the summer months, the NAO is best expressed in the winter and is therefore largely absent during JJA. For an equilibrium experiment such as this, it is impossible to say whether the negative phase is sustained (single mode) or whether it is simply more persistent (preferred mode) and therefore dominates the average winter condition.

When this winter pattern is compared to the winter effect of greenhouse gases alone and to solar forcing alone, it is evident that orbital forcing will temper some of the cooling at higher latitudes especially around northern North America and Greenland (figure 5.9)
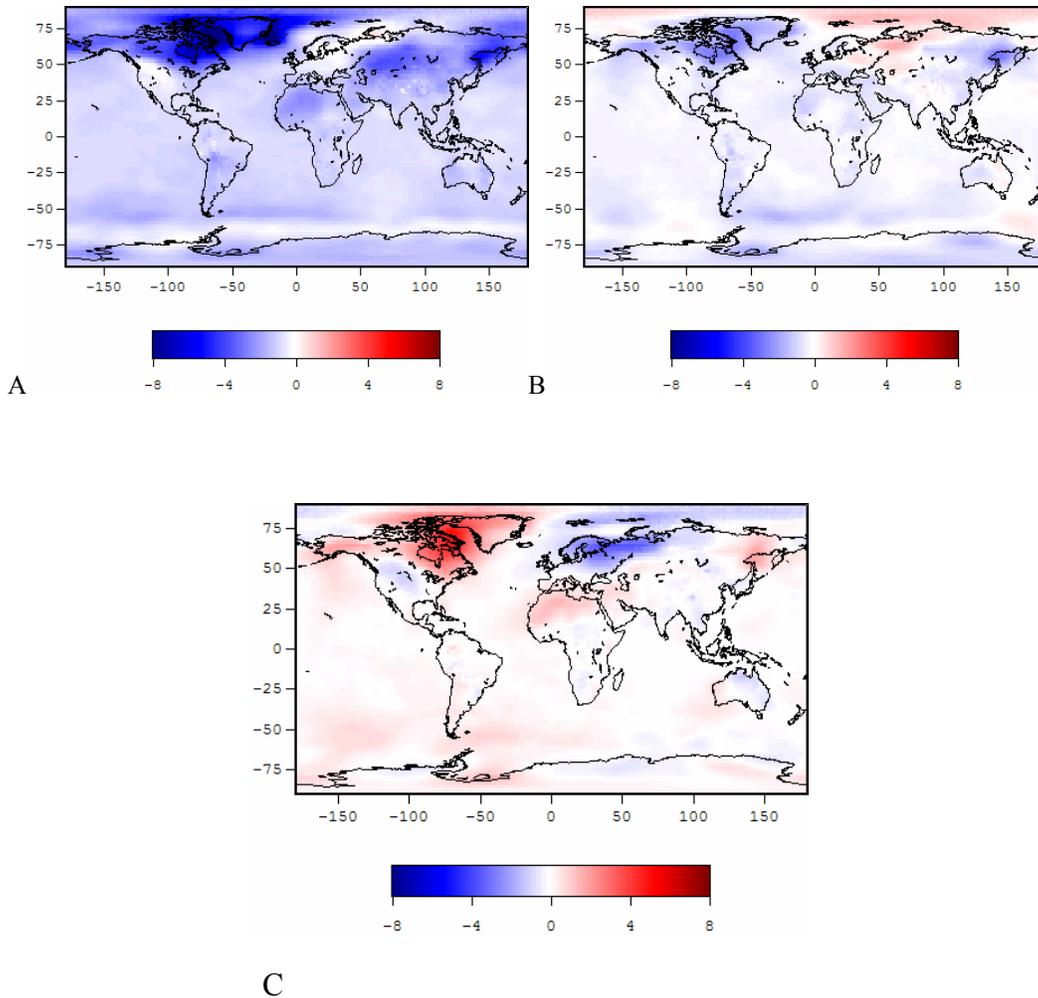
Figure 5.9 DJF temperature for A) SOLORBC-SOLORB (effect of CO_2 only), B) SOLAR-CONT (effect of solar only) and C) SOLORB-SOL (effect of orbital only), between the Maunder Minimum and present.

Maximum anomalies around Greenland for orbital forcing only are as much as 5ºC, compared to a maximum (negative) anomaly for the greenhouse gas only case of nearly 10ºC and compared to a solar only negative anomaly around Greenland of around 3ºC. Considering assumptions of linear additivity, the combined response in the vicinity of Greenland should be approximately 8ºC and indeed this is the case (figure 5.10a)
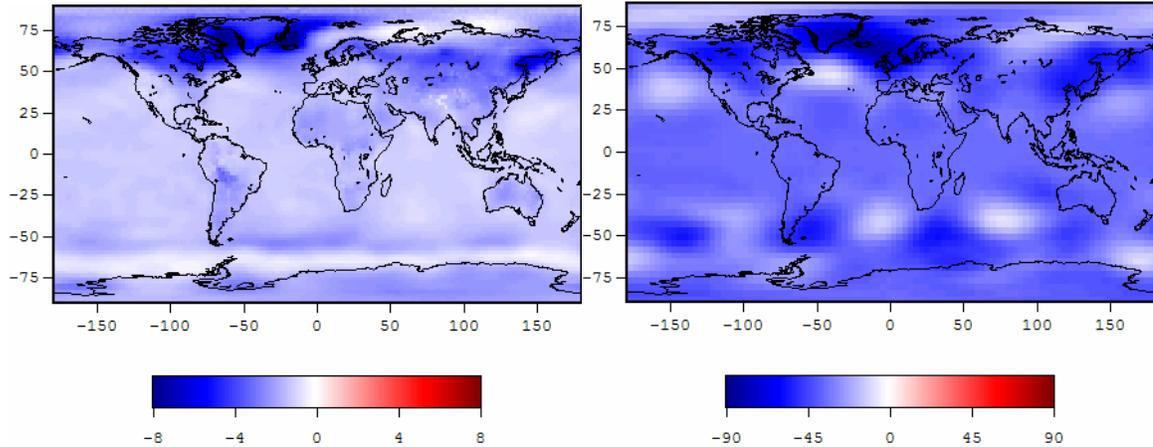
Figure 5.10 A) DJF temperature for SOLORBC-CONT - effect of combined forcing for the present minus Maunder Minimum, B) DJF 500 mb pressure for SOLORBC-CONT - effect of combined forcing for the present minus Maunder Minimum.

However, the disruption to the pressure pattern by including orbital forcing is also significant. As is shown in figure 5.10b, the Azores High is shifted much further to the northwest than in the case of greenhouse gas alone (figure 5.1f) and is therefore partially blocking movement of air from the relatively warmer North Atlantic to northern Europe, rather than promoting it. This results in cooler temperatures for Scandinavia than for greenhouse gases alone (compare 5.10a with 5.9a).

The resulting conclusion is that by including orbital forcing, the classic positive NAO-like signature, which is robust in both the solar and greenhouse gas case for the Maunder Minimum, breaks down to some degree. Although a pressure difference is maintained, it is strongest between Iceland and an area directly south of Greenland, rather than Iceland and the Azores (as in the typical pattern (Hurrell, 1995)), resulting in a cooling of

northern Europe. The air flow is more from the northwest than from the southwest, though due to the fact that Greenland is moderately warmer than in the greenhouse gas-only case, the cooling is also moderate. For northern Europe (around the area of Great Britain), the difference is approximately 1ºC between the two scenarios. SOLORBC minus CONT is 2.4ºC colder than present, while it is only 1.3ºC colder when ignoring the effects of orbital forcing, and for Scandinavia, as much as 3ºC (-3.7ºC compared to -0.8ºC, respectively). This mechanism and modulation of the regional temperature pattern is important to consider in observational studies of the Little Ice Age temperature in Europe in winter. Reconstructions of NAO indices prior to 1800 are in disagreement with each other (Jones *et al.* 2001) and these GENESIS experiments now give sufficient impetus for high resolution transient experiments to be run for the region with special focus on synoptic variability. Renewed effort to reduce errors in natural archives (proxy) of observed data should also be a priority.

5.4 Future scenarios

While there is no general consensus as to why the sun is occasionally in a magnetically quiescent state nor is there sufficient understanding among solar physicists to predict future quiescent episodes, there is no reason to suppose that the sun will not experience another Maunder Minimum-like event. As chapter 4 and 5 describe, the overall effect of a MM sun during the pre-industrial period is significant. And as researchers such as Lean *et al.* (1995) have shown, as well as earlier sections of this chapter, the climate effect of

the sun's inconstancy has diminished over recent decades in response to overwhelming forcing from increased atmospheric concentrations of greenhouse gases. The question remains as to whether a MM-like episode would significantly reduce the effect of further increased CO_2 concentrations.

Two further experiments were undertaken to determine the potential equilibrium sensitivity of climate under conditions of doubled CO_2 to a reduction in solar activity similar to that of the Maunder Minimum. A 'POST' experiment included the effects of a post-industrial equivalent doubled CO_2, such as is predicted to occur in the middle of the current century. The POST experiment keeps solar forcing at today's values (1365 W m^{-2}), while SOLARPOST includes doubled CO_2 and a reduced solar forcing of 1361 W m^{-2} (see table 5.1 for experiment summary and section 5.1 for discussion of solar forcing reduction).

As expected, experiment 'POST' is significantly warmer globally than CONT (+ 4.68ºC) with a dominant land-sea contrast (Figure 5.11). The effects of increased CO_2 in the GENESIS model have been investigated by others, (including Thompson and Pollard, 1995; Crane and Hewitson, 1998), and will not be discussed here, except in the context of the attenuating effect of a MM-like sun.
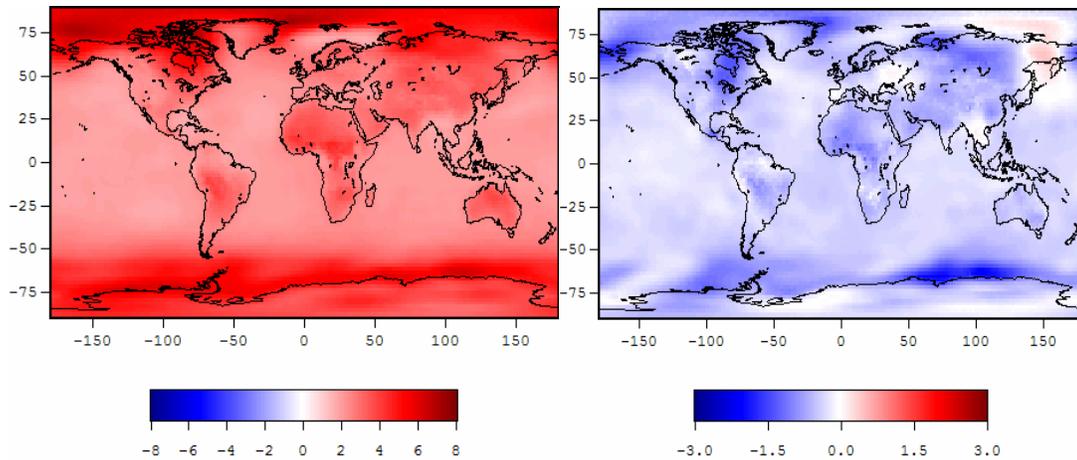
Figure 5.11 Annual temperature change for A) equivalent doubled CO_2 compared to present, and B) attenuation of temperature if solar forcing were reduced by 4 Wm^{-2} in the doubled CO_2 scenario. Note the different scales, used to increase clarity of pattern.

Figure 5.11b shows the decrease of the modeled global warming due to a 4 Wm^{-2} reduction in solar forcing at the top of the atmosphere intending to represent the equilibrium effect of a MM-like solar state. Average temperature for doubled CO_2 and a solar forcing of 1361 Wm^{-2}, compared to a run with doubled CO_2 and solar forcing of 1365 Wm^{-2}, results in a reduction of approximately 11% or 0.51°C. While the increase in global temperature as a result of increased CO_2 is greater over the land (figure 5.11a), the attenuation due to lower solar irradiance is also greater over the land surface (5.11b), as might be expected considering the prior conclusions (in section 5.22 and 4.23) noting that solar influence over land is greater than oceans. An 11% reduction is consistent with calculations expected from a linear response to forcing, since the surface forcing of solar irradiance is approximately -0.7 Wm^{-2}, compared to over 7 Wm^{-2} for equivalent CO_2.

The areas of greatest attenuation are centered around Hudson Bay, the Bering Strait and adjacent to the 'eastern' coast of Antarctica (60ºE-120ºE). This coincides with areas that are strongly influenced by increasing CO_2, indicating that there is very little pattern modification as a result of decreasing solar irradiance. Whereas in previous sections of this analysis it is clear that solar variability is able to modulate the known modes of variability, specifically the North Atlantic Oscillation, there is no such evidence for future warming scenarios. The feedbacks associated with a lower solar irradiance (increased sea-ice, pressure differences in the North Atlantic) are not initiated in a world that is warmer by over 4ºC.

As predicted by multiple global climate models (see chapter 9 of IPCC 2001), GENESIS global precipitation is higher with increased greenhouse gases (fig 5.12a). Globally, precipitation increases for $2xCO_2$ by 0.23mm/day, a percentage increase of approximately 7%. When solar forcing is reduced by 4 Wm^{-2} (at the top of the atmosphere) in the doubled CO_2 scenario, precipitation is increased by only 0.15 mm/day, an overall increase of around 5%, or in other words, a Maunder Minimum-like sun would attenuate the *increase* in precipitation by approximately 35 % (figure 5.12b) yielding a deviation from the concept of linear forcing and response for precipitation. This reinforces conclusions regarding an initially steep near-linear relationship between decreasing temperature and decreasing precipitation, transitioning to an asymptotic curve as significant drying occurs (see section 5.21)

The decrease in precipitation as a result of solar reduction is three times the relative

decrease in temperature *i.e.* 35% compared to 11%. The aforementioned high variability

in precipitation should be kept in mind when assessing the significance of precipitation

results however.
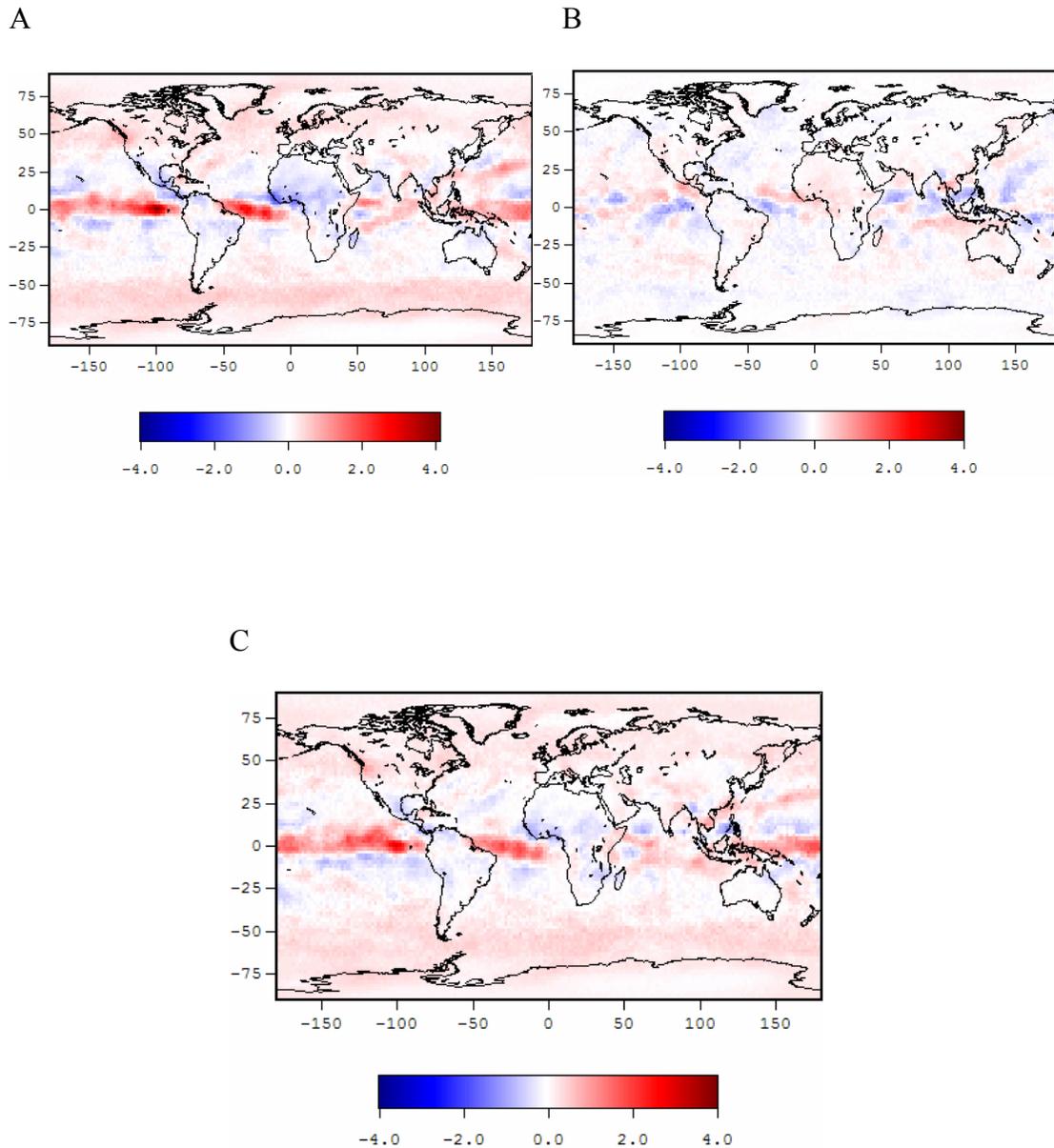
Figure 5.12 Change in precipitation for A) equivalent doubled CO_2 compared to present, and B) attenuation effect of solar forcing -4 Wm^{-2}, and C) Combined effect of doubled CO_2 and solar irradiance -4Wm^{-2}, compared to present.

The increase in precipitation for POST is fairly uniform in the mid- and high-latitudes, though Africa shows a drying under conditions of doubled CO_2 and the tropics in general show significant heterogeneity in the differences from CONT. For example, the ITCZ is more intense over the oceans, while over land, especially Africa and Central America, precipitation appears to be reduced, suggesting suppressed convection (increased subsidence) over land. However, the effect of reducing solar forcing (figure 5.12b and c) works to attenuate the increased ITCZ intensity while precipitation over Africa is less significantly diminished. Reducing solar forcing appears to have no effect in the high latitudes, where precipitation is also increased in response to increased greenhouse gases.

5.5 Summary of sensitivity experiments

A suite of General Circulation Model equilibrium sensitivity experiments were run to explore the relative influence of various global-scale forcing mechanisms during the Maunder Minimum compared to present. An additional experiment designed to gauge the sensitivity of a doubled CO_2 world to a decrease in solar irradiance was also conducted. Comparisons of these sensitivity tests provide insights into the influence of greenhouse gases, solar irradiance and orbital forcing relative to each other during the last several centuries and into the next few decades. They also provide the basis for further investigation into processes and regions deemed particularly sensitive to these forcing mechanisms.

These modeled results lead to the overall conclusion that all these forcing elements play an important role in modulating the global climate of the last several centuries. A reduction in global annual temperature of approximately half a degree when the model is run only in response to a negative change in solar forcing, agrees well with a range of transient experiments investigating solar-only effects for the Little Ice Age. This confirms assumptions that the dominance of the low-frequency portion of solar forcing approximates the dissipation timescale of the climate system and century-scale solar forcing is in near equilibrium with its climate response. The assumption of linear forcing and response is well demonstrated for temperature in all these experiments. However, precipitation sensitivity to forcing is not constant, and for Maunder Minimum compared to present, precipitation is significantly more sensitive to solar forcing than to greenhouse gases. This is likely a result of the non-normal distribution of precipitation and therefore the relationship of forcing to response changes as a value of zero is approached. As the climate dries during the Maunder Minimum and more closely approaches zero precipitation, greenhouse gases can exert little more influence than solar forcing during this time. However, solar forcing also exerts more relative influence on precipitation than on temperature when reduced to Maunder Minimum values for the 2060AD scenario – a period which is, on average, wetter than present.

Regional patterns of response in these equilibrium experiments match, in many respects, the Northern Hemisphere major mode of variability. The North Atlantic Oscillation is modulated (forced into a preferred positive mode) in response to negative forcing in the Maunder Minimum experiments. The expression of that response for temperature is

somewhat different between solar and greenhouse gas forcing as the warm air advection over Europe varies between scenarios. With greenhouse gas forcing only, consistently cooler SSTs in the North Atlantic provides for less warm air to advect (thus attenuating the temperature response in Europe). However, the NAO-like signature is stronger for precipitation for greenhouse gases than for solar, indicating that the NAO-influence (i.e. pressure difference) is also strong. Furthermore, sea-ice may be an important feedback in sustaining a preferred mode of the NAO. This preferred positive mode differs in phase from previous results for different models and for an empirical estimation.

The response in regional climate from changes in orbital forcing are larger than expected for the small forcing imposed over several centuries. A warming in the northern high latitudes tempers the opposite sign effect due to solar and greenhouse gases and influences the stability of the NAO-response. With the addition of orbital forcing, the NAO mode is likely not as frequent or strong, and/or the position of the quasi-stationary pressure systems, more particularly its southerly component, may shift to alter the dominant air flow direction over northern Europe. Orbital forcing is also a strong influence on the precipitation regime in Africa and is consistent with modeling studies and observational evidence that suggest increased Northern Hemisphere irradiance (from changing obliquity) would lead to a moistening of northern Africa. It is possible, given the obvious response across Africa to the small magnitude of forcing, that these equilibrium experiments are over-emphasizing the importance of orbital forcing. Nonetheless, it gives weight to conclusions regarding the necessity of including orbital forcing in further experiments exploring the climate of the last several centuries.

CHAPTER 6

SUMMARY AND DISCUSSION

6.1 Summary of research

A complementary approach of empirical and model-based analysis was used to determine if the climate effects of an estimated change in solar irradiance were significant in the pre-industrial era and what climate patterns emerge in response to reduced solar forcing at that time. Also investigated was the modification of solar-induced climate patterns by a hitherto under-represented forcing - changes in Earth's orbit - and how solar and orbital forcing compare to that of increasing atmospheric greenhouse gas concentration. Finally a brief analysis of the effects of a Maunder Minimum-like solar irradiance on a climate forced by doubled CO_2 was undertaken.

Many previous solar-climate investigations have found an important and robust relationship between the sun and surface climate. This study aims to build on these investigations, which are often based on data that are limited in spatial extent (*e.g.* Cook *et al.* 1997), or based on a broad-scale (hemispheric) long paleoclimate reconstruction, with no spatial resolution (e.g. Lean *et al.* 1995), or studies that are based purely on modeled results (e.g. Cubasch *et al.* 1997). In 1998, Mann and co-authors published a new paleoclimate reconstruction based on a variety of paleo-indicators that extended back to 1400 AD at annual resolution and resolve spatial patterns of temperature back to 1600?. This enabled a new empirical analysis of the solar influence on surface temperature for the pre-industrial period, emphasizing the spatial response. This

empirical analysis (contained mostly within chapter 4) facilitates comparison with

transient climate models (e.g. Cubasch *et al.* 1997), which also have reasonably high

spatial resolution, to gauge some indication of likely mechanisms for the temperature

patterns. In addition to the empirical analysis, a suite of model experiments of very high

spatial resolution were used to compare contributions of solar forcing to that of orbital

and greenhouse gas forcing over the Maunder Minimum-to-present period (chapter 5).

In order to isolate the effects of solar forcing on the climate, chapter 4 contains analysis

of an extended interval of time prior to industrialization (1650-1850) and the supposed

beginning of effects from the enhanced greenhouse effect. Indirect information (paleo-

indicators) was used by Mann *et al.* (1998) to reconstruct a large-scale temperature

history and Lean *et al.* (1995) provided the solar irradiance reconstruction preferred in

this study. The alternative solar reconstructions of Hoyt and Schatten (1993) and Wang *et*

al. (2005) were also compared given that certainty with regard to solar irradiance changes

remains elusive. Both global/hemispheric mean sensitivities to solar forcing and regional

patterns of response and their timescale dependence were examined. These were then

compared to general circulation model output to gain some insight into the possible

underlying mechanisms associated with the climate response.

For the global mean case, correlation between Lean *et al.* (1995) solar irradiance

estimates and the Mann *et al.* 1998 temperature reconstruction over the 1650-1850 time

period is 0.26, rising to 0.35 at a lag of 14 years. This is similar to results from Mann *et*

al. 1998 for the Northern Hemisphere. Converting regression into a more interpretable

diagnostic of sensitivity by applying formula (1) in section 4.2, an assessment of the change in temperature per Wm^{-2} forcing was obtained and compared to model output. Sensitivity is lower (0.17ºC/Wm^{-2}) in the empirical case than in the Cubasch *et al.* (1997) coupled model (0.36ºC/Wm^{-2}) and for the GISS atmospheric GCM (1.06ºC/Wm^{-2}). This is neither surprising nor inconsistent with the model results considering uncertainty in the time history of forcing, compared with the self-consistent nature of the models' forcing and response.

When the sensitivity calculations are applied to each grid cell of the Mann *et al.* (1998) reconstruction, large areas of coherent sensitivity are found to exist and these provide information regarding regional dynamics. The most notable feature of the spatial sensitivity pattern appears as large areas of positive sensitivity over the continental interiors and the western tropical Pacific. Low or negative sensitivity is apparent over the North Atlantic and northern North Pacific. This pattern is particularly clear when the low frequency variations are isolated. The empirical sensitivity is remarkably similar to the Cubasch *et al.* (1997) coupled model experiment, with the exception of the western Pacific. The delayed response in the North Atlantic in the empirical analysis, mirrored in the coupled model, appears to result from a slowing down of the thermohaline circulation and consequent reduction in the northward heat flux, in response to positive radiative forcing. Where the pattern between the model and the observations is dissimilar (i.e. the western Pacific) a possible mechanism for producing enhanced sensitivity in the western Pacific is discussed. A Bjerknes-type feedback may not be represented in climate models due to the inability of coarse resolution models to simulate sufficient ocean-atmosphere

coupling. The coarsely-resolved GISS AGCM shows widespread positive sensitivity and no time evolution of response. The higher-than-average model sensitivity, the lack of a dynamic ocean and the coarse horizontal resolution are major limitations of the GISS model for comparison in this case.

Isolation of the high frequency variability demonstrates far less evidence of the broad-scale features of the multidecadal timescale, which more closely approximate equilibrium conditions, but rather evidence of resonance with known modes of decadal variability is displayed. These modes are characterized by a strongly time-evolving component and this result is very much in line with previous empirical studies that note strong relationships between the 11-year solar cycle and intrinsic decadal modes of the climate system, especially during higher amplitude cycles.

Despite the close agreement between a solar forced coupled model and empirical calculations of the climate response to solar forcing, it is likely that other natural forcing mechanisms play some role both prior to the mid 1800s (i.e. the period analyzed in chapter 4) and certainly during the industrial era. A suite of equilibrium model experiments were run to gauge the relative impact of solar forcing compared with other known or estimated forcing at the decadal-to-centennial scale.

An equilibrium experiment isolating the effects of Maunder Minimum-like reduced solar irradiance (as estimated by Lean *et al.* 2005) was conducted and global temperature reduction was found to agree well with a range of transient experiments investigating

solar-only effects for the Little Ice Age time period. This reinforces conclusions regarding the dominance of the low-frequency band of solar forcing and provides evidence that century-scale solar radiative forcing produces a near-equilibrium response. When compared with other decade-to-century forcing, the dominance of greenhouse gas-forcing is clear for the present climate compared to the pre-industrial period. However, solar variability exerts more relative impact on global precipitation as the sensitivity changes in a drier climate (*i.e.* the colder Little Ice Age).

Regional patterns of response in the equilibrium experiments are reminiscent of the major modes of variability in the Northern Hemisphere. That North Atlantic Oscillation is forced into a preferred mode by both solar and greenhouse gas forcing and sea-ice is revealed as a critical feedback, possibly reinforcing the NAO mode. Though there are indications of a change in Hadley cell circulation and ITCZ position from solar and greenhouse gas forcing, significance is difficult to establish for tropical precipitation given the high interannual model variability.

For a future scenario examining the possible impact of a Maunder Minimum solar episode on equivalent doubled CO_2, some moderating effect on the widespread global warming was found to occur. Those areas that are most sensitive to an increase in greenhouse gases (e.g. the continental interiors) also displayed the greatest attenuation from a reduction in solar irradiance. Again, solar forcing induced a relatively stronger drying than expected for a linear response.

A larger than expected response from the small magnitude orbital forcing is found in the modeled experiments. Offsetting some of the forcing from solar and greenhouse gases in the high northern latitudes, orbital forcing influences the stability of the NAO response. Precipitation across Africa is also modulated, consistent with findings for larger magnitude orbital forcing for the mid-Holocene.

6.2 Discussion and Implications

Clear evidence is established herein for the ability of relatively small changes in solar irradiance to impact the global climate. Both at the century scale and at shorter periodicities, the variability of the solar 'constant' can help to define the global mean climate and more importantly, the regional characterization of that climate. Solar forcing influences the preferred mode of decadal variability – the North Atlantic Oscillation for example – thereby altering the mean climate for northern Europe and the North Atlantic region. The global response for temperature is found to be near-linear, while precipitation is more complex. Excitation of important feedbacks, such as sea-ice, plays an important role in determining the resulting pattern of response and ensures that even a much smaller forcing (solar variability) can produce a similar fingerprint to that of a larger forcing (greenhouse gases). Orbital forcing, typically excluded from model experiments for simulations involving recent decades and centuries, is found to provide important modification of regional response and may be critical for determining a more accurate 'forecast' for future climate. In addition, models of relatively coarse scale may fail to

capture important dynamical feedback mechanisms (e.g. in the western Pacific) crucial for gauging regional sensitivity.

The implications of this research for the future are far-reaching. As a global community, it is less likely that we will be concerned with global mean climate change in the coming decades and more likely that we will need to understand and predict the modulation of the climate signal in regions where the population and environment appears vulnerable. Despite the limited attenuation that a low solar phase would have on global mean warmth under the enhanced greenhouse gas effect, there may be significant regional impacts, perhaps especially in those areas that are most likely to feel the influence of higher CO_2. This may be critical in offsetting regionally large changes or delaying the transition across critical climate system thresholds, such as a change in thermohaline circulation. Modulation of precipitation may prove especially important in determining the adaptability of regional populations and this research indicates that a reduced irradiance may have more relative impact on that precipitation in the face of greenhouse gas induced warming.

Clearly there are forcings and feedbacks which are under-represented in many current climate models – elements such as a coupled dynamic sea-ice model, and forcing such as orbital parameters, which may prove to be critical in determining the regional response for past and future decades. We know that millennial scale orbital forcing can have a large impact on African moisture and given the likely sensitivity of this region and its current marginal viability for support of a sustainable population, any modulation of the

precipitation pattern on the decade-century scale will be of critical importance for future planning.

This research has shown the importance of including smaller magnitude global-scale forcing and its ability to influence not only the global mean response, but also the regional scale climate patterns. The inclusion of solar forcing and orbital forcing increases our ability to identify a deterministic response in the current and future climate system. Further research is necessary to analyze other important possible feedbacks (such as stratospheric ozone) and to improve model capability such that more confidence in precipitation estimates is possible. Equilibrium climate models allow us to attempt a variety of experiments in relatively little time and to gauge a relative sensitivity and possible climate pattern outcome. In order to reduce forecast uncertainty further, those experiments must be used primarily to indicate which areas of the globe and aspects of climate dynamics need closer attention in transient and coupled simulations. An important limitation of equilibrium models is the inability to see how the resulting climate pattern developed over time and which specific elements of climate dynamics were more influential in nudging the climate into a certain pattern or phase.

6.3 Future Research

There are several different elements that comprise the uncertainty in this research and can be addressed in future research to some degree. Perhaps the largest element of uncertainty in looking at the climate response to solar forcing is the solar forcing itself. While there is

much research analyzing the properties of the changing sun, there is limited community agreement as to the multidecadal changes in magnitude of irradiance impinging on the Earth. This continued research is very much within the purview of solar physicists, and atmospheric scientists are consequently limited by progress within that community. Nonetheless, recent interdisciplinary interaction has heightened awareness as to the importance of long-term irradiance estimates. Meanwhile, we are able to conduct research based on a range of irradiance possibilities (as here).

Proceeding with the assumption that we are using reasonable estimates of solar irradiance for the past, and acknowledging the impact of the sun on past and future climate, an important follow-up question is the degree to which future changes in irradiance may delay or offset the abrupt changes hypothesized to occur in response to further greenhouse gas warming. Intriguing modulation of the greenhouse gas induced pattern has been demonstrated in this research and further investigation may reveal critical conclusions regarding the projections of likely climate in the 21st century. For example, if a warmer, wetter climate and increased ice cap melting would lead to a cessation or slowing down of the thermohaline circulation of the oceans, what is the likelihood that reduced solar radiation in the future would change the timing or severity of that response? This can only be answered with a coupled ocean-atmosphere transient model – one that includes the components of the model used in chapter 5 – a coupled dynamic sea ice model and orbital forcing as an additional input.

Uncertainties in the strength of coupling between the troposphere and stratosphere as well as the role of the ocean in solar-driven experiments are at present limiting confidence in modeled results. Though some research has been undertaken regarding the feedback of ozone (*e.g.* Shindell *et al.* 2001) there is still disagreement regarding the role of solar forcing on the troposphere as modulated by ozone feedbacks in the stratosphere. For example, the model that Shindell *et al.* used had a very coarse horizontal resolution and did not include a coupled ocean component. Similar experiments can be performed with a more complex model to assess different processes.

Lastly, this research reveals a larger role of orbital forcing than previously anticipated and this area of research requires more focused attention. More empirical research at the century scale as well as model experiments can help us gain further insight into this climate forcing and its interaction with other, likely more dominant forcing.

APPENDIX

A NOTE ON THE ESTIMATE OF SENSITIVITY FROM LINEAR REGRESSION OF

FORCING AND TEMPERATURE SERIES

Courtesy of M. E. Mann

One can estimate s' (see e.g., Cubasch *et al.*, 1997), the linear sensitivity with respect to a

given forcing F through linear regression,

$$s'_f = <FT>/<F^2> \qquad (A1)$$

where $<FT>$ is the covariance of F and T, and $<F^2>$ is variance in the forcing series F.

Since T can be considered as a sum of the forced response to F and a residual "noise

term" N (which actually consists of the response to other forcings as well as internal

climate noise), we can write,

$$T = T_f + N \qquad (A2)$$

This allows us to write the estimated sensitivity s' in terms of the true sensitivity s as,

$$s'_f = s_f \, (1 + <FN>/<F \, T_f>) \qquad (A3)$$

where

$$s_f = <F\ T_f>/<F^2> \qquad\qquad (A4)$$

is the correct theoretical sensitivity. It is thus evident that the sensitivity as estimated

through direct application of (A1) will in general differ from the true estimate of

sensitivity (A4) for at least two distinct possible reasons:

1) *random errors:* sensitivity will differ from the true sensitivity by some additive

fraction (second term in A3) which depends on the signal-to-noise ratio through the ratio

of the signal and noise covariances with the forcing for the given realization. This error

term can be quite large in a relatively short single-realization, but in principle can be

reduced if it is possible to average over an ensemble of more than one noise realization or

over a very long interval of time (e.g., Cubasch *et al.*, 1997--in an infinite ensemble, this

term should of course average to zero). It is also possible to reduce the expected

amplitude of this random error if the forcing and temperature series are filtered in bands

where the signal-to-noise ratio for the forcing is greatest.

2) *systematic bias:* This is largely an issue only for empirically estimated sensitivities,

which are based on statistically independent estimates of forcing and response, wherein

calibration uncertainties and random errors can both lead to systematic errors in estimates

of sensitivity [This is in contrast with the model-forcing experiments, wherein errors in

the estimate of the actual forcing are immaterial, as it is only the self-consistent response

of the model to any supplied forcing which is used to ascertain sensitivity]. These

systematic errors fall into two basic categories. The first will always lead to an underestimate of sensitivity, while the second can lead to either an underestimate or overestimate of sensitivity:

a) Any random uncertainties in the estimate of the true history of the forcing will increase the variance of the forcing (the denominator in A1) but not (on average) the covariance of the forcing and temperature estimate (the numerator in A1), consequently leading to an underestimate of the true sensitivity.

b) A systematic overestimate (underestimate) of variance in the calibration of the solar irradiance reconstruction will systematically decrease (increase) the sensitivity estimate, while a systematic overestimate (underestimate) of variance in the calibration of the temperature reconstructions will systematically increase (decrease) the sensitivity estimate.

Neglecting the calibration uncertainties (i.e., "b" above) or at least being unable to determine *a priori* the likely sign of the associated bias in either case, we are left to conclude that the considerable uncertainty in the information used to extend solar estimates back in time insures substantial *random* uncertainty (i.e., "a" above) in the forcing estimate, and necessitates that we consider the empirically estimated sensitivity patterns fundamentally as lower-bound estimates of the true sensitivity. Because several of the possible sources of bias discussed above are likely to exhibit timescale dependence, examination of the sensitivity in independent frequency bands may however provide a means of establishing more confidence in the estimates. Estimates of sensitivity

confined to frequency bands wherein the forcing history is most accurately estimated are less likely to lead to underestimates of sensitivity vis error source "a".

REFERENCES

ACIA. (2005). *Arctic climate impact assessment*. Cambridge: Cambridge University
Press.

Appenzeller, C., Stocker, T.F. and Anklin, M. (1998). North Atlantic oscillation
dynamics recorded in Greenland ice cores. *Science, 282*, 446-449.

Bard, E., Raisbeck, G., Yiou, F. and Jouzel, J. (2000). Solar irradiance during the last
1200 years based on cosmogenic nuclides. *Tellus, 52B*, 985-992.

Beer, J., Mende, W., and Stellmacher, R. (2000). The role of the sun in climate forcing.
Quaternary Science Reviews, 19, 403-415.

Benestad, R.E. (2002). *Solar activity and Earth's climate*. Berlin and Heidelberg: Praxis-
Springer

Berger, A. L., Loutre, M.. F., and Tricot, C., (1993). Insolation and Earth's orbital
periods. *Journal of Geophysical Research, 98*(10), 341–10 362.

Berger, A. L. and Loutre, M. F. (1991). Insolation values for the climate of the last 10
million years. *Quaternary Science Reviews, 10*, 297-317

Berger, A. L. (1978). Long Term Variations of Daily Insolation and Quaternary Climatic
Changes. *Journal of the Atmospheric Sciences, 35*(12), 2362-2367

Bradley, R. S., (1999). *Paleoclimatology: Reconstructing climates of the Quaternary*. San
Diego: Harcourt, Academic Press.

Bradley, R.S. and Jones, P.D., (1993). 'Little Ice Age' summer temperature variations:
their nature and relevance to recent global warming trends. *Holocene, 3,* 367-376.

Briffa, K.R., Jones, P.D., Schweingruber F.H. and Osborn T.J. (1998). Influence of
volcanic eruptions on Northern Hemisphere summer temperature over the past
600 years. *Nature, 393*, 350-354.

Brostrom, A., Coe, M., Harrison, S. P., Gallimore R., Kutzbach J. E., Foley J., Prentice
I.C., and Behling P. (1998) Land surface feedbacks and palaeomonsoons in
northern Africa. *Geophysical Research Letters, 25*, 3615-3618.

Cane, M.A., Clement, A.C., Kaplan, A., Kushnir, Y., Pozdnyakov, D., Seager, R.,
Zebiak, S.E., and Murtugudde, R. (1997). Twentieth-century sea surface
temperature trends. *Science, 275*, 957-960

Charbonneau, P. and White, O.R. (1995). The sun: a pictorial introduction. http://www.hao.ucar.edu/public/education/slides/slides.html. National Center for Atmospheric Research.

Claussen, M.,. Kubatzki, C., Brovkin, V., Ganopolski, A., Hoelzmann, P., and Pachur, H. J. (1999). Simulation of an abrupt change in Saharan vegetation in the mid-Holocene. *Geophysical Research Letters, 26*, 2037-2040.

Clement, A.C., Seager, R., Cane, M.A. and Zebiak, S.E. (1996). An ocean dynamical thermostat. *Journal of Climate, 9*, 2190-2196.

Cook, E., Meko, D.M., and Stockton, C.W. (1997). A new assessment of possible solar and lunar forcing of the bidecadal drought rhythm in the western United States. *Journal of Climate, 10*, 1343-1356.

Coyne, G.V. (1991). Sunspots: The historical background. In Sonett, C.P., Giampapa, M. S., and Matthews, M.S., (Eds.) *The sun in Time*. Tucson: Arizona University Press.

Crane, R. G. and Hewitson, B.C. (1998). Doubled CO2 precipitation changes for the Susquehanna Basin: Downscaling from the GENESIS general circulation model, *International Journal of Climatology, 18*, 65-76.

Cubasch, U., Voss, R, Hegerl, G.C., Wazskewitz, J. and Crowley, T.J. (1997). Simulation of the influence of solar radiation variations on the global climate with an ocean-atmosphere general circulation model. *Climate Dynamics, 13*, 757-767

Crowley, T.J. and Kim, K-Y (1996). Comparison of proxy records of climate change and solar forcing. *Geophysical Research Letters, 23*(4), 359-362.

Crowley, T.J. and Kim, K-Y (1999). Modeling the temperature response to forced climate change over the last six centuries. *Geophysical Research Letters, 26*(13), 1901-1904.

Damon, P. E., and Peristykh, A.N. (2005). Solar forcing of global temperature change since AD 1400, *Climatic Change, 68*(1-2), 101

Damon, P.E., and Sonnett, C.P., (1991). Solar and terrestrial components of the atmospheric 14C variation spectrum. In Sonett, C.P., Giampapa, M. S., and Matthews, M.S., (Eds.) *The sun in Time*. Tucson: Arizona University Press.

Damon, P.E., and Peristykh, A.N. (1999). Solar cycle length and 20th century northern hemisphere warming. *Geophysical Research Letters, 26*(16), 2469-2472.

Delworth, T.L., Manabe, S. and Stouffer, R.J., (1993). Interdecadal variations of the thermohaline circulation in a coupled ocean-atmosphere model. *Journal of Climate, 6*, 1993-2011.

Delworth, T.L., Manabe, S. and Stouffer, R.J., (1997). Multidecadal climate variability in the Greenland Sea and surrounding regions: a coupled model simulation. *Geophysical Research Letters, 24*, 257-260.

Delworth, T.D., and Mann, M.E., (2000). Observed and simulated multidecadal variability in the North Atlantic. *Climate Dynamics, 16*, 661-676

deMenocal, P., Ortiz, J., Guilderson, T., Adkins, J., Sarnthein, M., Baker, L., and Yarusinsky, M., (2000). Abrupt onset and termination of the African Humid Period: rapid climate responses to gradual insolation forcing. *Quaternary Science Reviews, 19*, 347-361.

Deser, C. and Blackmon, M., (1993). Surface climate variations over the North Atlantic ocean during Winter: 1990-1989. *Journal of Climate, 6*, 1743-1753.

Deser, C., Walsh, J. E., Timlin, M. S. (2000). Arctic Sea Ice Variability in the Context of Recent Atmospheric Circulation Trends. *Journal of Climate, 13*, 617-633

DKRZ model-user support group (1993). Report no.6: The ECHAM3 general circulation model. Max-Planck Institute für Meteorologie, Hamburg.

Drijfhout, S.S., Haarsma, R.J., Opsteegh, J.D., Selten, F.M. (1999). Solar-induced versus internal variability in a coupled climate model. *Geophysical Research Letters, 26*(2), 205-208.

Eddy J. (1976) The Maunder Minimum. *Science, 192*, 1189-1202.

Fligge, M., Solanki, S.K. (2000). The solar spectral irradiance since 1700. *Geophysical Research Letters, 27*(14), 2157–2160

Folland, C.K., Palmer, T.N. and Parker, D.E. (1986). Sahel rainfall and worldwide sea temperatures. *Nature, 320*, 602-606.

Friis-Christensen, E. and Lassen, K. (1991). Length of a solar cycle: an indicator of solar activity closely associated with climate. *Science, 254*, 698-700.

Fröhlich, C. and Lean, J. (1998). The sun's total irradiance: cycles, trends and related climate change uncertainties since 1976. *Geophysical Research Letters, 25*(23), 4377-4380.

Fröhlich, C. and Lean, J. (2004). Solar radiative output and its variability: evidence and mechanisms. *Astronomy and Astrophysics Review, 12*, 273—320.

Graham, N.E. (1994). Decadal-scale climate variability in the 1970's and 1980's: observations and model results, *Climate Dynamics, 10*, 135-162.

Haigh, J.D. (1994). The role of stratospheric ozone in modulating the solar radiative forcing of climate. *Nature, 370*, 544-546.

Haigh, J. (1996). The impact of solar variability on climate. *Science, 272*, 981-984.

Hansen, J., Russell, G., Rind, D., Stone, P., Lacis, A., Lebedeff, S., Ruedy, R., and Travis, L. (1983). Efficient three-dimensional global models for climate studies: models I and II. *Monthly Weather Review, 111*(4), 609-662

Hastenrath, S. (1990). Decadal-scale changes of the circulation in the tropical Atlantic sector associated with Sahel drought. International *Journal of Climatology, 10*, 459-472.

Honda, M., Yamazaki, K., Tachibana, Y., and Takeuchi, K. (1996). Influence of Okhotsk sea-ice extent on atmospheric circulation. *Geophysical Research Letters, 23*, 3595–3598.

Honda, M., Yamazaki, K., Nakamura, H., and Takeuchi, K. (1999). Dynamic and thermodynamic characteristics of atmospheric response to anomalous sea-ice extent in the Sea of Okhotsk. *Journal of Climate, 12*, 3347–3358.

Hoyt, D.V. and Schatten, K.H. (1993). A discussion of plausible solar irradiance variations, 1700-1992. *Journal of Geophysical Research, 98*(A11), 18,895-18,906.

Hoyt, D. V., Schatten, K.H., and Nesme-Ribes, E. (1994). A new reconstruction of solar activity, 1610-1993. NATO Advanced Research Workshop Proceedings. The Solar Engine and Its Influence on Terrestrial Atmosphere and Climate.

Hoyt, D.V. and Schatten, K.H. (1997). *The role of the sun in climate change*. New York: Oxford University Press.

Hughes, M.K., and Diaz, H.F. (1994). Was there a `Medieval Warm Period" and if so, where and when? *Climatic Change, 26*, 109-142.

Hurrell, J.W. and van Loon, H. (1997). Decadal variations in climate associated with the North Atlantic oscillation. *Climatic Change, 36*, 301-326.

Hurrell, J.W. (1995). Decadal trends in the North Atlantic Oscillation regional temperatures and precipitation. *Science, 269*, 676-679.

Intergovernmental Panel of Climate Change (2001). *Climate Change 2001: The Scientific Basis.* Houghton J. T., Ding Y., Griggs D. J., Noguer M., van der Linden P. J., Dai X., Maskell K., Johnson C.A. (Eds.). Cambridge: Cambridge University Press.

Intergovernmental Panel of Climate Change (1996). Climate Change 1995: The science of climate change. edited by Houghton J.T., Meira Filho L.G., Callander B.A., Harris N., Kattenberg A. and Maskell K. (Eds.). Cambridge: Cambridge University Press.

Intergovernmental Panel of Climate Change (1990). Climate Change: The IPCC Scientific Assessment. edited by Houghton J.T., Jenkins G.J., Ephraums J.J. (Eds.). Cambridge: Cambridge University Press.

Jones, P.D., Osborn, T.J., Briffa, K.R., Folland, C.K., Horton, E.B., Alexander, L.V., Parker, D.E. and Rayner, N.A., (2001). Adjusting for sampling density in grid box land and ocean surface temperature time series. *Journal of Geophysical Research, 106*, 3371-3380.

Jones, P.D., Briffa, K.R., Barnett, T.P., and Tett, S.F.B. (1998). High-resolution palaeoclimatic records for the last millennium: interpretation, integration and comparison with general circulation model control run temperatures. *Holocene, 8*, 477-483.

Joussaume, S., Taylor, K. E., Braconnot, P., Mitchell, J. F. B., Kutzbach, J. E., Harrison, S. P., Prentice, I. C., Broccoli, A. J., Abe, O.-A., Bartlein, P. J., Bonfils, C., Dong, B., Guiot, J., Herterich, K., Hewitt, C. D., Jolly, D., Kim, J. W., Kislov, A., Kitoh, A., Loutre, M. F., Masson, V., McAvaney, B., McFarlane, N., De, N.-N., Peitier, W. R., Peterschmitt, J. Y., Pollard, D., Rind, D., Royer, J. F., Schlesinger, M. E., Syktus, J., Thompson, S., Valdes, P., Vettoretti, G., Webb, R. S. and Wyputta, U. (1999). Monsoon changes for 6000 years ago: results of 18 simulations from the Paleoclimate Modeling Intercomparison Project (PMIP). *Geophysical Research Letters, 26*, 859-862.

Khanderkar, M.L., Murty, T.S. and Chittibabu, P. (2005). The global warming debate: A review of the state of science. *Pure and Applied Geophysics, 162*, 1557-1586

Kushnir, Y., (1994). Interdecadal variations in North Atlantic sea surface temperature and associated atmospheric conditions. *Journal of Climate, 7*, 141–157.

Kutzbach, J. E. and Liu, Z. (1997). Response of the African monsoon to orbital forcing and ocean feedbacks in the middle Holocene. *Science, 278,* 440-443.

Kutzbach, J. E. and Street-Perrott, F. A., (1985). Milankovitch forcing of fluctuations in the level of tropical lakes from 18 to 0 kyr BP. *Nature, 317*, 130-134.

Labitzke, K. and van Loon, H. (1988). Associations between the 11-year solar cycle, the QBO and the atmosphere. part I: the troposphere and stratosphere in the northern hemisphere in winter. *Journal of Atmospheric and Terrestrial Physics, 50*(3), 197-206.

Labitzke, K. and van Loon, H. (1992). Association between the 11-year solar cycle and the atmosphere, part V: summer. Journal of Climate 5, 240-251.

Labitzke, K. and van Loon, H. (1993). Some recent studies of probable connections between solar and atmospheric variability. *Annales Geophysicae, 11*, 1084-1094.

Larkin, A., Haigh, J.D. and Djavidnia, S. (2000). The effect of solar UV irradiance variations on the Earth"s atmosphere. *Space Science Reviews, 94*, 199 – 214

Latif, M., and Barnett, T.P. (1994). Causes of decadal climate variability over the North Pacific and North America. *Science, 266*, 634-637.

Laut, P. (2003). Solar activity and terrestrial climate: An analysis of some purported correlations. *Journal of Atmosphere and Solar-Terrestrial Physics, 65*, 801–812.

Lean, J. (1991). Variations in the sun's radiative output. *Reviews of Geophysics 29*(4), 505-535.

Lean, J., Skumanich, A., and White, O. (1992). Estimating the sun's radiative output during the maunder minimum. *Geophysical Research Letters 19*, 1591-1594.

Lean, J., and Foukal, P., (1988). A model of solar luminosity modulation by magnetic activity between 1954 and 1984. *Science, 240*, 906-908.

Lean, J., Beer, J. and Bradley, R.S. (1995). Reconstruction of solar irradiance since 1610: implications for climate change. *Geophysical Research Letters, 22*(23), 3195-3198

Lean, J. and Rind, D., (1998). Climate forcing by changing solar radiation. *Journal of Climate, 11(*12), 3069-3064

Lean, J. (2000). Evolution of the Sun's spectral irradiance since the Maunder Minimum. *Geophysical Research Letters, 27*(16), 2425-2428

Mahasenan, N., Watts R.G. and Dowlatabadi, H. (1997). Low-frequency oscillations in temperature-proxy records and implications for recent climate change. *Geophysical Research Letters, 24(*5), 563-566

Maier-Reimer, E. and Mikolajewicz, U. (1992). Report no.2: The Hamburg large-scale geostrophic ocean general circulation model, cycle 1. Max-Planck-Institute für Meteorologie, Hamburg.

Manabe, S. and Stouffer, R.J. (1994). Multiple-century response of a coupled ocean-atmosphere model to an increase of carbon dioxide. *Journal of Climate, 7,* 5-23.

Mann, M.E., Lall, U., Saltzman, B., (1995b). Decadal-to-century scale climate variability: Insights into the Rise and Fall of the Great Salt Lake. *Geophysical Research Letters, 22,* 937-940.

Mann, M.E. and Park, J. (1993). Spatial correlations of interdecadal variation in global surface temperatures. *Geophysical Research Letters, 20,* 1055-1058.

Mann, M.E. and Park, J. (1994). Global scale modes of surface temperature variability on interannual to century time scales. Journal *of Geophysical Research, 99*, 25819-25833.

Mann, M.E. and Park, J. (1996). Joint spatio-temporal modes of surface temperature and sea level pressure variability in the northern hemisphere during the last century. *Journal of Climate, 9*, 2137-2162.

Mann, M.E. and Park, J. (1999). Oscillatory spatiotemporal signal detection in climate studies: A multiple-taper spectral domain approach. *Advances in Geophysics, 41*, 1-131.

Mann, M.E., Park, J., and Bradley, R.S. (1995a). Global interdecadal and century-scale climate oscillations during the past five centuries. *Nature, 378*, 266-270.

Mann, M.E., Bradley, R.S. and Hughes, M.K. (1998). Global-scale temperature patterns and climate forcing over the past six centuries. *Nature, 392*, 779-787.

Mann, M.E., Bradley, R.S. and Hughes, M.K. (1999a). Northern hemisphere temperatures during the past millennium: inferences, uncertainties, and limitations. *Geophysical Research Letters, 26*, 759-762.

Mann, M.E., Bradley, R.S., and Hughes, M.K., (2000a). Long-term variability in the el nino southern oscillation and associated teleconnections. In Diaz H.F. and Markgraf V. (Eds) *El nino and the southern oscillation: Multiscale variability and its impacts on natural ecosystems and society*. Cambridge: Cambridge University Press.

Mann, M.E., Gille, E., Bradley, R.S., Hughes, M.K., Overpeck, J.T., Webb, R.S. and Keimig, F.T. (2000b). Annual temperature patterns in past centuries: An interactive presentation. *Earth Interactions, 4-4*, 1-29.

Marshall, S., Oglesby, R.J., Larson, J. and Saltzman, B. (1994). Comparison of GCM sensitivity to changes in CO2 and solar luminosity. *Geophysical Research Letters, 21(23),* 2487-2490.

Marshall, S., Mann, M.E., Oglesby, R., and Saltzman, B. (1995). A comparison of the CCM1-simulated climates for pre-industrial and present-day C02 levels. *Global and Planetary Change, 10*, 163-180.

McHargue, M.R. and Damon, P.E. (1991). The global Beryllium 10 cycle. *Reviews of Geophysics, 29*, 141-158

Meehl, G.A., and co-authors, (2004). Combinations of natural and anthropogenic forcings and 20th century climate. *Journal of Climate, 17*, 1584

Meehl, G.A. and Washington, W.M. (1996). El Niño–like climate change in a model with increased atmospheric CO2 concentrations. *Nature 382,* 56–60.

Meldrum, C. (1872). On a periodicity in the frequency of cyclones in the Indian Ocean south of the equator. *British Association Report, 42*, 56–58

Miller, A.J., Cayan, D.R., and White, W.B. (1998). A decadal change in the North Pacific thermocline and gyre-scale circulation. Journal *of Physical Oceanography, 27*, 2023-2039.

Minobe, S. (1997) A 50-70 year climatic oscillation over the North Pacific and North America. Geophysical *Research Letters, 24*, 683-686.

Morfill, G.E., Scheingraber, H. and Voges, W. (1991). Sunspot number variations: stochastic or chaotic? In Sonett, C.P., Giampapa, M.S. and Matthews, M.S., (Eds.) *The sun in time*. Arizona: University of Arizona Press.

Ogilvie, A.E.J. (1992). Documentary evidence for changes in the climate of Iceland, A.D.1500 to 1800. In Bradley, R.S. and Jones, P.D. (Eds.) *Climate since A.D.1500*. London: Routledge

Overpeck, J., Hughen, K., Hardy, D., Bradley, R., Case, R., Douglas, M., Finney, B., Gajewski, K., Jacoby, G., Jennings, A., Lamoureux, S., Lasca, A., MacDonald, G., Moore, J., Retelle, M., Smith, S., Wolfe, A. and Zielinski, G. (1997). Arctic environmental change of the last four centuries. *Science, 278*, 1251-1256.

Phillips, K.J.H. (1992). *Guide to the Sun*. Cambridge: Cambridge University Press.

Ram, M., Stolz, M. and Koenig, G. (1997). Eleven year cycle of dust concentration variability observed in the dust profile of the GISP2 ice core from central Greenland: possible solar cycle connection. *Geophysical Research Letters 24(19),* 2359-2362.

Reid, G.C. (1991). Solar total irradiance variations and the global sea surface temperature record. *Journal of Geophysical Research, 96(D2),* 2835-2844

Rigor, I. G., Wallace, J. M., Colony, R. L. (2002). Response of Sea Ice to the Arctic Oscillation. *Journal of Climate, 15*, 2648-2663

Rind, D. and Overpeck, J. (1993). Hypothesized causes of decade-to-century-scale climate variability: climate model results. *Quaternary Science Reviews 12*, 357-374

Rind, D., Lean, J. and Healy, R. (1999). Simulated time-dependent response to solar radiative forcing since 1600. *Journal of Geophysical Research, 104(D2),* 1973-1990.

Rind, D., Shindell, D., Perlwitz, J., Lerner, J.,Londergan, P., Lean, J., McLinden, C. (2004). The relative importance of solar and anthropogenic forcing of climate change between the Maunder Minimum and the present. *Journal of Climate, 17,* 906-929

Schaefer, B. (1997). Sunspots that changed the world. *Sky and Telescope, April*, 34-38.

Schlesinger, M.E., and Ramankutty, N. (1994). An oscillation in the global climate system of period 65-70 years. *Nature, 367*, 723-726.

Schove, D. J. (1983). *Sunspot cycles*. Pennsylvania: Hutchinson Ross.

Schulz, M., Paul, A. (2002). Holocene climate variability on centennial-to-millennial time scales: Climate records from the North-Atlantic realm. In: Wefer, G., Berger, W. H., Behre, K.-E. and Jansen, E. (Eds.). *Climate development and history of the North Atlantic Realm.* Berlin: Springer Verlag.

Shindell, D.T., Schmidt, G.A., Mann, M.E., Rind, D., and Waple, A. (2001). Solar forcing of regional climate change during the Maunder Minimum. *Science, 294*, 2149-2152.

Stearns, S.D. and David, R.A. (1988). Signal processing algorithms. A.V. Oppenheim, (Ed) New Jersey: Prentice-Hall Signal Processing Series, Prentice-Hall, Inc.

Stocker, T.F. and Schmittner, A. (1997). Influence of CO2 emission rates on the stability of the thermohaline circulation. *Nature, 388*, 862-865

Stuiver, M. (1961). Variations in Radiocarbon Concentration and Sunspot Activity. *Journal of Geophysical Research 66*, 273 -76.

Svensmark, H. and Friis-Christensen, E. (1997). Variation of cosmic ray flux and global cloud coverage - a missing link in solar-climate relationships. *Journal of Atmospheric and Solar-Terrestrial Physics, 59*(11), 1225-1232

Sun, B. and Bradley, R. S. (2002). Solar influences on cosmic rays and cloud formation: A reassessment, Journal *of Geophysical Research, 107(D14),* 4211-4220.

Tett, S.F.B., Stott, P.A., Allen, M.R., Ingram, W.J. and Mitchell, J.F.B. (1999). Causes of twentieth-century temperature change near the Earth's surface. *Nature, 399*, 569-572

Thompson, S.L., and Pollard, D. (1997). Greenland and Antarctic mass balances for present and doubled atmospheric CO_2 from the GENESIS version-2 global climate model. *Journal of Climate, 10*, 871-900.

Thompson, S.L. and Pollard, D. (1995b). A global climate model (GENESIS) with a land-surface-transfer scheme (LSX). Part 2: CO2 sensitivity. *Journal of Climate 8*, 1104-1121.

Timmerman, A., Latif M., Voss, R. and Grotzner, A. (1998). Northern hemispheric interdecadal variability: A coupled air-sea mode. *Journal of Climate 11*, 1906-1931.

Tinsley, B.A. (1988). The solar cycle and QBO influence on the latitude of storm tracks in the North Atlantic. *Geophysical Research Letters 15*, 409-412.

Tourre, Y., Rajagopalan, B. and Kushnir, Y. (1999). Dominant patterns of climate variability in the Atlantic over the last 136 years. *Journal of Climate, 12*, 2285-2299.

Trenberth, K.E. (1990). Recent observed interdecadal climate changes in the Northern Hemisphere. *Bulletin of the American Meteorological Society 71*, 988-993.

Trenberth, K.E. and Hurrell, J.W. (1994). Decadal atmospheric-ocean variations in the Pacific, *Climate Dynamics, 9*, 303-309.

Voss, R., Sausen, R., Cubasch, U. (1997). Periodically synchronously coupled integrations with the atmosphere-ocean general circulation model ECHAM3/LSG. Rep 229, Max-Planck-Institut Für Meteorologie, Bundesstr. 55, Hamburg, Germany

Wang, Y.-M., Lean, J.L., and Sheeley, Jr. N.R. (2005). Modeling the Sun's magnetic field and irradiance since 1713. *The Astrophysical Journal, 625*, 522-538

Waple, A., Mann, M.E., Bradley, R.S. (2002). Long-term patterns of solar irradiance forcing in model experiments and proxy-based surface temperature reconstructions. *Climate Dynamics, 18*, 563-578.

White, W.B., Lean, J., Cayan, D.R. and Dettinger, M.D., (1997). A response of global upper ocean temperature to changing solar irradiance. *Journal of Geophysical Research, 102*, 3255-3266.

White, W.B., Cayan, D.R. and Lean, J. (1998). Global upper ocean heat storage response to radiative forcing from changing solar irradiance and increasing greenhouse gas/aerosol concentrations. *Journal of Geophysical Research 103C*, 21355-21366.

White, W.B., and Cayan, D.R. (1998). Quasi-periodicity and global symmetries in interdecadal upper ocean temperature variability, *Journal of Geophysical Research 103C*, 21335-21354.

Wigley, T.M.L. and Kelly, P.M. (1990). Holocene climatic change, $_{14}$C wiggles and variations in solar irradiance. *Philosophical Transactions of the Royal Society of London. A330*, 547-560.

Withbroe, G. L. and Kalkofen, W. (1994). Solar variability and its terrestrial effects. In Withbroe, G. L. and Kalkofen, W (Eds) *The sun as a variable star: Solar and stellar irradiance variations.* Cambridge: Cambridge University Press.

Willson, R.C. (1997). Total solar irradiance trend during solar cycles 21 and 22. *Science, 277*, 1963-1965.

Willson, R.C. and Hudson, H.S. (1991). The sun's luminosity over a complete solar cycle. *Nature 351*, 42-44

Zhang, Y., Wallace, J.M., and Battisti, D.S. (1997). ENSO-like interdecadal varibility: 1900-93. *Journal of Climate 10*, 1004-1020